

**Development and characterization of stimuli-responsive drug  
delivery systems to prevent HIV infection and the treatment of  
chronic wounds**

by

Yannick Leandre Traore

A thesis  
presented to the University of Waterloo  
in fulfillment of the  
thesis requirement for the degree of  
Doctor of Philosophy  
in  
Pharmacy

Waterloo, Ontario, Canada, 2021

© Yannick Leandre Traore 2021

## **Examining Committee Membership**

The following served on the Examining Committee for this thesis. The decision of the Examining Committee is by majority vote.

External Examiner	DR. AFSANEH LAVASANIFAR Professor, Faculty of Pharmacy and Pharmaceutical Sciences, University of Alberta
Supervisor	DR. EMMANUEL A. HO Associate Professor, Graduate Officer, School of Pharmacy
Internal Member	DR. SHAWN D. WETTIG Professor, School of Pharmacy, Associate Dean, Graduate Studies (Science)
Internal Member	DR. JONATHAN BLAY Professor, School of Pharmacy
Internal-External	DR. BRIAN DIXON Professor, Department of Biology

## **Author's Declaration**

This thesis consists of material all of which I authored or co-authored: see Statement of Contributions included in the thesis. This is a true copy of the thesis, including any required final revisions, as accepted by my examiners.

I understand that my thesis may be made electronically available to the public.

## **Statement of Contributions**

Yannick Leandre Traore was the sole author of Chapters 5 and 6 which were written under the supervision of Dr. Emmanuel Ho and were not written for publication.

This thesis consists in part of four manuscripts written for publication. Exceptions to sole authorship of material are as follows:

### **Research presented in Chapter 1:**

This research was conducted at the University of Waterloo by Yannick Leandre Traore under the supervision of Dr. Emmanuel Ho. Yannick Leandre Traore designed the study with consultation from Dr. Emmanuel Ho, did the research, and wrote the manuscript. Dr. Emmanuel Ho helped edit the manuscript. Dr. Yufei Chen contributed to the manuscript writing and draft editing.

Citation:

Yannick L. Traore, Yufei Chen, Emmanuel A. Ho. Current State of Microbicide Development. *Clinical Pharmacology & Therapeutics*, 2018 104(6):1074-1081 Vol. doi.org/10.1002/cpt.1212

### **Research presented in Chapter 2:**

This research was conducted at the University of Manitoba by Yannick Leandre Traore under the supervision of Dr. Emmanuel Ho. Yannick Leandre Traore designed, performed, completed the data analysis and wrote the manuscript with assistance from Dr. Emmanuel Ho. Dr. Jijin Gu provided intellectual input and Miral Fumakia helped with data collection and manuscript

drafting and editing.

Citation:

Yannick L Traore, Miral Fumakia, Jijin Gu and Emmanuel A Ho. Dynamic mechanical behaviour of nanoparticle loaded biodegradable PVA films for vaginal drug delivery. *Journal of Biomaterials Applications* 2018, Vol. 32(8) 1119–1126 DOI: 10.1177/0885328217739451

### **Research presented in Chapter 3:**

This research was conducted at the University of Manitoba by Yannick Leandre Traore under the supervision of Dr. Emmanuel Ho. Yannick Leandre Traore designed, performed, completed the data analysis and wrote the manuscript with assistance from Dr. Emmanuel Ho. Dr. Yufei Chen contributed to study design, performed the cytotoxicity study of hydroxychloroquine on Sup-T1 cells, VK2/E6E7, and ECT-1/E6E7. He also helped with manuscript editing. Dr. Anne-Marie Bernier helped with intellectual input, study designed, and manuscript editing.

Citation:

Yannick Traore, Yufei Chen, Anne-Marie Bernier, and Emmanuel A. Ho. Evaluating the Impact of Hydroxychloroquine-Loaded Polyurethane Intravaginal Rings on Lactobacilli. 2015 *Antimicrob Agents Chemother* 59:7680–7686. doi:10.1128/AAC.01819-15.

#### **Research presented in Chapter 4:**

This research was conducted at the University of Waterloo by Yannick Leandre Traore under the supervision of Dr. Emmanuel Ho. Yannick Leandre Traore designed, performed, completed the data analysis, and wrote the manuscript with assistance from Dr. Emmanuel Ho. Dr. Yufei Chen helped with the study design. Fernanda Padilla helped with the data collection of the pH-responsive film dissolution study.

#### **Citation:**

Yannick Leandre Traore, Yufei Chen, Fernanda Padilla and Emmanuel A. Ho. Segmented intravaginal ring for the combination delivery of hydroxychloroquine and anti-CCR5 siRNA nanoparticles as a potential strategy for preventing HIV infection. *Drug Delivery and Translational Research* 2021 (Currently In Press)

As lead author of these four chapters, I was responsible for contributing to conceptualizing study design, collecting and analysing data, drafting and submitting manuscripts. My coauthors provided guidance and feedback on draft manuscripts.

## Abstract

Patient compliance is very important and highly depends on the drug dosage form which correlates with the success of therapy. Drug delivery systems can be adapted to different pharmaceutical ingredients and to different delivery routes depending on the application. This thesis focuses on the development and characterization of different types of drug delivery systems with a focus on stimuli-responsive biomaterials. Stimuli-responsive biomaterials are a promising approach for achieving on-demand drug release. They are intended to deliver their active compound at the appropriate time and site of action in response to specific triggers. The aim of this thesis was the development and characterization of a pH-responsive intravaginal ring (IVR) and a thermo-responsive wound dressing. The IVR is intended for the prevention of HIV infection while the wound dressing is to treat chronic wounds that develop as a co-morbidity associated with immune-compromised patients.

The behavior of polyvinyl alcohol (PVA) films containing nanoparticles (NPs) for vaginal drug delivery was evaluated first. In this study, we demonstrated that the amount of NPs had little effect on film dissolution and on the storage and loss modulus. However, the percentage of PVA used and the amount of plasticizer (polyethylene glycol) and carrageenan (a film forming agent) greatly affected the physico-mechanical properties of the film and play an important role in film dissolution time and nanoparticle (NP) release.

Secondly, we fabricated an IVR with polyurethane HP-60D-35 containing hydroxychloroquine (HCQ) as a prevention strategy against HIV. The safety of the IVR and HCQ were assessed on the vaginal epithelial cells VK2/E6E7, the ecto-cervical cells ECT1 and more importantly, on vaginal normal microflora *Lactobacillus crispatus* and *jensenii*. No significant

toxicity was observed.

We then designed a segmented IVR with half of the ring delivering HCQ while the second-half was coated with a pH-responsive polymer to deliver anti-CCR5 siRNA NPs. HCQ was released continuously for over 25 days with a mean daily release of  $31.17 \pm 3.06$   $\mu\text{g/mL}$ . Anti-CCR5 siRNA NPs were released from the pH-responsive coated segment only when the pH was 7.3 (e.g. in the presence of simulated seminal fluid) with a total release of  $5.12 \pm 0.9$  mg compared to vaginal fluid simulant alone ( $0.42 \pm 0.19$  mg). Anti-CCR5 siRNA NPs knocked down CCR5 gene expression by  $83 \pm 5.1\%$  in vitro in the CD4<sup>+</sup> T-cell line Sup-T1.

In the second part of the thesis, we made a thermo-responsive wound dressing using gelatin crosslinked with chitosan. LL37 and vancomycin were encapsulated into solid lipid nanoparticles (SLN) and mixed into the gelatin-chitosan hydrogel. The hydrogel itself liquefied rapidly (30min) at 33°C (human skin temperature) than at room temperature (remained semisolid). We evaluated LL37/vancomycin-SLN using a microtiter plate-based biofilm assay formed using *S. aureus*. 6mg/mL of LL37/vancomycin was capable of significantly reducing *S. aureus* biomass. Overall, the development of stimuli-responsive drug delivery systems is appealing as it can release drugs only when needed, which will reduce toxicity and unwanted side-effects. Furthermore, it can potentially improve patient compliance resulting in improved therapeutic efficacy.



## **Acknowledgments**

I would like to sincerely express my gratitude to my supervisor Dr. Emmanuel A. Ho for his constant support and guidance. I wouldn't be able to make it that far without his mentorship. I am so grateful to him for believing in me and inspiring me to become a great scientist. I am extremely honored and feel very lucky to be under his mentorship. His contagious enthusiasm for research made a significant impact in my life and made me the person I am today who is aspiring to be a great leader tomorrow. I will forever be grateful.

I would like to thank the members of my Ph.D. committee, Dr. Shawn Wettig and Dr. Brian Dixon for their constructive criticism throughout the years. I am grateful to my external examiner Dr. Afsaneh Lavasanfar and Dr. Jonathan Blay for been part of my examining committee. I would like to express my gratitude to my former committee members from the University of Manitoba Dr. Frank Burczynski and Dr. Song Liu. They helped me jump-start my Ph.D. research. I am thankful to Dr. Anne-Marie Bernier for all her support throughout my undergraduate and graduate studies. I am sincerely thankful to all my colleagues from Laboratory for Drug Delivery and Biomaterials for their support through all those years. Special thanks to Dr. Yufei Chen for all the knowledge he passed down to me and his friendship. I am grateful to Dr. Sidi Yang for all the training and advice on nanoparticle preparation and gene knockdown and her friendship. Thank you to Dr. Jijin Gu for all the training he provided me. I would like to thank Miral Fumakia for her wonderful friendship and her great support throughout my graduate studies. Thanks to Dr. Seungil Kim for all your help and support. Last but not least, I would like to thank all the summer students and co-op students, Fernanda Padilla, Vincent Jiminez, Gabriel Luo, Benita Patel, HyoJin Son, and Jennifer Rett who helped me with my projects throughout my graduate studies.

I am grateful to the Ontario Graduate Scholarship, Natural Sciences and Engineering Research Council of Canada, and University of Waterloo scholarships for their financial support.

## **Dedication**

I would like to dedicate this thesis to my parents Etienne and Marguerite Traore. Thank you for always believing in me and for your unconditional love and support. Thanks to my sisters Carine and Geraldine for all your support.

## Table of Contents

Examining Committee Membership .....	ii
Author's Declaration .....	iii
Statement of Contributions .....	iv
Abstract .....	vii
Acknowledgments.....	ix
Dedication .....	xi
List of Figures .....	xix
List of Tables .....	xxi
List of Abbreviations .....	xxii
Chapter 1: Introduction .....	1
1.1. HIV infection .....	2
1.1.1. Human immunodeficiency virus.....	2
1.1.2. Epidemiology .....	3
1.1.3. HIV transmission .....	3
1.1.4. HIV entry into target cells.....	5
1.1.5. Viral replication cycle.....	6
1.1.6. Clinical sign of infection.....	7
1.1.7. Sex differences in HIV infection .....	8
1.1.8. Current state of microbicide development.....	9
1.1.8.1. HIV prevention strategies .....	9

1.1.8.1.1. An overview .....	9
1.1.8.1.2. Preexposure and postexposure prophylaxis.....	9
1.1.8.1.3. Induction of T Cell immune quiescence at the FGT as a preventative strategy .....	12
1.1.8.1.4. Passive immunization.....	13
1.1.8.2. Microbicide dosage forms.....	14
1.1.8.2.1. Vaginal and rectal formulations .....	14
1.1.8.2.2. Vaginal films and gels .....	16
1.1.8.2.3. Intravaginal ring .....	17
1.1.8.2.4. Rectal microbicides .....	19
1.1.8.2.5. Nanotechnology-based systems.....	20
1.1.8.2.6. Stimuli-responsive formulations.....	22
1.1.8.2.7. Electrospun fibers .....	23
1.1.8.2.8. Modified microbiota for microbicide drug delivery.....	24
1.1.8.2.9. Challenges in microbicide drug delivery .....	27
1.1.9. Intravaginal ring design .....	31
1.1.9.1. Discreet use of IVR for women and adherence .....	32
1.1.9.2. Effect of intravaginal ring on vaginal mucosa and biofilm formation.....	33
1.1.10. Gene therapy as a potential strategy for preventing HIV infection .....	34
1.1.10.1. Mechanism.....	35
1.1.10.2. siRNA-directed inhibition of HIV-1 infection.....	35
1.1.10.3. siRNA delivery vehicle in the vaginal mucosa.....	37
1.1.10.4. pH-responsive polymers .....	38

1.2.	Immunocompromised patients and chronic wounds.....	39
1.2.1.	Chronic Wound.....	39
1.2.2.	Physiology of wound healing.....	40
1.2.3.	Chronic wound vs Acute wound.....	41
1.2.4.	Biofilms and inflammation in chronic wounds.....	42
1.2.5.	Thermo-responsive polymer scaffold .....	45
1.3.	Project rationale, hypothesis and objectives. ....	46
Chapter 2: Dynamic mechanical behaviour of nanoparticle loaded biodegradable PVA films for vaginal drug delivery .....		
		50
2.1.	Abstract.....	51
2.2.	Introduction.....	52
2.3.	Materials and Methods.....	53
2.3.1.	Preparation of nanoparticle-loaded film .....	54
2.3.2.	Dynamic mechanical analysis.....	54
2.3.3.	Determination of the glass transition temperature ( $T_g$ ).....	55
2.3.4.	Determination of storage and loss modulus.....	55
2.3.5.	In vitro drug release .....	56
2.3.6.	Determination of mechanical properties.....	56
2.3.7.	Scanning electron microscopy .....	56
2.4.	Statistical analysis.....	57
2.5.	Results.....	57
2.6.	Discussion.....	66

2.7. Conclusion .....	70
Chapter 3: Evaluating the impact of hydroxychloroquine-loaded polyurethane intravaginal rings on lactobacilli.....	
3.1. Abstract.....	72
3.2. Introduction.....	72
3.3. Materials and Methods.....	74
3.3.1. Materials .....	74
3.3.2. Fabrication of IVRs.....	75
3.3.3. HCQ/HPMC semi-solid preparation and HCQ extraction.....	76
3.3.4. HPLC Method.....	77
3.3.5. In vitro release studies .....	77
3.3.6. Sensitivity test of HCQ on Lactobacilli, vaginal/ectocervical epithelial and immune cells .....	78
3.3.7. Cytotoxicity evaluation of IVR segments on lactobacilli and vaginal/ectocervical cell lines .....	79
3.3.8. In vitro evaluation of IVR segments on vaginal epithelial cell layer integrity .....	80
3.4. Results.....	81
3.4.1. In vitro release studies .....	81
3.4.2. Sensitivity test of HCQ on Lactobacilli, vaginal/ectocervical epithelial and immune cells .....	84
3.4.3. Cytotoxicity evaluation of IVR segments on lactobacilli and vaginal/ectocervical epithelial cell lines .....	86

3.4.4. Assessment of transepithelial electrical resistance (TEER) of VK2/E6E7 .....	88
3.5. Discussion.....	89
Chapter 4: Segmented intravaginal ring for the combination delivery of hydroxychloroquine and anti-CCR5 siRNA nanoparticles as a potential strategy for preventing HIV infection.....	94
4.1. Abstract.....	95
4.2. Introduction.....	96
4.3. Materials and Methods.....	100
4.3.1. Materials .....	100
4.3.2. IVR fabrication .....	101
4.3.3. HCQ loading in reservoir-type IVR.....	101
4.3.4. Nanoparticle fabrication.....	102
4.3.5. pH-responsive coating preparation .....	103
4.3.6. In vitro release studies from the reservoir-type and matrix-type IVR segment.....	104
4.3.7. In vitro cytotoxicity studies of IVR containing NPs.....	105
4.3.8. In vitro CCR5 gene knockdown study .....	106
4.4. Results.....	108
4.4.1. IVR fabrication. ....	108
4.4.2. NP fabrication. ....	109
4.4.3. pH-responsive coating preparation .....	109
4.4.4. In vitro release.....	112
4.4.5. Determination of the in vitro cytotoxicity of IVR containing SLNs .....	114
4.4.6. In vitro CCR5 downregulation study .....	115



4.5.	Discussion .....	117
4.6.	Conclusion .....	121
Chapter 5: Thermo-responsive hydrogels for reducing biofilm formation on chronic wounds.		123
5.1.	Introduction.....	124
5.2.	Materials and Methods.....	127
5.2.1.	Materials .....	127
5.2.2.	Solid lipid nanoparticles preparation. ....	128
5.2.3.	Hydrogel preparation .....	128
5.2.4.	C6 SLNs release study from hydrogel.....	129
5.2.5.	Preparation of microtiter plate-based biofilm model .....	129
5.2.6.	Quantification of the biofilm using crystal violet and resazurin assays .....	130
5.2.7.	Biofilm treatment with SLNs containing LL37 and vancomycin.....	131
5.3.	Results.....	131
5.3.1.	Solid lipid nanoparticles preparation. ....	131
5.3.2.	Hydrogel preparation .....	132
5.3.3.	C6 SLNs release study from the gelatin-chitosan formulation. ....	134
5.3.4.	Quantification of the biofilm using crystal violet and resazurin assays .....	135
5.3.5.	Biofilm treatment with SLNs containing LL37 and Vancomycin.....	137
5.4.	Discussion: .....	138
5.5.	Conclusion .....	141
Chapter 6: Conclusion.....		142
6.1	Significance of the study.....	143

6.2	Summary of results .....	145
6.3	Future directions. ....	147
	References.....	150

## List of Figures

Figure 1.1: Potential activity of microbicides to prevent HIV infection. ....	15
Figure 1.2: Schematic of the CCR5 expression inhibition by siRNA .....	36
Figure 2.1: Determination of storage and loss modulus of film samples (Plot from DMA analysis software) .....	59
Figure 2.2: Determination of storage and loss modulus of film samples. ....	60
Figure 2.3: In vitro cumulative release of 2% and 5% PVA films loaded with 3mg or 5mg fluorescent NPs. (A) Amount of NP released (B) Percentage of NPs released.....	63
Figure 2.4: Tensile strain of 2% and 5% PVA films loaded with 3 mg or 5 mg of NPs .....	65
Figure 2.5: SEM images of 2% and 5% PVA films containing 3 mg or 5 mg of NP loading (2000 X). ....	66
Figure 3.1: Aluminum mold for the fabrication of reservoir-type IVR segments .....	76
Figure 3.2: Release study of HCQ in sodium acetate from PU-93A .....	82
Figure 3.3: Release study of HCQ in sodium acetate and MRS broth .....	83
Figure 3.4: The effects of 24 h HCQ treatment on vaginal normal flora, vaginal ecto-cervical and epithelial cells and CD4+ immune cells. ....	85
Figure 3.5: Elution assay on <i>Lactobacillus crispatus</i> and <i>jensenii</i> and vaginal cells VK2/E6E7 and Ect1/E6E7 .....	87
Figure 3.6: Cytotoxicity study from HCQ released from IVR segment on <i>Lactobacillus crispatus</i> and <i>jensenii</i> . ....	88
Figure 3.7: Evaluation of TEER on a monolayer of VK2/E6E7 cells. ....	89
Figure 4.1: SLN preparation and conjugation to anti-CD4 antibody.....	103
Figure 4.2: Segmented intravaginal ring (IVR). ....	108

Figure 4.3: HCQ release in VFS .....	113
Figure 4.4: Release of C6-SLNs in VFS and SFS. ....	114
Figure 4.5: Cytotoxicity evaluation of IVR coated with Eudragit L100 on VK2/E6E7 epithelial vaginal cells .....	115
Figure 4.6 Evaluation of CCR5 gene expression using real-time PCR .....	116
Figure 4.7: Evaluation of coated IVR segment on CCR5 knockdown .....	117
Figure 5.1: Picture of lyophilised 3% gelatin at 25°C and at 33°C after 25 min.....	133
Figure 5.2: Amount of C6 NP Released Over Time.....	134
Figure 5.3: Percentage cumulative release of C6-SLN over time .....	135
Figure 5.4: Assessment of <i>S. aureus</i> biomass using 0.05% crystal violet in a 96-well plate .....	136
Figure 5.5: Evaluation of living <i>S.Aureus</i> bacteria present in the biofilm using resazurin .....	136
Figure 5.6: Biofilm treatment with LL37/vancomycin-SLNs .....	137

## List of Tables

Table 1.1 Milestone PrEP clinical trials .....	11
Table 1.2: Engineered microbiota as microbicides to prevent HIV infection .....	26
Table 1.3. Other Novel HIV prevention strategies evaluated pre-clinically or in clinical trials ..	29
Table 2.1: Glass transition temperature determined using two different parameters .....	61
Table 2.2: Disintegration time for PVA films. ....	61
Table 4.1: CCR5 siRNA-encapsulated SLN size, zeta potential, and encapsulation efficiency.	109
Table 4.2: Eudragit L100 properties in different organic solvents and their impact on polyurethane.....	110
Table 4.3: Impact of varying amounts of Eudragit L100 and PEG 400 dissolved in isopropanol on film formation. ....	111
Table 4.4: Eudragit L100 film disintegration time .....	111
Table 5.1: LL37-Vancomycin SLN characterisation.....	132
Table 5.2: Gelatin hydrogel phase transition. ....	133
Table 5.3: Liquefaction time of different ratio of gelatin/chitosan.....	133

## List of Abbreviations

Ago:	argonaute 2
AIDS:	acquired immunodeficiency syndrome
AMP:	anti-microbial peptide
API :	pharmaceutical active ingredient
ARV:	antiretroviral
ASA:	acetylsalicylic acid
bNAbs :	broadly neutralizing antibodies
BSA:	bovine serum albumin
BV:	bacterial vaginosis
C6:	coumarin 6
CAD:	computer aid design
CCR5:	chemokine receptor type 5
CD38:	cluster of differentiation 38
CD4:	cluster of differentiation 4
CD69:	cluster of differentiation 69
cDNA:	complementary DNA
CV:	crystal violet
CXCR4:	chemokine receptor type 4
DMA:	dynamic mechanical analyzer
DNA:	deoxyribonucleic acid
DPV:	dapivirine
DSPE PEG:	1,2-distearoyl-sn-glycero-3-phosphoethanolamine-poly(ethylene glycol)

dsRNA:	double-stranded RNA
ECM:	extracellular matrix
EDC:	1-ethyl-3-(3-dimethylaminopropyl) carbodiimide
EDTA:	ethylenediaminetetraacetic acid
EPS:	extracellular polymeric substance
EVA:	ethylene-co-vinyl acetate
FBS:	fetal bovine serum
FDA:	Food and Drug Administration (United State)
FGT:	female genital tract
FTC:	emtricitabine
Gag:	HIV group-specific antigen
GAPDH:	glyceraldehyde 3-phosphate dehydrogenase
gp120:	glyco-protein 120 kilodalton
HAART:	highly active antiretroviral therapy
HCQ:	hydroxychloroquine
HEC:	hydroxyethyl cellulose
HESN:	HIV-exposed seronegative
HIV:	human immunodeficiency virus
HLA-DR:	human leukocyte antigen – DR
HMA:	human microbiota-associated
HPLC:	high-performance liquid chromatography
HPMC:	hydroxypropyl methylcellulose
IVR:	intravaginal ring

K-SFM:	keratinocyte-(serum-free medium)
LCST:	lower critical solution temperature
MES:	2-(N-morpholino) ethanesulfonic acid
miRNA:	micro-RNA
MMP:	matrix metalloproteases
mRNA:	messenger RNA
MRS :	Man, Rogosa & Sharpe
MSM:	men who have sex with men
MTP:	microtiter plate-based
MTS:	3-(4,5-dimethylthiazol-2-yl)-5-(3-carboxymethoxyphenyl)-2-(4-sulfohenyl)-2H-tetrazolium
N9:	nonoxynol-9
NHS:	N-hydroxysuccinimide
NK:	natural killer
NNRTI:	non-nucleoside reverse transcriptase inhibitor
NP:	nanoparticle
NP-Ab:	antibody-conjugated NP
PBMC:	peripheral blood mononuclear cells
PBS:	phosphate-buffered saline
PEG:	polyethylene glycol
PEI:	polyethylenimine
Pep:	post-exposure prophylaxis
PIC:	pre-integration complex



PLGA:	poly(lactic-co-glycolic acid)
PrEP:	pre-exposure prophylaxis
PU:	polyurethane
PVA:	polyvinyl alcohol
RISC:	RNAi-induced silencing complex
RNA:	ribonucleic acid
RNAi:	RNA interference
ROS:	reactive oxygen species
RPMI:	Roswell Park Memorial Institute media
RT:	reverse transcriptase
RT-PCR:	real-time polymerase chain reaction
SC:	subcutaneous
SD:	standard deviation
SEM:	scanning electron microscopyFD
SFS:	seminal fluid simulant
shRNA:	short hairpin RNA
siRNA:	short interfering RNA
SIV:	simian immunodeficiency virus
SLN:	solid lipid nanoparticle
TDF:	tenofovir disoproxil fumarate
TEER :	trans-epithelial electric resistance
TFV:	tenofovir
TIMP:	tissue inhibitors metalloproteinases

TSB: tryptic soy broth  
UCST: upper critical solution temperature  
VCF: vaginal contraceptive film  
VFS: vaginal fluid simulant

## **Chapter 1: Introduction**

The first part of the introduction was adapted from the following scientific article:

Yannick Traore, Yufei Chen, Emmanuel A. Ho *Clinical Pharmacology & Therapeutics*,

2018 104(6):1074-1081 Vol. [doi.org/10.1002/cpt.1212](https://doi.org/10.1002/cpt.1212)

## **1.1. HIV infection**

### **1.1.1. Human immunodeficiency virus**

Human immunodeficiency virus (HIV) keeps spreading among vulnerable and resource-limited populations worldwide. HIV is an enveloped lentivirus, member of the family retroviridae [1], and replicates using reverse transcription. HIV-1 and HIV-2 are two closely related but different strains of HIV that can induce acquired immunodeficiency syndrome (AIDS). Both originate from the parent virus simian immunodeficiency virus (SIV) [2]. HIV-1 and HIV-2 share 30-60 % of their genome but have comparable genomic organization [3]. They have similar transmission routes and the capacity to bind CD4 molecules on immune cells, but HIV-2 infection is much slower than HIV-1 [4]. HIV-2 is much less virulent hence bearing the definition of long-term non-progressors disease that keeps the viral load under the limit of detection [5]. The CD4 T cell counts are maintained in the normal range for decades, and less CD4 T cell activation has been reported in HIV-2 patients [6, 7]. The resistance of dendritic cells and the reduced rate of replication in macrophages may explain the moderate infection of HIV-2 compared to HIV-1 [8]. The focus of this thesis will be on HIV-1, the most common virus found in HIV-positive patients. HIV-1 infection originated in Central Africa [9]. HIV-1 is subdivided into different groups listed as M, N, O, and P. The most virulent group is the M which is further subdivided and represented by the letters A to K [10]. HIV-1 spreads by sexual intercourse, neonatal and percutaneous routes. More than 80% of adults infected by HIV-1 occur sexually, thus making sexual intercourse the main infection route for the virus [11].

### **1.1.2. Epidemiology**

It has been estimated that in 2019, more than 38 million people lived with HIV in the world. Approximately 96% of people that acquired HIV-1 infection live in developing countries [12]. Many efforts have been made to further reduce the infection rate in the past decade, but still, around 690 000 people died from HIV in 2019 [12]. Those numbers are not negligible, so many efforts have to be made to further decrease HIV incidence in the world. Investigations into sub-Saharan Africa revealed that there is a decrease in condom usage, but an increase in sexual intercourse among young people [13]. There was also no reduction in the transmission of HIV among sex workers or in homosexual partners over time [13]. Sexual intercourse is the most common HIV transmission route with injection drug users being second. For example, in Asia, more than 28% of HIV-infected people are drug users [13]. A lot of effort must be done to reduce HIV incidence.

### **1.1.3. HIV transmission**

HIV-1 utilizes three major infection routes including sexual contact across mucosal surfaces, mother-to-infant transmission and percutaneous inoculation [14]. Heterosexual transmission accounts for more than 70% of HIV infection, which is much greater than men having sex with men and mother-to-child infections [14]. The genital and the gastrointestinal tract are the primary infection sites for HIV. They are rich in HIV target cells such as primary T cells, dendritic cells and macrophages [11]. The female genital tract (FGT) and the ectocervix offer a larger surface area that provides more possibility for HIV entry even though the squamous epithelium layers that cover their surface offer a tremendous physical barrier against HIV entry. The endocervix constitutes only one layer of columnar epithelium and will allow easy passage of the virus. There is an abundant population of T-cells in the junction where the ectocervix transitions into the endocervix, offering an ideal site for virus entry [15]. The upper vaginal tract may become

more susceptible to HIV penetration during ovulation marked by an increase in estrogen level [15]. The mucus present in FGT is intended to block the virus movement, but this can also present as a downside by keeping the virus longer within the vaginal tract increasing infection [16]. Free HIV virion released into the mucosa by an infected donor crosses the epithelial barrier by transcytosis, endocytosis, followed by exocytosis. A free virion can also penetrate through the gaps between epithelial cells causing an active infection. Even though HIV has more affinity for immune cells, it can also penetrate into epithelial cells in the mucosa via transcytosis. Thus, HIV can find a path through the cervicovaginal epithelium to the draining lymphatic via transport by lymphocytes and macrophages [17]. It has been shown that within 30-60 min of exposure, HIV can penetrate the cervicovaginal epithelium. The primary host for HIV infection are CD4<sup>+</sup> T cells and Langerhans cells in the FGT. Langerhans cells also called dendritic cells can project their dendrites through the intercellular spaces of the vaginal epithelium and appear at the surface. Free virion can promptly bind to those dendrites and infect the cells [18]. During sexual intercourse, mechanical tearing of the cervicovaginal epithelium will increase access of HIV to its target cells, located in the basal epithelium underlying the stroma [18]. Infectious micro-organisms like herpes simplex virus or syphilis can create genital ulcers and inflammation leading to a gathering of HIV target cells and facilitate the entry of the virus through the epithelium and further to the lymph node. For example, the popular spermicide nonoxynol-9 (N9) has been used as a contraceptive and evaluated for its anti-viral properties against the herpes simplex virus and HIV. Unfortunately, N9 can induce an inflammatory response within the FGT attracting more immune cells increasing viral infection rates [19, 20].

The male genital tract is also a site of HIV entry. The mechanism of HIV uptake is similar to the FGT uptake. Removal of the foreskin during circumcision will significantly reduce HIV

target cells making the virus entry more difficult [21]. The surface of the penis is covered by a keratinized squamous epithelium that presents a great physical barrier for HIV entry, but the urethra is covered by a non-keratinized epithelium that shows the same weaknesses as the female cervicomucosa [22].

#### **1.1.4. HIV entry into target cells.**

HIV target cells are essentially T cells, macrophages, and dendritic cells. HIV binds to its target cells using a portion of its envelope called gp120 (glyco-protein 120 kilodalton). When gp120 interacts with the cell surface receptor CD4, it will create new rearrangements of gp120 loops that will allow the binding to a co-receptor, the chemokine receptor type 5 (CCR5), or to the chemokine receptor type 4 (CXCR4). Once gp120 binds to CD4, a portion of the virus envelope called gp41 will be inserted into the host membrane and create a fusion of the viral envelope and the plasma membrane of the cell [23].

The Langerhans cells present in the sub-mucosa of the genital tract express the HIV receptor CD4, CCR5 and the C-type lectin receptor (plays a major role in cell adhesion and endocytosis) but not CXCR4. The internalization of the virus seems to be mostly through Langerhans cells where it is picked up by endocytosis and released to the other side of the epithelium to be picked up by other HIV target cells such as lymphocytes [24]. Langerhans cells can harbour the virus and transfer it to virus-free T-cells causing its activation [25]. CD4<sup>+</sup>T cells are found in the connective tissue lying beneath the epithelium known as lamina propria of the human vagina, and below the ectocervix and endocervix[26]. Most of them are memory T cells with a higher expression of the surface receptor CCR5 compared to the T cells found in the blood [27]. Hladik et al. found that within 2 hours after exposure to a virion, it can bind to the vaginal CD4<sup>+</sup>T cell and begin fusion [28]. This implies that ideal therapy against HIV-1 infection should

be effective within 1-2 hours of exposure from an infected donor. Active T-cells present at their surface a MHC II cell surface receptor called HLA-DR. An active T-cell presenting HLA-DR (HLA-DR<sup>+</sup>) receptor will have more affinity for HIV and increased susceptibility to viral infection. Studies have shown that even resting T-cells not presenting HLA-DR can fuse with HIV virion. Resting T cells (HLA-DR<sup>-</sup>) have also been reported to play an essential role in the early stages of HIV infection but are less susceptible to infection than HLA-DR<sup>+</sup> cells [29]. Macrophages are a target of HIV in the initial infection but to a lesser extent than T cells and they are the primary target cells for HIV strains that use the co-receptor CCR5 and CXCR4 [30]. Monocyte-derived macrophages can internalize HIV by a process called macropinocytosis without the intervention of any specific cell surface receptor and store the virus for several days transmitting to T cells. The virion can also penetrate those monocytes using syndecans that are single transmembrane domain protein that enables the interaction with diverse ligands and HIV-1 gp120 protein [15]. Natural Killer (NK) cells and B lymphocytes have also been reported to transmit HIV to T cells in trans infection [31, 32].

#### **1.1.5. Viral replication cycle.**

The envelope of the virus fuses with the plasma membrane of host cells, allowing all of its contents to be released in the cytoplasm of the host cell including its genome and proteins. The genome of the virus is double-stranded RNA. Upon its transfer into the host cytoplasm, the genome is reverse transcribed into complementary DNA (cDNA) using reverse transcriptase (RT). The reversed transcription process will follow with the formation of the pre-integration complex (PIC) that will then be translocated into the nucleus. Inside the nucleus, the double-stranded DNA will merge with host genome using a viral protein called integrase. The machinery of the cell will carry on a regular cell division cycle with the genome of the virus integrated. The genome of the virus



can be silent in the host and multiply while remaining latent. To infect other cells, the provirus may be reactivated [33]. The viral genome is used to translate mRNA into viral proteins and genome. All the essential viral proteins will be fabricated using the host machinery. The virion components after being translated into proteins will be transported to the plasma membrane for the assembly. Once the entire parts are together, new virions will bud at the plasma membrane where they acquired their lipid envelope. Each newly created virus is composed of 3 major elements, which are the envelope, the viral proteins and the capsid that contains the viral genome [34].

#### **1.1.6. Clinical sign of infection**

After HIV-1 infection, the virus will undergo the eclipse phase where it will not be detectable in the blood but multiply in immune cells. After 1 or 2 weeks, the virus will reach the lymph node and the gut-associated lymphoid tissue where there is an important number of CD4<sup>+</sup> cells that will be infected, followed by mass production of virions [35]. The acute phase of HIV infection occurs when the viral markers are detectable in the blood, followed by massive death of CD4<sup>+</sup> T lymphocytes due to apoptosis or pyroptosis [35]. The chronic phase is the last phase of HIV infection and last 10 to 20 years. During this phase, both immune cells and the virus replicate with a continuous depletion of the number of CD4<sup>+</sup> T lymphocytes. The CD4<sup>+</sup> T lymphocyte count is crucial to distinguish the severity of the disease. CD4<sup>+</sup> T lymphocyte counts < 200 cells/ $\mu$ l signifies a patient with severely compromised health increasing susceptibility to opportunistic infections like tuberculosis [36]. These opportunistic diseases are usually the cause of death for HIV-positive patients. This late phase is called AIDS (Acquired immunodeficiency syndrome).

### **1.1.7. Sex differences in HIV infection**

The UNAIDS reported that 52% of HIV-infected persons are women. In the same report, it is mentioned that the percentage of women aged 15-24 infected with HIV is twice that of young men. After decades of research on AIDS, gender consideration is now a prime concern in an effort to stop the spread of the virus and the application of an effective treatment [13]. Women are more exposed to HIV than men for biological and socio-cultural reasons. The mucosal surface area of the FGT is greater than the male genital tract increasing exposure to HIV. Furthermore, semen remains longer within the FGT leading to a higher vulnerability. In developing countries, women are most of the time unable to negotiate condom usage, fearing a violent retort from their partners [37]. A young girl in the third world is more likely to marry an older HIV-positive man who is already in a polygamous relationship. The lack of education for girls in those countries makes them less aware of HIV infection and the different protection strategies [38, 39]. Well-educated women will be able to make their own choices regarding their sexual life. Protecting women from HIV will help decrease the number of HIV-born children via mother-to-child transmission. Most children are infected by their mothers during pregnancy, labour or breastfeeding. A promising study has shown that the rate of mother-to-child transmission has declined in developed countries because of the availability of drugs that can protect the child during the pregnancy [40]. Microbicide development for women is an encouraging strategy that will significantly impact the evolution of HIV infection in the world.

## **1.1.8. Current state of microbicide development**

### **1.1.8.1. HIV prevention strategies**

#### **1.1.8.1.1. An overview**

Efforts in developing an effective vaccine for HIV-1 are challenging as HIV strains are highly variable with the capability of undergoing recombination with high error rates during the reverse transcription process [41]. These highly variable conserved regions are usually thermostable and concealed with heavy glycosylation coverage [42], leading to significant difficulties for anti-HIV antibodies to recognize and neutralize the virus efficiently. Therefore, in the absence of an effective vaccine against HIV, consistent usage of condoms is still the cornerstone of prevention. Due to the lack of condom accessibility in some developing countries and the unwillingness of condom usage by sexual partners due to socio-cultural factors, other alternative interventions have been studied to be employed as additional prevention strategies such as male circumcision and the use of antiretroviral drugs for the treatment of HIV infection [43]. These proposed biomedical prophylactic interventions include postexposure prophylaxis (PEP), preexposure prophylaxis (PrEP) [44], and more recently, the induction of T-cell immune quiescence (IQ) at the FGT [45].

#### **1.1.8.1.2. Preexposure and postexposure prophylaxis**

Thanks to advancements in antiretroviral therapy, HIV is no longer considered a terminal disease but a manageable condition that can be controlled under a long-term intervention using antiretroviral drugs. PrEP and PEP were proposed as such strategies that utilize antiretroviral drugs to prophylactically intervene in HIV infection before and after an incident of HIV viral exposure.

In a case-control study where individuals were given the prophylactic zidovudine post-viral exposure, there was an 81% reduction in infection [46]. However, due to ethical and logistical concerns, further initiation of a randomized controlled clinical trial aiming to systemically evaluate PEP regimens is considered not feasible. PrEP, on the other hand, is currently the most promising HIV prevention strategy which involves the administration of antiretroviral drugs on a daily basis to HIV-negative persons prior to potential exposure to the virus. The rationale behind PrEP is to inhibit viral replication immediately after viral exposure, resulting in the abolishment of the infection (Table 1.1). Two promising nucleoside/nucleotide reverse transcriptase inhibitors, tenofovir (TFV) and emtricitabine (FTC), showed high effectiveness and toleration in HIV treatment with evidential HIV prevention effects in clinical studies. As a result, this combination treatment is now sold under the brand name Truvada<sup>®</sup> and approved for PrEP against HIV. However, it should be kept in mind that the most important prerequisite to maintain PrEP efficacy is to achieve high levels of drug adherence as shown in failed clinical trials such as FEM-PrEP [47] and VOICE [48] trials, where both trials had poor patient adherence of <40% and <30%, respectively. Thus, to improve drug concentrations at the FGT and increase patient adherence, other PrEP-derived prophylaxis interventions are currently being explored for both males and females.

**Table 1.1 Milestone PrEP clinical trials**

<b>Clinical Trial</b>	<b>Study Population</b>	<b>Mode of HIV Infection</b>	<b>Regimen</b>	<b>Estimated Efficacy of HIV Prevention (%)</b>	<b>Ref</b>
TDF2 trial	Heterosexual men and women	Vaginal or penile	Truvada®; once oral daily	63%	[49]
Partners PrEP trial	Heterosexual men and women	Vaginal or penile	TDF (200 mg) only; TDF (300 mg) + FTC (200 mg); once oral daily	67% in TDF only arm; 75% in TDF/FTC arm	[50]
iPrEx trial	MSM and transgender women	Rectal	Truvada®; once oral daily	44%	[51]
PROUD trial	MSM	Rectal	TDF (245 mg) + FTC (200 mg); once oral daily	86%	[52]
Bangkok TFV trial	Injection drug users	Vaginal or penile	TFV (300 mg); once oral daily	49%	[53]
FEM-PrEP trial	Women	Vaginal or penile	Truvada®; once oral daily	stopped early due to lack of efficacy	[47]

Abbreviations: FTC, emtricitabine; MSM, men who have sex with men; TDF, tenofovir disoproxil fumarate; TFV: tenofovir

### **1.1.8.1.3. Induction of T Cell immune quiescence at the FGT as a preventative strategy**

Elevated immune activation systemically and locally at the FGT [54] is one of the hallmarks during HIV infection. The resulting systemic and local mucosal inflammation can significantly contribute to the progression of HIV transmission, which is usually represented by increased immune cell activation (activated HIV-target cells such as T cells, dendritic cells, etc.) coupled with elevated production of pro-inflammatory mediators [54]. Activated immune cells are necessary for HIV replication and are more prone to HIV infection compared to their resting counterparts [45]. However, a lower base level of immune activation was observed in some HIV-exposed seronegative (HESN) individuals who are naturally resistant to HIV-1 infection [45]. T cell IQ status was observed in these HESN individuals [45] which showed lower expression of T cells activation markers such as CD69, CD38, HLA-DR, Ki67, and CCR5. At the same time, it is found that these individuals with high levels of quiescent T cells are still able to initiate normal antigenic and mitogenic responses [55]. Therefore, if T cell IQ can be pharmacologically induced at local HIV transmission sites such as the FGT, it may inhibit local HIV infection due to decreased availability of activated T cells leading to less productive transmission and replication of HIV. Eventually, the clearance of acutely infected cells may be achieved through local HIV-specific cytotoxic T cells with the assistance of regulatory T cells or other innate mechanisms [45], or by antiretroviral drug intervention. Our group recently developed a polyurethane vaginal implant delivering the immunomodulatory drug HCQ within the vaginal tract of rabbits. Our results showed that the implant was capable of attenuating pro-inflammatory mediator production and decrease gene expression of CCR5 and CD69 in isolated vaginal mucosal T cells even after challenge with the surfactant N9 [56].

#### **1.1.8.1.4. Passive immunization**

Currently, there is a lack of an effective vaccine against HIV, but passive immunization approaches using broadly neutralizing antibodies (bNAbs) against HIV administered either systemically or locally at the FGT to prevent HIV-1 infection in the vaginal mucosa has demonstrated promise in preclinical studies and early-stage clinical trials [57]. A phase 1 clinical trial utilizing a vaginal microbicide containing a combination of bNAbs 2F5, 2G12, and 4E10 formulated in a gel was recently completed, showing that 12-day vaginal delivery of 50 mg of each antibody can be achieved safely in the female participants [57]. Another phase 1 trial examined the safety and pharmacokinetics of intravenously or subcutaneously administered bNAb VRC01 over a 28-day period, revealing that VRC01 retained neutralizing activity in serum without anti-VRC01 antibody responses [58]. The efficacy of systemic delivery of VRC01 to prevent HIV infection is currently on-going with healthy women that are considered at high risk of HIV acquisition [59]. Kang et al. are currently evaluating the safety of a genetically modified and killed whole-HIV-1 in phase 1 clinical trials. The SAV001 vaccine study was safe for all participants and the antibodies produced in the plasma recognized HIV-1 envelope protein on the surface of infected cells. The antibodies exhibited broad neutralizing activity inhibiting tier I and II of HIV-1 B, D and A subtypes [60].

## **1.1.8.2. Microbicide dosage forms**

### **1.1.8.2.1. Vaginal and rectal formulations**

Microbicides are topical therapies developed to prevent HIV and other sexually transmitted infections during intercourse (Figure 1.1). Microbicides applied vaginally or rectally are intended to prevent HIV infection at the site of transmission by either preventing viral replication or inhibiting its entry into immune cells. Some possible mechanisms of action of microbicides are to hinder HIV entry into its target cells, to boost the immune system's fight against the viral infection, or prevent the virus from replicating once inside the target host cells [61].



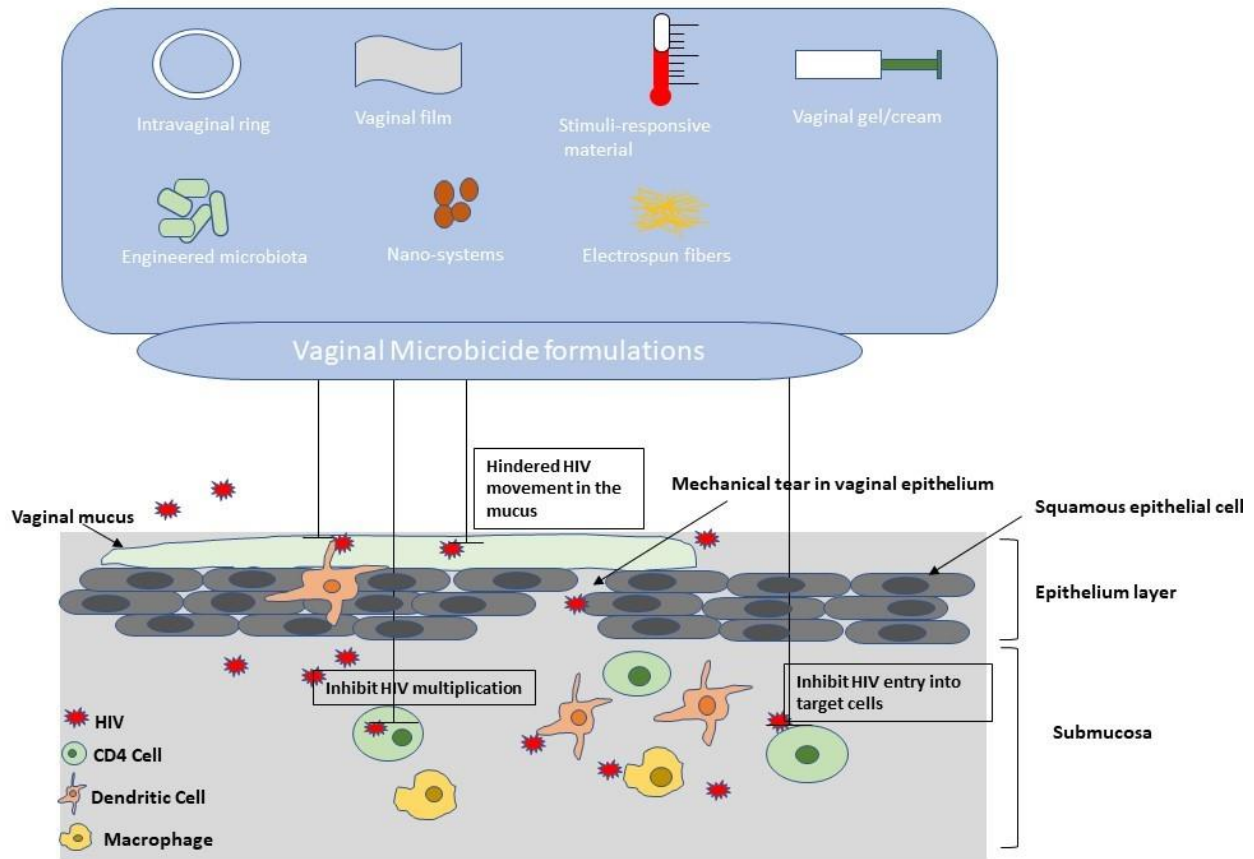


**Figure 1.1: Potential activity of microbicides to prevent HIV infection.** [62] A free virion at the mucosal surface can rapidly cross the mucosal epithelial barrier to infect its target cells. Microbicides can act at different stages of viral infection. Microbicides can hinder virus movement in the mucus prior to cell infection. Once inside the target cells, the delivery of some inhibitors like nucleoside and non-nucleoside reverse transcriptase inhibitors can prevent the virus multiplication.

#### **1.1.8.2.2. Vaginal films and gels**

Vaginal films have been formulated to deliver therapeutics in the FGT. Vaginal films are solid dosage forms that rapidly dissolve in contact with vaginal fluid, are mainly composed of polymers, plasticizers and the active therapeutic agent. The films are designed to prevent or decrease HIV infection. Two main manufacturing processes used for the fabrication of vaginal films include solvent casting and hot melt extrusion methods [61]. The latter is used only if the drug is stable at high temperatures. An example of an approved vaginal film is the contraceptive N9 film from Apothecus Pharmaceutical Corporation (VCF® Vaginal Contraceptive film). Numerous film formulations have been developed during the past several years as potential microbicides against HIV infection [63]. In a recent phase 1 clinical trial, dapivirine vaginal film was evaluated for patient compliance, safety, and drug distribution in healthy women. In this study, HIV-negative women were randomly subjected daily for seven days to either a hydroxyethylcellulose (HEC) placebo gel, 0.05% dapivirine gel, placebo film, or film containing 1.25 mg of dapivirine [64]. Researchers found that the plasma concentration of dapivirine was four  $\log_{10}$  lower than the concentration in cervical and vaginal tissue. The gel users had a higher content of the drug in the tissue but both formulations significantly reduced HIV infection *ex vivo*. Participants in the study preferred the film formulation since it is not linked to any messiness, but found the gel was easier to apply than the film. TFV film formulations have also been evaluated in a clinical setting in HESN women [65]. This study investigated a single-dose vaginal film or gel application and found that the film formulation gave a higher concentration of the drug in the plasma and vaginal tissues during the first days compared to the gel formulation, but after day 3-7, both groups demonstrated similar concentrations [65]. Unfortunately, *ex vivo* HIV challenge studies using the film or the gel formulation failed to protect against infection. The authors claim

that the failure to protect against infection is due to the decrease in drug concentration over time after a single dose regimen [65]. These studies suggest that multiple dosing with film may be necessary to maintain protective concentrations of drug before HIV challenge.

#### **1.1.8.2.3. Intravaginal ring**

IVRs, initially introduced for contraception and hormone replacement therapy, received much attention recently as novel anti-HIV microbicides to provide prolonged and controlled drug delivery [66]. IVRs are commonly fabricated using high-temperature methods such as hot-melt extrusion or hot injection molding. Thanks to the flexible choice of thermoset or thermoplastic polymers ranging from silicone, ethylene-vinyl acetate, to polyurethane [66], different pharmaceutical agents can be incorporated into IVRs in a large quantity to achieve cumulative drug release in a sustainable and predictable manner [66]. There are two major categories of conventional IVRs involving matrix-based and reservoir-based IVRs. In a matrix-based IVR system, the pharmaceutical active ingredients (APIs) are dispersed uniformly within the polymeric matrix of the IVR during the fabrication. The drug release is correlated with both drug loading and the surface area of the device and demonstrates a diffusion-permeation release mechanism [66]. In a typical reservoir-based IVR system, however, the APIs are usually formulated into a semi-solid dosage form with release rate-controlling excipients and then loaded into a semi-permeable hollow tubing, in which the drug release rate is determined by both the surface area of the device and the physico-chemical properties of the polymers used to fabricate the semi-permeable tubing and excipients used to form the drug-excipient core [67]. For example, our group developed a polyurethane IVR system capable of sustained delivery of HCQ over a two-week period that did

not present any significant cytotoxicity in vitro towards vaginal epithelial cells and vaginal flora [68, 69].

Currently, there is increased interest in multi-purpose microbicide development. Several innovative designs of IVRs targeting different pathogenesis of sexually transmitted diseases or targeting different types of sexually transmitted infections or possessing extra protection from unwanted pregnancy have been developed. For example, a pod-insertion silicone-based IVR was described to deliver five drugs simultaneously in a sheep model [70]. Each IVR carried 32 mg of TFV, nevirapine, saquinavir, and estradiol along with 20 mg of etonogestrel. The constant release of these drugs into sheep FGT was achieved over 28 days. In addition, IVRs can also be developed to allow the long-term delivery of heat-sensitive macromolecules, offering an attractive platform to develop vaginal mucosal vaccines for inducing vaginal mucosal immunity against HIV or direct delivery of HIV neutralization antibodies against HIV. McKay et al. recently described a novel antigen-releasing IVR capable of releasing human HIV-1 recombinant protein CN54gp140 and its adjuvant R848, yielding a 30-fold increase in mucosal IgA response and higher presence of antigen-specific B cells in the genital draining lymph nodes of the sheep model [71].

IVRs also offer improved user adherence in comparison to other delivery systems as it requires minimal action on the part of the user to achieve product adherence since daily, intermittent, or coitally-associated application of an active ingredient is not required [66]. An on-demand release of API IVR system was developed by Kim et al., with an insertion-type intravaginal ring with reversible pH-responsive polyurethane membranes to control drug release [72]. Very small pore sizes are observed in the membranes at vaginal pH, but larger pore size begin to appear at high basic pH, mimicking the presence of seminal fluid during sexual intercourse.

#### **1.1.8.2.4. Rectal microbicides**

Unlike vaginal microbicides that mostly protect women against HIV infection during sexual intercourse, rectal microbicides must be designed to protect both in the case of men who have sex with men (MSM) or rectal heterosexual intercourse. People engaged in receptive anal intercourse mostly do not use condoms compared to those engaged in vaginal intercourse [73]. Microbicides for rectal delivery are usually formulated as a gel, fluid (enema), or suppository. An excellent review by McGowan et al. summarized the different types of rectal microbicides and the drugs used in the formulations [73]. In this review, we will focus on current formulations that have already been completed or currently in clinical phase of testing. In terms of rectal microbicides, not many have made it to clinical trials. TFV, dapivirine, and UC-781 are the drugs that have been most evaluated. A clinical trial published in 2011 assessing the acceptability, safety and ex vivo efficacy of the reverse-transcriptase UC-781 showed some promising results [74]. Although this study did demonstrate that the gel formulation with UC-781 was safe, with high adherence and was effective in preventing HIV infection ex vivo, to the best of our knowledge we could not find any subsequent clinical trials further evaluating this product probably because of its extremely poor water solubility that makes it difficult in formulation development [75]. TFV has been extensively evaluated in clinical trials for the formulation of rectal microbicides. A phase 2 randomized clinical trial compared daily oral emtricitabine/tenofovir disoproxil fumarate, daily use of reduced-glycerin 1% tenofovir rectal gel and reduced-glycerin 1% TFV rectal gel before and after receptive anal intercourse [76]. After the 8-week study, there was more than 80% adherence for patients in the rectal application before and after rectal intercourse group compared to the daily oral formulation group (41%) and the daily rectal gel application group (29%). It is not a surprise that the daily gel application group exhibited low adherence since it is very

inconvenient to apply the rectal gel daily when there is no sexual intercourse. Naturally, the formulation for the gel application before and after rectal intercourse must have sufficient active compound in order to rapidly reach therapeutic levels when used during those two times. A similar phase 2 trial published by Cranston et al. corroborated the previous findings [77].

#### **1.1.8.2.5. Nanotechnology-based systems**

Nanomedicine is a fast-emerging field during the past several decades. NPs have been massively used in health research for the prevention, treatment, and diagnosis of different diseases. NP formulations are typically categorized as viral-based or non-viral NPs. Viral NPs mainly use viral components for gene delivery. This method can achieve high transfection efficiency but can result in severe adverse reactions [78], and as a result, will not be focused on in this review. The majority of NPs evaluated for HIV prevention or treatment have been non-viral based and are composed of lipids and/or polymers. When developed as a microbicide, NPs play essential roles in drug solubility, protection of the drug formulation, enhancing targeted drug delivery, modification of drug safety and toxicity, and can influence pharmacokinetics and pharmacodynamics of certain drugs [79].

One of the well-known nano-systems used as a microbicide and has entered phase 1 clinical trial is the SPL 7013 dendrimer gel Vivagel<sup>®</sup> [80]. This dendrimer is designed to interact with gp120 to inhibit direct entry of HIV and has demonstrated virucidal activity on certain strains of HIV. In a phase 1 trial, Vivagel<sup>®</sup> when used by women, was safe and had high tolerability [80]. The likelihood of this microbicide to work depends highly on its adherence, but unfortunately, in the same study, participants raised the same problems known with gel formulations mainly the leakiness and the hindrance with sexual intercourse in some cases. NPs have been used in gene

therapy to hinder HIV infection or viral replication via the delivery of nucleic acids [79] and for the delivery of small molecule drugs such as saquinavir [44].

Polymeric NPs present numerous advantages such as biodegradability and good biocompatibility, as well as mucoadhesive properties, which, for example, allow the NPs to remain longer in the FGT providing sustained drug release. In a study by Lakshmi et al., the team developed a combination platform against HIV [81]. In this study, lactoferrin, which has direct anti-HIV properties, was used to encapsulate efavirenz and curcumin. These NPs had a size of 40-70nm and were able to encapsulate up to 63% of curcumin and 61% of efavirenz. Furthermore, improved tissue and plasma concentrations were reported with the NP group compared to free drug[81]. In addition, poly(lactic-co-glycolic acid) (PLGA) conjugated to polyethylene glycol carrying siRNA against SNAP23, a gene involved in HIV escape from immune cells, has also been evaluated for its potential as a vaginal microbicide [82]. In these studies, the NPs were attached to anti-HLA-DR antibody for active targeting to dendritic cells. The mucus at the mucosal surface of the FGT can hinder viral movement but can also slow down NPs crossing the mucosal barrier into the submucosa. Maisel et al. designed polystyrene NPs densely coated with low-molecular-weight poly-ethylene-glycol (PEG) to prevent interaction with the mucus which enhanced NP penetration [83]. This NP formulation was capable of rapidly crossing the mucosal layer in a mouse model [83].

Lipids are also useful materials for developing NP-based microbicides. For example, a commercially available liposomal formulation called novasome<sup>®</sup> used for the encapsulation of 2-RANTES, a synthetic homolog of RANTE, demonstrated promise in a non-human primate SHIV challenge model [84]. In the study, 2-RANTES was used to block the CCR5 co-receptor to prevent

SHIV infection. Solid lipid NPs functionalized with polylysine-heparin have also been developed by Alukda et al. to encapsulate tenofovir as a drug model [85].

Hybrid NPs comprised of polymers and lipids have also been investigated for anti-HIV applications. For example, Boyapalle et al. evaluated a NP formulation mixing chitosan and lipids to form a chimera called chlipid nanocomplexes [86]. The nanocomplex was used to encapsulate and deliver siRNA for anti-HIV/SHIV evaluation. The nanocomplex was delivered in a cream formulation intravaginally to non-human primates and demonstrated a significant reduction in SHIV viral titer [86].

#### **1.1.8.2.6. Stimuli-responsive formulations**

Stimuli-sensitive materials for applications in drug delivery are a promising approach for achieving on-demand drug release. Stimuli-responsive polymers are able to deliver their active compounds at the appropriate time and site of action in response to specific triggers [87]. Different stimuli can be considered in the design of drug delivery systems such as temperature, pH, light, electric and magnetic fields, or enzymatic [87]. The FGT has a normal pH around 3.8-4.5 [88] which is a property that can be utilized to design drug delivery systems that respond to changes in the acidity of the vaginal area. In fact, during sexual intercourse, the presence of seminal fluid (pH 7-8.5) [88] can increase the pH of the FGT up to around neutral for 6 to 8 hours [89]. In a study published by Mahalingam et al., the authors developed a synthetic mucin-like polymer that will crosslink upon increases in pH to impede the movement of free HIV [90]. This pH-responsive polymer was made of phenylboronic acid and salicylhydroxamic acid copolymerized with 2-hydroxypropyl methacrylamide. At vaginal pH, the polymer is partially crosslinked and can slow down the viral movement with a relaxation time of 0.9 s and elastic modulus of 11 Pa. In the



presence of basic semen, the crosslinking becomes denser with a relaxation time of 60 s and an elastic modulus of 1800 Pa. Movement of HIV was reduced with a diffusion coefficient of  $1.60 \times 10^{-4} \mu\text{m}^2/\text{s}$ .

Besides using change in pH in the vaginal tract to trigger drug delivery, Clark et al. evaluated a vaginal delivery system using enzymes as a release trigger [91]. In this study, microgel particles containing the HIV-1 entry inhibitor sodium poly(styrene-4-sulfonate) were fabricated with a crosslinker containing a peptide substrate for serine proteases present in seminal fluid called prostate-specific antigen. Upon ejaculation in the FGT, the enzymes contained in the ejaculate degrades the crosslinkers and releases the therapeutic compound. The study revealed that after 30 min of exposure, the concentration released ( $10 \mu\text{g}/\text{mL}$ ) is equivalent to the published  $\text{IC}_{90}$  for the drug. Recently, a research article published by Coulibaly et al. utilized HIV-1 gp120 fragment's ability to interact with the drug carrier to trigger drug release [92]. In this study, TFV was encapsulated in a mannose responsive particle using calcium carbonate, concanavalin A and glycogen. This study was intended to address the unnecessary drug release while the virus is not present. Stimuli-responsive drug delivery systems are also known as “smart delivery systems” and may help to tailor drug delivery in a specific situation to prevent unnecessary drug release as a strategy to reduce adverse effects when the drug is not needed.

#### **1.1.8.2.7. Electrospun fibers**

Electrospinning has been around for a while, but its usage in microbicide development is still at an early stage. Ball et al. defined the electrospinning process as “the transformation of polymer melts or solution into collections of fine fibrous strands of material using a strong electric field. The resulting materials are typically opaque, soft, foldable sheets of polymer capable of

taking nearly any shape” [93]. There is an excellent review covering the different electrospinning techniques and materials used in the electrospinning process [93]. For example, In a study by Huang et al., TDF (Tenofovir Disoproxil Fumarate ) (Viread), a pro-drug of TFV, and Etravirine (TMC 125) were mixed with cellulose acetate phthalate and electrospun into fibers to protect the drugs from releasing in normal vaginal pH but released in the presence of human semen [94]. The fibers did not present any cytotoxicity towards vaginal epithelial and *lactobacilli* cells in vitro, appeared safe in a mouse model and prevented HIV infection in vitro [94]. Recently, Tyo et al., published on the pH-responsive delivery of the broad-spectrum antiviral protein griffithisin from electrospun fibers [95]. Electrospun fibers are a compelling platform that should be further explored as potential microbicide formulations.

#### **1.1.8.2.8. Modified microbiota for microbicide drug delivery**

The FGT is dominated by bacteria specifically those from the lactobacillus family, playing an important role in protecting against external infections. Studies have shown that lactobacilli present in the FGT were able to protect against HIV infection by the acidification of the medium, and also the nature of the lactic acid produced was able to inhibit the virus even if the pH was increased to 6.9 [96]. They also found the bacteria themselves have a direct virucidal effect [96]. Unfortunately, this natural defense is not sufficient to completely protect against HIV infection. Since bacteria can be engineered to produce specific proteins of interest, scientists have attempted to modify the natural flora to produce anti-HIV moieties capable of preventing HIV infection (Table 1.2) [97]. Lagenaur et al. published a study where they prepared a stable lyophilized tablet containing *Lactobacillus jensenii* engineered to express the HIV-1 entry inhibitor cyanovirin-N (mCV) [98]. Five tablets were inserted into the FGT (one tablet per day over five days) of

macaques. The tablets were completely disintegrated in 2 mins and colonization of the FGT by the modified bacteria was 66% after 14 days and 83% after 21 days. Western blot was used to confirm the presence of mCV-N. Although this is a promising platform to fight against HIV infection, this technique involving the use of genetically modified organisms will require additional studies to be conducted to demonstrate long-term safety and stability of the engineered bacteria before moving into clinical trials.

**Table 1.2: Engineered microbiota as microbicides to prevent HIV infection**

Engineered bacteria	Encoded inhibitors	Target	Ref
Lactobacillus jensenii	2D CD4	Entry inhibitor (gp120)	[99]
Lactobacillus reuteri RC-14	CD4 D1 D2	Entry inhibitor (gp120)	[100]
Lactobacillus jensenii	C1C5 CCL5	Entry inhibitor (CCR5)	[101]
Lactobacillus gasseri	CCL5; CCL3	Entry inhibitor (CCR5)	[102]
Lactobacillus jensenii	Modified cyanovirin-N; LB- mCV	Entry inhibitor (gp120)	[97]
Lactobacillus jensenii	Cyanovirin-N	Entry inhibitor (gp120)	[98]

#### 1.1.8.2.9. Challenges in microbicide drug delivery

Microbicide development was intended to be a breakthrough in the combat against HIV infection particularly in the absence of an effective vaccine. The ideal formulation should be reasonably easy to use, comfortable to increase patient adherence, must be capable of delivering sufficient drug uniformly throughout the FGT and rectum, and preferentially remain at the site for prolonged periods of time to provide complete and effective protection against HIV [103]. Table 1.3 presents some novel HIV prevention strategies evaluated in pre-clinical or in clinical trials. The majority of microbicide formulations are considered “single-use”, meaning that it is to be applied immediately before and after sexual intercourse. This can pose as a major inconvenience to patients resulting in a significant decrease in adherence. A potential solution to address some of these challenges is to formulate the microbicide into an IVR, which theoretically is not considered messy, does not require the patient to apply at the time of sexual intercourse, and can provide prolonged protection e.g. >21 days. Drug transporters and metabolizing enzymes may also play an important role in the therapeutic efficacy of the delivered drug. Zhou et al., examined the expression profile of 22 transporters and 19 metabolizing enzymes found in the FGT [104]. Certain antiretroviral drugs were shown to be affected by transporters such P-gp, BCRP, OCT2, and ENT1 and were more highly expressed in the lower genital tract compared to the liver. As for the metabolic enzymes, CYP isoforms were absent in the FGT while UGT1A1 was highly expressed [104]. Understanding all the factors around drug metabolism and transport will significantly help in the design of more effective microbicides.

Recently, a series of research has investigated the potential impact of the microbiome on the efficacy of microbicides evaluated in clinical trials. In the study published by Klatt et al., it was shown that women with impaired microbiota with a high content of *Gardnerella vaginalis*

experienced reduced effectiveness when they received 1% TFV gel [105]. In a previous study, *Gardnerella vaginalis* which causes bacterial vaginosis in the absence of *lactobacilli*, was found to exacerbate the production of inflammatory cytokines, which may facilitate HIV infection [106]. In an in vitro study, the authors found that *Gardnerella vaginalis* rapidly degraded TFV by 50.6% compared to *Lactobacillus iners*, *Lactobacillus crispatus*, and control without any bacterium [105]. This study highlighted the importance of vaginal microbiota while delivering TFV and possibly other anti-HIV drugs.

**Table 1.3. Other Novel HIV prevention strategies evaluated pre-clinically or in clinical trials**

Strategy	Preclinical or Clinical Research	Study Population	Targeted HIV Infection Route	Drug Delivery System	Regimen	Antiviral Agents	Efficacy of HIV Prevention (%) or Other Notes
On-demand PrEP[107]	Phase 3 clinical trial	MSM	Rectal	Oral tablet	two tablets 2-24 hr prior to sex followed by one tablet each at 24 hr and 48 hr post sex	Truvada®; TDF (300 mg) + FTC (200 mg)	86%
PrEP derived[108]	Phase 1 clinical trial	Women	Vaginal or penile	IVR	14-day IVR insertion	TDF (365±15 mg)	N/A
PrEP derived[109]	Phase 3 clinical trial	Women	Vaginal or penile	IVR	4 weeks	DPV (25 mg)	Overall 27%; 37% for high adherence group
IQ[54]	Pilot trial study	Women	Vaginal or penile	Oral tablet	daily administration	HCQ (200 mg) or ASA (81 mg)	Reduced HIV target cells at FGT; decreased CCR5 expression on mucosal CD4+ T cells
IQ[56]	Pre-clinical animal study	Rabbit model	N/A	Vaginal implant	6-day implantation	HCQ (80 mg)	Attenuated inflammation at FGT; decreased protein expression of HLA-DR and decreased gene expression of CCR5 and CD69 on mucosal T cells

Passive Immunization[110]	Phase 1 clinical trial	Women	Vaginal or penile	Vaginal gel	12 days	Vaginal gel containing bNAbs 2F5, 2G12, and 4E10, 50 mg each	Safety demonstrated over test period
Passive Immunization[111]	Phase 1 clinical trial	HIV-uninfected adults	Systemic	Intravenous; subcutaneous	Once or twice IV or SC administration of VRC01 in a dose escalation plan over 28 days	bNAbs VRC01	Safety and retained neutralizing activity demonstrated over test period

Abbreviations: ASA, acetylsalicylic acid; bNAbs, broadly neutralizing antibodies; DPV, dapivirine; FTC, emtricitabine; HCQ, hydroxychloroquine; IQ, immune quiescence; IV, intravenous; IVR, intravaginal ring; MSM, men who have sex with men; SC, subcutaneous; TDF, tenofovir disoproxil fumarate



### **1.1.9. Intravaginal ring design**

An IVR is a torus-shaped polymer that can deform when pinched into a figure-eight shape. Three principal polymers are used in microbicides notably the thermoset silicones, the thermoplastic poly (ethylene-co-vinyl acetate) EVA and thermoplastic polyurethanes [112]. From those polymers, four types of IVRs are usually used to deliver active compounds within the vaginal lumen. First, there are matrix-type IVRs where the drug is distributed homogeneously throughout the ring. A second type is the reservoir-type, which is similar to hollow tubing where the drug will be loaded into the lumen, and the two ends will be sealed together to form a ring shape [113]. The third type is an insert-type IVR. Small drug cores can be fabricated separately and coated with a rate-controlling membrane before inserted into the IVR. The fourth type is the segmented IVR allowing the combination of multiple segments from different polymers containing different drugs that are joined together to form the torus shape [114]. The matrix-type IVR will usually demonstrate a first-order release which means that the amount of drug released is proportional to the concentration at the present moment, e.g., more drug present in the ring will result in faster drug release. However, with the reservoir-type IVR, zero-order kinetics can be achieved, providing a constant rate of release. It is important to take into consideration the nature of the drug and the chosen polymer for controlled drug release, e.g., the solubility of the drug in the elastomer, the diffusion coefficient of the drug in the elastomer and the solubility of the drug in vaginal fluid. The volume of vaginal fluid produced and the partition coefficient of the drug between the IVR and the vaginal tissue are also essential [112, 114].

For an IVR to be able to release a drug for an extended period, it depends on its ability to stay in place within the vaginal lumen. Therefore, a typical IVR must not be able to deform easily within the vaginal tract or fall out. This can happen during daily activities such as coughing or running. On the other hand, if the ring is too rigid, it will cause irritation or damage to the vaginal

tissue resulting in severe inflammation [115]. Every woman is different including the size of their FGT. As a result, an IVR must be designed taking into consideration an optimum size that will allow the ring to fit into most vaginal tracts without causing any damage. Studies have shown that IVRs designed with an outer diameter of around 55 mm and with a cross-sectional diameter between 5 and 6mm are safe for humans [116].

#### **1.1.9.1. Discreet use of IVR for women and adherence**

In the third world, some women have difficulties negotiating the use of condoms with their partners. Sex workers are not always able to negotiate safer sex with their clients in fear of retaliation or reduced incomes. Microbicides will empower women to protect themselves against an infected partner without their consent. Women can place the IVR discreetly in the genital tract without the knowledge of their partner. Many of the previous intravaginal devices require a healthcare professional for insertion/placements e.g. intrauterine devices. IVRs can be inserted/removed easily and rapidly by women without professional help. Since the ring can be inserted for a long period of time, this will reduce the burden associated with daily application, which will improve patient adherence.

It is important to understand the difference between patient acceptability and patient adherence. Acceptability is defined as the extent to which a product is desirable to the target user population, and adherence is the extent to which users obey specified dosing instructions [117]. A study conducted by Novak & al. showed that 66% of participants chose oral contraceptives instead of the ring at the beginning, but after using it for a while, 81% were happy with the ring [118]. 85% of the women in the study never or rarely noticed the presence of the ring during intercourse, and 74% of their partners hardly noticed the presence of the ring. 94% of women's partners had

little or no concern about the use of the ring. The acceptability of the ring was high because of the simplicity in its usage and improved convenience (the ring can be used for a prolonged period) [118].

#### **1.1.9.2. Effect of intravaginal ring on vaginal mucosa and biofilm formation**

An IVR is a foreign device to the human body fabricated from medical grade polyurethane to improve biocompatibility and reduce the risk of inflammation. The vaginal environment is complex and involves a lot of microorganisms. An alteration of the vaginal flora can severely decrease the number of lactic acid-producing bacteria naturally present in the FGT and keep the acidic pH. A decrease of those bacteria will follow an increase of the vaginal pH >4.5 and lead to the installation of other microorganism pathogens [119]. The presence of foreign pathogens in the genital tract can lead to an inflammatory response called vaginitis. The most common vaginitis is bacterial vaginosis caused by *Gardnerella vaginalis* [120]. Numerous studies have shown that bacterial vaginosis may ease HIV infection [121-123]. The impact of the IVR on the vaginal microbiota must be carefully monitored so that it does not create unnecessary inflammation and enhance HIV infection.

On the other hand, the vaginal flora can also have an impact on the ring. It is possible for an IVR that stays longer than three weeks in the vaginal tract to develop biofilm formation on the surface of the ring. The biofilm growth can affect the release rate of the active compound from the ring. Not many studies have been done to evaluate this, but Manjula et al. reported the presence of a layer of dead epithelial cells on the surface of the ring worn by six female pig-tailed macaques for 28 days. They found the presence of two different phenotypes of bacterial biofilm on the ring. The phenotype I formed a bacterial mat with a thickness of approximately 5µm. The phenotype II,

less common than the first one, created a mat of 40  $\mu\text{m}$  [124]. Unfortunately, this study did not focus on the effect of those biofilms on drug release. More studies must be done regarding the impact of the IVR on the microbiome and the effect of the microbiome on the IVR in long-term use.

#### **1.1.10. Gene therapy as a potential strategy for preventing HIV infection**

Gene therapy offers continuous interference with viral replication. It can be a good alternative if there is no chemotherapy to act on a specific target or to reduce drug resistance. There are different approaches for gene therapy to prevent HIV infection. One of the main approaches is using RNA-based agents as prevention strategy. For example, RNA interference (RNAi) is a process whereby double-stranded RNA (dsRNA) can induce post-transcriptional gene silencing in cells [125]. RNAi uses small interfering RNA (siRNA) or short hairpin RNA (shRNA) to knockdown a specific gene expression to prevent HIV replication. Gu et al. demonstrated siRNA can be used to silence the expression of synaptosome-associated 23-KDa as a strategy to prevent HIV virion to escape the host cell [82]. Another example of RNA-based gene therapy molecule is RNA aptamers. They have a high affinity to bind to a specific target. For example, Ramalingam et al. raised HIV-1 Gag protein RNA aptamers to prevent HIV replication [126]. Duclair et al. used RNA aptamers to inhibit HIV-1 protease activity and also prevent viral replication [127]. Another gene therapy strategy to genetically modified host cells to produce anti-viral particles in effort to prevent HIV infection. For example, Falkenhagen et al, modified  $\text{CD4}^+$  using plasmid to produce soluble CD4 that inactive the virus by binding to the envelope glycoproteins [128].

#### **1.1.10.1. Mechanism**

In the process of RNAi, the RNase III Dicer processes dsRNA of 21-25 nucleotides long called siRNA or micro-RNA (miRNA). siRNA is incorporated into the RNAi-induced silencing complex (RISC) where it promotes the degradation of the target mRNA in a sequence-specific manner by Argonaute 2 (Ago) or hindering its translation into proteins in the cytoplasm [129]. After the dicer has processed the dsRNA, the resultant siRNA is double-stranded and contains three overhangs of two nucleotides. If the synthetic siRNA is directly injected into the cell, it can bypass the requirement for dsRNA processing by Dicer and immediately be incorporated into the RISC complex. The double-strand siRNA is unwound by a helicase in RISC. The untwisted anti-sense strand is matched to messenger RNA (mRNA) that carries a high degree of sequence complementarity (the gene of interest). The mRNA will then be cleaved. The cleavage of the mRNA is directed by an Ago protein, which is an important part of the RNAi machinery associated with siRNA. The RNAi processing gives two small interfering RNAs that are siRNA and miRNA. Dicer enzymes can cleave long dsRNA and stem-loop precursors into siRNA or miRNA in an ATP-dependent manner, respectively. The Dicer does cleave not only the RNAi but also helps the siRNA-RISC loading. It has been reported as well that siRNA with 3' overhang in the antisense operate better than siRNA with asymmetric sense strand overhang [130, 131].

#### **1.1.10.2. siRNA-directed inhibition of HIV-1 infection**

siRNAs are used to target many stages of the HIV-1 infection and replication cycle including the knockdown of host cell membrane receptors such as CD4, CXCR4, and CCR5. For example, Novina et al. showed a decrease in HIV entry by silencing the expression of CD4 receptor. Transfection with CD4-siRNA reduced CD4 expression by 75%, which also resulted in

a four-fold decrease in HIV infection [132]. Using gene therapy against HIV has many advantages. For example, in the absence of drugs to act on a specific target, siRNA can be individually customized to target the gene of interest. Systemic toxicity and off-target effects associated with a conventional drug can be reduced as well as decreases in the development of drug resistance by microorganisms.

As discussed before, CCR5 co-receptor is the dominant receptor involved in HIV-1 entry into target cells along with the CD4 receptor. A report stated that people lacking CCR5 genes are resistant to HIV-1 infection [23]. In this project, we will be using siRNA to knockdown the expression of CCR5 gene as a strategy for preventing HIV entry into its target cells (Figure 1.2).

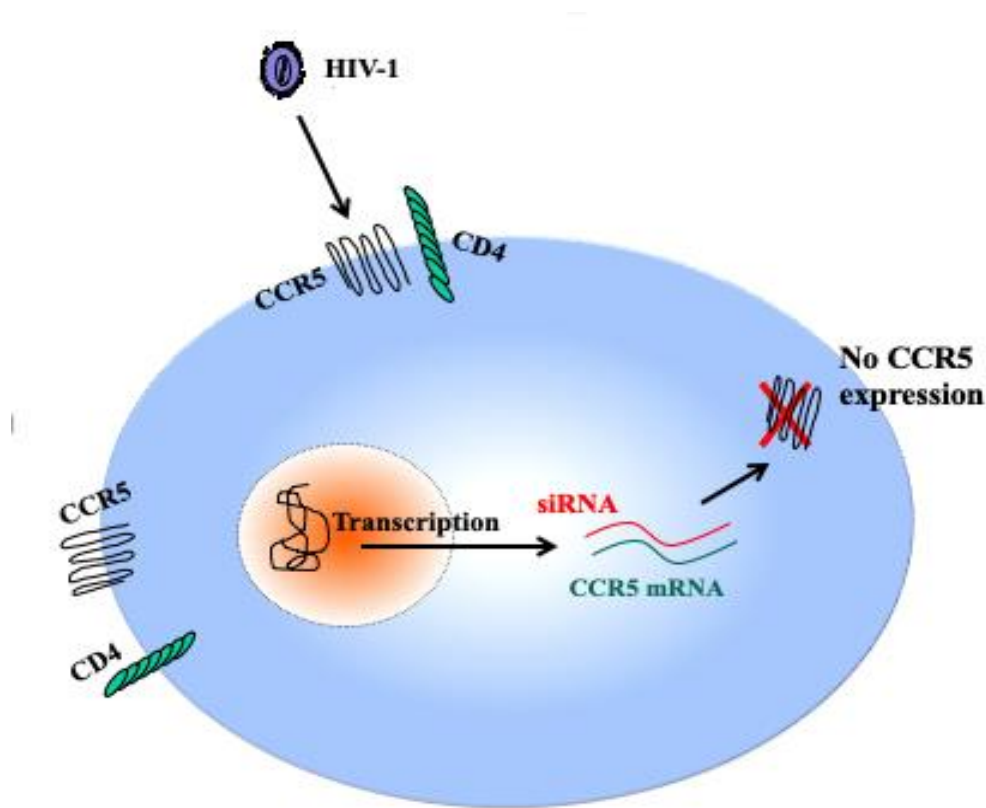


**Figure 1.2: Schematic of the CCR5 expression inhibition by siRNA**

### **1.1.10.3. siRNA delivery vehicle in the vaginal mucosa**

Naked siRNA has a net negative charge and is hydrophilic, preventing it from crossing the plasma membrane and entering cells. Naked siRNA can trigger an immune response and become degraded before it reaches its target. Enzymatic degradation by RNase is a significant risk for naked siRNA [133]. Thus, siRNA needs a protective carrier capable of targeting the cell of interest.

There are two main categories of carrier systems for the delivery of siRNA - viral and non-viral based vectors. The viral vectors present some limitations such as the difficulty of the vector production, broad tropism and ability to trigger the activation of the immune system. Certain viral vectors were found to be carcinogens and have insufficient space for packing large quantities of siRNA [134]. Non-viral vectors are simpler to synthesize, can load more genetic material and have less immunogenicity [134]. The non-viral vectors include lipid-based transfection reagents, macromolecule nanocarriers, and polymer-based NPs.

Polymer-based NPs as a vehicle for siRNA delivery are often used in the past several decades. Poly(lactic-co-glycolic acid) (PLGA) is an example of a FDA approved biodegradable and biocompatible polymer, extensively used to deliver siRNA. PLGA demonstrated an enhanced efficacy to encapsulate small molecules, nucleic acids, and proteins. Furthermore, PLGA NPs are easy to customize to attached targeting moieties at the surface and also used for imaging [135].

Solid lipid nanoparticles (SLNs) have also gained a lot of interest in the past decade. The lipid-based nanocarriers may be composed of a solid lipid core dispersed in an aqueous surfactant solution at room temperature. The surface of SLNs can be modified to attach targeting moieties for the drug to be released in a specific type of cell. SLNs are easy to synthesize using techniques such as high-pressure homogenization, solvent evaporation, ultra-sonication [136].

#### 1.1.10.4. pH-responsive polymers

Polymeric materials that are capable of responding to external physical and chemical stimuli such as pH, ionic strength, light, electric field, and temperature by changing their behaviors are extensively investigated in pharmaceuticals and medicine [137, 138]. pH-responsive polymers are defined as materials that can respond to the pH changes of the surrounding medium by varying their morphologies and conformations due to the protonation-deprotonation equilibrium of the functional groups in the polymer chains [139]. Cationic pH-sensitive polymers will have a different response than anionic pH-sensitive polymers in various pH buffers. For example, poly(acrylic acid) contains carboxylic acid groups (-COOH) that are ionizable at basic pH. In contrast, poly(N,N'-diethyl-aminoethyl methacrylate) has amino groups (-NH<sub>2</sub>) that are ionized and dissolves at acidic pH [140]. A pH-responsive polymer, cellulose acetate phthalate (anionic pH-responsive polymer) was used to coat vaginal tablets to provide a slow release of IQP-0528. The antiretroviral (IQP-0528) presented a slow release at the acidic pH (vaginal < pH4.5) and provide burst release at pH > 7.2 mimicking the presence of semen in the vaginal tract [141, 142]. This controlled release prevents a continuous exposure of the drug to the vaginal tract when not necessary (absence of sexual intercourse) and provide a high release in the presence of semen during sexual intercourse.

In our study, we will use polyacid polymers for triggering drug release only when the pH of FGT increases to mimic the presence of seminal fluid. At low pH, polyacid polymers will not swell because of the protonation of the acid group, hence ionized. When the pH increases, the acidic group will be deprotonated and become negatively charged. The repulsion between those negative charges makes the polymer swell to make bigger pores with a subsequent release of all



the entrapped molecules. The release of a therapeutic compound at desired pH (pH>6) will greatly decrease the amount of drug used and reduce unnecessary toxicity.

## **1.2. Immunocompromised patients and chronic wounds**

### **1.2.1. Chronic Wound**

Chronic wounds or non-healing wounds are those that do not progress through the healing process in a timely manner and turn into a severe healthcare concern [143]. Individuals with low immune profiles tend to not be able to heal properly. Immunocompromised patients tend to develop bacterial infections, diabetes, and other comorbidities [144]. Those comorbidities can cause chronic wounds [145]. People infected with HIV can easily develop chronic wounds and are more susceptible to develop wound complications after surgery [146, 147]. For example, Popovich et al. showed the colonisation of HIV-infected patient body by methicillin-resistant staphylococcus aureus [148]. This colonization makes it easy to infect a wound on HIV patients and establish a biofilm. Chronic wounds include diabetic ulcers, vascular ulcers, and pressure ulcers [149]. Diabetic foot ulcers will affect almost 15% of people living with diabetes, and the recurrence of these wounds is seen in over 70% of patients within five years [150]. Diabetes causes arterial damage and neuropathy that can create ulcers in the foot area. Often, bacterial infections can worsen those ulcers and spread them to the bone of the foot [151]. In the case of vascular ulcers, which are mostly associated with venous diseases, venous stasis can create damage to the venous systems of the leg and cause hypertension and reduce blood flow [152]. Pressure ulcers or bedsores are ulcers resulting from prolonged pressure on the skin commonly seen in patients with reduced mobility like in residential care homes or hospitals [153]. Although researchers know the classifiable cause of the ulcer capable of creating a chronic wound, resolving the underlying cause

will not necessarily lead to healing [149]. In this thesis, we propose to develop a new scaffold made of a thermo-sensitive material that can rapidly release an active compound formulated into a NP for targeted and prolonged release inside the biofilm. The NP with sustained-release will increase the exposure of the active compound to the bacteria which might help destroy the bacteria. The thermo-sensitive material will be gel-based at room temperature to hold the NPs. Upon application on the skin, the temperature will rise and the gel will liquefy allowing the release of NPs. It is also important that the wound dressing/scaffold for delivering the active compound is easily removed without causing any pain or the reopening of the wound. This new scaffold design will not stick to the wound and won't reopen it when it is taken off.

### **1.2.2. Physiology of wound healing**

The wound healing will occur through a systematic process of 4 overlapping phases: Hemostasis, inflammation, proliferation, and maturation [154]. After an injury, the vasoconstriction of the blood vessel and blood clot will occur through the hemostasis phase to prevent blood loss. The thrombocytes (platelets) at the site of the injury produce growth factors and cytokines to attract endothelial cells, immune cells, and fibroblasts. This will initiate the inflammatory phase carried out by neutrophils and macrophages [149]. Neutrophils are the first on-site responding to platelet degranulation, complement activation, and bacterial degradation. Neutrophils will produce proteolytic enzymes like matrix metalloproteases (MMPs), elastase, cathepsin G, anti-microbial proteins (AMPs; multi-functional cationic peptides capable to induce cytokines production, to attract immune cells, and directly kill pathogens and promote wound healing), reactive oxygen species (ROS) and cytokines in an effort to clean the wound bed [155]. While wound healing is progressing, neutrophils are slowly replaced by monocytes, which will differentiate and become macrophages to continue the cleaning process by phagocytosis of

microorganisms. The macrophages are sensitive to their environment via Toll-like receptors, complement receptors, and Fc receptors. The inflammation phase will end with the apoptosis of immune cells [156]. The third phase of the healing process, the proliferation phase, is characterized by tissue granulation, angiogenesis (new blood vessels), and epithelialization. This phase overlaps with the last phase where remodeling will assist in the wound contraction, collagen remodeling, and extracellular matrix degradation [155].

### **1.2.3. Chronic wound vs Acute wound**

Unlike acute wounds, chronic wounds do not follow the standard wound healing process. Chronic wounds present a persistent pro-inflammatory phase that prevents the wound from healing. This persistent inflammatory phase is mostly due to repetitive tissue trauma, tissue hypoxia, tissue breakdown and necrosis, and more importantly, a substantial bacterial burden [157]. There is an imbalance in the production of pro-inflammatory cytokines, chemokines, proteases. Neutrophils and activated macrophages present at the wound site release pro-inflammatory cytokines TNF-alpha and IL-1 beta that increase the production of MMP and reduce the synthesis of tissue inhibitors of metalloproteinases (TIMPs), which will induce more degradation of extracellular matrix (ECM), reduce fibroblast proliferation and collagen synthesis[158]. Immune cells also will produce ROS intended to provide defense against microorganisms in low concentrations. But in the case of chronic wounds, the production of ROS is exacerbated and causes damage to ECM proteins and cells [159]. Another downside of chronic wounds is the massive presence of senescent cells with impaired proliferation and secretory capacities. In fact, those cells are very slow or completely unresponsive to wound healing signals with a limited cell proliferation capacity that impedes wound healing. It has been reported that the senescent phenotype of cells, in this case, is due to the DNA damage caused by oxidative stress or

abnormal metabolic changes observed in diabetic patients. In this regard, recent researchers have focused on mesenchymal stem cell applications in chronic wound healing [160]. They developed a scaffold that mimics the dermal structure and uses it to deliver mesenchymal stem cells to the wound bed. Those cells have the ability to differentiate into various cell types and also can recruit different cells needed for faster regeneration [160].

#### **1.2.4. Biofilms and inflammation in chronic wounds**

Biofilms consist of microorganisms (bacteria or fungi) enclosed in an extracellular matrix composed of hydrated polymers and debris. The bacteria in biofilm differ from their planktonic peers in structure, genetic make-up, interaction with the host, and resistance to antibiotics [161]. Mature biofilm formations are more resistant to antibiotics than younger, less established biofilms. The bacteria separated from the biofilm or if the biofilm is re-suspended in culture media, increase the vulnerability to antibiotics [162]. The presence of necrotic tissues and impaired host immune system make the chronic wound an ideal environment for bacterial growth and biofilm implantation. About 60% of chronic wounds are populated with biofilms compared to 6% in acute wounds [163]. Studies have shown that the biofilm formation inside chronic wounds is due to the concerted action of many bacterial species instead of only one. The most populated bacteria found in wound biofilms are *Pseudomonas*, *Staphylococcus*, *Janthino-bacterium*, *Corynebacterium*, and *Propionibacterium acnes*. The amount of different bacterial species present in a wound is highly dependent for each specific patient case [155, 164, 165]. The biofilm presence in chronic wounds plays a critical role in the prolonged inflammatory phase as discussed above, such as the excessive release of cytokines, the extended presence of neutrophils and macrophages, the changes in oxygen concentration, and the pH in the wound [166]. A chronic wound with biofilm present shows much more neutrophil infiltration. For example, *Pseudomonas* attracts neutrophils in the wound area

using their quorum-sensing system and lyses them [167]. These bacteria protect themselves from phagocytosis by neutrophils through their rhamnolipid protective shield. The bacterial DNA in biofilm also is reported to stimulate neutrophils [167]. Another example of a study conducted on a mouse model shows that the presence of *Staphylococcus aureus* in the wound was capable of exacerbating macrophage infiltration but changing their function by suppressing microbicidal activity and increasing cell death [168]. The inflammatory cytokines are increased dramatically by the presence of biofilms as depicted by a study showing the levels of IL-2, IL-4, IL-6, IL-12, IL-17, and TNF-  $\alpha$  caused by the presence of *S. aureus* [169]. MMP-1 and MMP-3 production were increased using in-vitro keratinocyte culture challenged with biofilm [170]. From these observations, microbial presence appears to contribute to the prolonged inflammatory phase. Eliminating the microbial growth from the surface of chronic wounds will tremendously speed up the wound healing process. Unfortunately, the bacteria present in a biofilm have particular resistance to antibiotics, which seems to be an important mechanism for biofilms survival. The extracellular polymeric substance might prevent the efficient diffusion of antibiotics. Also, antibiotics act on metabolic activities, and unfortunately, since bacteria present in a biofilm are quiescent with slow metabolic activity, the antibiotics will tend to be ineffective. The stress response, nutrition supply, and oxidative stress may induce mutations to the bacteria and slow down growth and metabolic activity making them resistant to antibiotics. Besides surgery, which is the most effective way of treating chronic wounds, other current strategies used for biofilm disruption and wound treatment, are summarized in Table 1.4. As suggested by Zhao et al., to be able to kill microorganisms in a biofilm, a high dosage of the medication applied directly on the wound for a prolonged period might help to get rid of the bio-burden [166].

**Table 1.4: Current therapies for treating chronic wounds**

Type/ Compound Base	Actives	Mechanisms Addressed		Bacterial Resistance
		Physical and Chemical Disruption of Biofilm Supportive Structures (Matrix)	Preservation of Host Healing Cells	
Quaternary ammonia (detergents) [171]	Benzethonium chloride	No	Not significant at low concentration	Development of microbial resistance
Polyhexamethylene/betaine/biguanide [171]	Undecylenamidopropyl betaine, polyaminopropyl biguanide	Polyhexamethylene biguanide (PHMB) solutions may block microbial attachment to surfaces;	Low concentrations of betaines and biguanides may not harm host tissue, depending upon chemical structure.	Poor chance of development of resistance to PHMB; resistance not reported.
Collagen with PHMB [171]	PHMB	No published evidence showing effectiveness of collagen-PHMB dressings against biofilm.	Unknown	Poor chance of Development of resistance to PHMB; resistance not reported.
Hypochlorite [172]	Bleach; chlorine	Yes at high concentration	May induce tissue injury associated with inflammation; toxic to fibroblasts and keratinocytes.	Reports of development of acquired resistance to certain pathogens to chlorine are very limited.
Silver [173]	Ionic silver; silver sulfadiazine	No	Silver nitrate and silver dressings have been found to be cytotoxic in vitro. No in vivo data	Microbial resistance is rare
Topical antibiotics [174]	Bacitracin zinc salt, neomycin, polymyxin B; mupirocin	No	Various concentrations of topical antibiotics have shown in vitro tissue toxicity.	Increased resistance Associated with increased use of neomycin, bacitracin, and mupirocin.
Iodine [175]	Cadexomer iodine	Limited in vivo, and in vitro evidence that cadexomer iodine reduces biofilm in wounds and may destroy biofilm structures	May be safe for host, but controversies remain regarding potential cytotoxicity and systemic absorption with prolonged use	No bacteria resistance. Iodine-resistant microbial strains are exceptionally rare.

### **1.2.5. Thermo-responsive polymer scaffold**

A thermo-responsive polymer will undergo property changes upon changes in temperature. There are two different groups of thermo-responsive polymers: a group that forms solution upon heating, and a group that forms solution upon cooling. The polymer that forms solution upon heating present an upper critical solution temperature (UCST) and the opposite group presents a lower critical solution temperature (LCST) in their phase diagram [176]. An excellent review by Aseyev et al. discussed the extensive applications of thermo-responsive polymers used in chromatography, temperature-triggered drug release, bio-separation, targeted drug delivery just to name a few [177].

In our study, we will design a wound dressing using gelatine as a thermo-responsive material to help deliver the medication to biofilms present in chronic wounds. Gelatine has an UCST of around 32°C, which is slightly closer to the skin temperature of 33°C. Gelatine is derived from collagen extracted from connective tissues, skin, and bone of animals. The gelatin has a triple helix chain in the form of a coil conformation. When the gelatin is heated past its melting temperature, the hydrogen bonds between the chains become fragile and disordered and turn to a liquid form. Upon cooling, the gelatin can revert to its triple-helical state [178]. The amplitude of the gelatine helical state transformation depends on the concentration, temperature, stress, solvent, and the presence of crosslinking agents [178]. Gelatin has been extensively used as a drug delivery material since it is natural, biodegradable, biocompatible, easy to modify and safe [179-181].

In this study, we propose a combination therapy consisting of the delivery of vancomycin and LL37, encapsulated in SLN formulated in a thermo-responsive gelatin scaffold for rapid release of the payload upon application on the wound.

### **1.3. Project rationale, hypothesis and objectives.**

Project #1:

The first part of my thesis focused on the development of a microbicide in an effort to prevent HIV infection. In the absence of an effective vaccine, they are an excellent alternative to condoms to help reduce male-to-female transmission. Unfortunately, several microbicide trials previously demonstrated limited efficacy due to the fact that gel dosage forms are messy, can be easily “washed out” of the FGT, and requires high patient compliance (e.g. gel needs to be applied before and after sexual intercourse) [182]. An IVR can be a suitable alternative strategy that can provide controlled, sustained delivery (>14 days) of drugs within the FGT [183]. In this project, we propose to develop a segmented combination IVR whereby one-half of the IVR will be loaded with HCQ and the other half of the IVR will be coated with a pH-responsive film for the rapid release of small interfering RNA (siRNA)-encapsulated nanoparticles as a novel strategy for protecting against HIV infection. It is widely documented that drug resistance is a concern with conventional antiretroviral therapy. As a result, delivering a combination of drugs of different classes (e.g siRNA and chemotherapeutics) targeting different steps in the HIV infection process is expected to be more effective. Studies have shown that quiescent (resting) CD4+ T cells are less susceptible to HIV infection [184]. HCQ is an immunomodulatory drug approved for the treatment of malaria, systemic lupus erythematosus, and rheumatoid arthritis [185]. It is capable of reducing HIV viral load and the activation of T-cells, resulting in reduced viral infection [186, 187]. While T-cells are activated, there will be an increased expression of cell surface markers such as HLA-DR, CD69, and CD38 increasing the susceptibility for HIV infection [188]. HCQ at has the ability to increase the lysosomal pH and impairing the expression of T-cells activation markers such as HLA-DR, CD69, and CD38 [189]. In addition, HCQ has been shown to inhibit the production of



HIV-1 gp120 by increasing the lysosomal pH of the cell and altering the enzymes required for glycoprotein 120 production [190]. RNA interference via the use of siRNA is a strategy for knocking down gene expression. When there are no drugs available to act on a specific target, using siRNA as a therapeutic agent could be a highly effective alternative. Furthermore, siRNA can be designed to specifically target the knockdown of a single gene, reducing systemic toxicity and off-target effects associated with conventional drug therapy. Unfortunately, siRNA cannot readily traverse cell membranes, hence, a drug carrier such as nanoparticles is required for delivering siRNA into the cytosol of the target cells. In this project, solid lipid nanoparticles (SLN) encapsulated with CCR5 siRNA will be functionalized with anti-CD4 antibody to specifically target and deliver to CD4+ immune cells (HIV target cells) and knock down the expression of CCR5, a co-receptor involved in HIV-1 infection.

### **Hypothesis:**

It is expected that at normal vaginal pH (3.5-4.3) there will be no release of siRNA-loaded nanoparticles. During heterosexual intercourse, the vaginal pH becomes elevated due to the presence of seminal fluid, resulting in elevated pH (>6.2) [191]. As a result, it is expected that at pH>6.2, the IVR will provide rapid release of siRNA-nanoparticles while HCQ will be released continuously (>14 days) at both acidic and neutral pH to prevent immune activation of T-cells.

### **Specific Aims:**

- 1) Develop and characterize a segmented combination pH-responsive IVR delivery system.
- 2) In vitro evaluation of HCQ release and siRNA gene knockdown.

## Project #2:

The second part of my thesis focused on the development of a thermo-responsive chronic wound dressing designed to reduce biofilm formation on chronic wounds and facilitate the healing process. The current and widely used wound dressings present some disadvantages. For example, gauzes are dry and not able to maintain the optimum moisture of the wound bed and can easily adhere to the wound which makes it difficult to remove without creating another trauma with residue remaining into the wound [192]. The current hydrogel wound dressings have been found to be non-adherent with a high water content that reduces their absorptive ability therefore cannot be used on wounds with high exudate [193]. An ideal wound dressing as described by Sood et al, should provide an optimum moist environment capable of removing excess exudate, protect the wounds, can conform to wound shape, and should be easy use and to remove without trauma [192].

In this project, I propose the development of a thermo-responsive hydrogel dressing made of gelatin-chitosan capable of delivering SLN containing LL37 and vancomycin to reduce the bioburden and improve wound healing. Vancomycin and LL37 SLN have been shown to synergistically enhance antibacterial activity against *S. aureus* [194]. LL37 is derived from the cathelicidin precursor protein hCAP18 produced by human neutrophils, mast cells, and natural killer cells. Proteinase 3 cleaves hCAP18 and the C-terminal becomes LL37 with 37 peptides [195, 196]. Although LL37 has been shown to promote wound healing while acting on cell proliferation, differentiation, it is also a potent anti-microbial [197, 198]. Shahmiri et al, showed that LL37 exhibits two different modes of action against bacteria. The peptide might interact with bacteria membrane can create pores in bilayers of unsaturated phospholipids or can create the formation of tubular structures by acting like a membrane modulating agent [199]. On the other hand,

vancomycin is a glycopeptide that has been used for many decades. It has been shown to be very potent against gram-positive bacteria. Vancomycin binds to the acyl-D-ala-D-ala portion of the bacterial peptidoglycan cell wall and prevents their cross linking altering the cell wall formation. The bacterium reacts by producing more peptidoglycans that accumulates and triggers an enzyme against the peptidoglycans which contributes to the breakdown of the cell wall [200, 201]. The use of LL37 alongside vancomycin might improve biofilm reduction and promote wound healing.

**Hypothesis:**

The development of a thermo-responsive hydrogel scaffold capable of delivering LL37/vancomycin-SLNs upon application on a chronic wound will be capable of decreasing the biofilm burden and potentially enhance wound healing.

**Specific Aims:**

- 1) Preparation of LL37 and vancomycin encapsulated SLNs
- 2) Preparation of a thermo-sensitive scaffold from gelatin and chitosan to incorporate the SLNs.
- 3) In vitro model of biofilm for evaluating the scaffold.

## **Chapter 2: Dynamic mechanical behaviour of nanoparticle loaded biodegradable PVA films for vaginal drug delivery**

Adapted from the following research article:

Yannick L Traore, Miral Fumakia, Jijin Gu and Emmanuel A Ho, *Journal of Biomaterials Applications* 2018, Vol. 32(8) 1119–1126 DOI: 10.1177/0885328217739451

## **2.1. Abstract**

In this study we investigated the viscoelastic and mechanical behaviour of polyvinyl alcohol (PVA) films formulated along with carrageenan, plasticizing agents (PEG and glycerol), and when loaded with nanoparticles (NP) as a model for potential applications as microbicides. The storage modulus, loss modulus and glass transition temperature were determined using a dynamic mechanical analyzer (DMA). Films fabricated from 2% and 5% PVA containing 3 mg or 5 mg of fluorescently-labeled NPs were evaluated. The storage modulus and loss modulus values of blank films were shown to be higher than the NP-loaded films. Glass transition temperature determined using the storage modulus was between 40-50°C and 35-40°C using the loss modulus. The tensile properties evaluated showed that 2% PVA films were more elastic but less resistant to breaking compared to 5% PVA films (2% films break around 1N load and 5% films break around 7N load). To our knowledge, this is the first study to evaluate the influence of NP and film composition on the physico-mechanical properties of polymeric films for vaginal drug delivery.

## **KEYWORDS**

Poly (vinyl alcohol), nanoparticles, dynamic mechanical analysis (DMA), modulus, glass transition temperature, thermal stability.

## 2.2. Introduction

Polymeric films are increasingly gaining attention as drug delivery systems due to their ability to provide rapid drug release and bio-adhesive properties that may increase the retention time at the target tissue. Film-formulated products offer user compliance as well as ease of application. Recently, a number of researchers have focused on the development of polymeric vaginal films as contraceptives and microbicide formulations [202-206]. The potential of vaginal films for contraceptive or microbicide applications is mainly due to their ability to overcome several challenges related to acceptability, compliance, and efficacy in comparison to gel-based formulations [206-208]. For example, gels are messy and may leak resulting in reduced drug concentrations. Despite films demonstrating to be a promising drug delivery platform, the type of bioactive being delivered will affect the mechanical, chemical and physical properties of the film, which in turn will also alter drug release rates [208].

Polyvinyl alcohol (PVA) is a polymer that is widely used in a variety of applications due to its biodegradability and its ease in preparation [209]. PVA is a water-soluble and crystalline polymer. This material can form films that are biocompatible with good mechanical properties allowing its use in various industrial and medical applications. It has been used in pharmaceuticals as a drug delivery system due to its high water solubility and rapid disintegration rate [204, 210]. Polymeric films can be designed to be highly resistant to repeated flexure or creasing [211]. Some of the film properties such as tensile strength, and permeability to gases or water vapour may be important features to consider when developing a drug delivery system [212]. Studies have shown that thin polymeric films tend to degrade in the presence of destabilizing forces such as heat and mechanical stress at the film's interface [211, 213]. Quantitatively, such instabilities affect the

thermal and mechanical characteristics of the film [211, 213]. Depending on the plasticizer, excipients, or drug loaded into the films, it can exhibit different physico-chemical behaviours.

Numerous studies are using polymeric film formulations to deliver nanoparticles (NPs) [214, 215]. The nanocarrier is used to protect the active compound from its external environment, can assist in active targeted delivery, and can provide controlled, sustained drug release [216]. They have been used to address the concerns of physicochemical instability of drugs, low cellular uptake and the need for multiple dosing [217]. For example, different PVA films with different thickness have been formulated to deliver varying concentrations of poly(D,L-lactic-co-glycolic acid)-poly(ethylene glycol) NPs containing siRNA as a therapy for preventing HIV infection within the female genital tract [205].

Hence, the objective of this study was to experimentally determine the influence of NP content and film composition on the physico-mechanical properties of NP-loaded PVA films subjected to varying temperature ranges.

### **2.3. Materials and Methods**

Degradex® fluorescent PLGA NPs were purchased from phosphorex (Hopkinton, Massachusetts, USA). PVA (98-99% hydrolyzed; MW 31,000-50,000) and  $\lambda$ -carrageenan were purchased from American Custom Chemicals Corp (San Diego, CA, USA). Phosphate-buffered saline (PBS; pH 7.4) was purchased from Lonza (Allendale, NJ, USA). Double distilled water (ddH<sub>2</sub>O) was purified using Millipore Simplicity System, which was used for all the experiments.

### **2.3.1. Preparation of nanoparticle-loaded film**

PVA films were prepared by a solvent casting method as previously described [205]. Briefly, PVA and carrageenan were dissolved overnight in distilled water at 80°C. The PVA solution was allowed to cool down to room temperature and diluted to either 5% or 2% solution (w/v). 240 µL of glycerol and 80 µL of PEG400 were mixed in 8 mL of the solution and allowed to stir for 1h. Commercially available fluorescent NPs (200 nm) were added and mixed for an additional 1h to prepare 5% film containing NPs with the ratio of 1:88 [w (NP)/w (PVA+carrageenan)] for 5 mg NPs loading and 1:146.6 for 3 mg NPs loading. For the 2% film solution, a ration of 1:40 and 1:66.6 were used for 5mg and 2 mg NPs loading respectively. Fluorescent Degradex® PLGA was made by Phosphorex Inc by standard oil/water emulsion and encapsulating a hydrophobic dye. The mixture was poured into a Teflon™ dish (30 cm<sup>2</sup>) and placed in the oven at 40°C overnight to evaporate the solvent and to form the film.

### **2.3.2. Dynamic mechanical analysis**

Dynamic mechanical analysis (DMA) of the films was performed using a DMA Q800 (TA Instruments, New Castle, USA) in tensile mode. Film samples (2% and 5% PVA blank films or NP-loaded films) were cut into sizes between 5-6.5 mm in width, 20-30 mm in length, and 0.5-0.7 mm in thickness in order to conform to the dimensional limits required for the tensile film clamp test fixture. The average thickness for each film sample was based on three separate measurements, taken at the two ends and in the middle. The DMA test procedure was as follows: after mounting the film sample on the DMA tension film clamp, the furnace was sealed and the mechanical properties were measured from 25 °C to 80 °C at a ramp rate of 3 °C per min under a preload of 0.5 N. Measurements were performed at a constant frequency of 1 Hz and strain



amplitude of 10  $\mu\text{m}$ . This setup was used to determine the glass transition temperature and the real (storage) modulus  $E'$ , imaginary (loss) modulus  $E''$  using thermal analysis software (TA Instrument Universal Analysis 2000) included with the DMA apparatus to analyse the data. The software automatically detects using the signal change on the analysis curve. The inflection point on the curve of the modulus can be considered as the glass transition and it is determined by using the tangent of the onset point and the end point [218, 219]. 3 different were performed for each film formulation throughout this paper.

### **2.3.3. Determination of the glass transition temperature ( $T_g$ )**

The DMA machine was set to the multi-strain mode using the tensile film clamp at a single-frequency temperature ramp of 1 Hz and a ramp rate of 3°C per min. The glass transition temperature was recorded at a temperature range of 25 °C to 80 °C using a ramp rate of 3 °C per min, a fixed frequency of 1 Hz and amplitude of 10  $\mu\text{m}$ .

### **2.3.4. Determination of storage and loss modulus**

Using the tensile film clamp, the DMA machine was set to the multi-strain mode. The real (storage) modulus  $E'$ , imaginary (loss) modulus  $E''$ , and loss factor  $\tan \delta$  were recorded as a function of increasing temperature from 25 °C to 80 °C using a ramp rate of 3 °C/min, a fixed frequency of 1 Hz and an amplitude of 10  $\mu\text{m}$  using thermal analysis software (TA Instrument Universal Analysis 2000) included with the DMA apparatus.

### **2.3.5. In vitro drug release**

PVA film samples (2% and 5% fluorescent NP-loaded films cut to around 20 mg) were suspended in 1 mL release medium (PBS pH 7.4). The fluorescent NP-loaded film suspension was transferred to an orbital shaker maintained at 37 °C at a speed of 100 rpm (VWR, Edmonton, Canada). 200 µL aliquot of samples were periodically removed for analysis and were replenished with equal volume of fresh medium. The fluorescent NP concentration in the samples was analyzed on a microplate reader (BioTek Synergy) with an excitation wavelength of 530 nm and an emission wavelength of 590 nm. Samples were taken and analyzed in triplicate for each time point. Films disintegration have been evaluated also by immersing 50 mg of each film in 3 mL of ddH<sub>2</sub>O in 20 mL vial and place in the orbital shaker at 37 °C at a speed of 100 rpm. Visual inspection is used to record the disintegration rate.

### **2.3.6. Determination of mechanical properties**

Mechanical analysis was performed on an Instron tensile machine model 5943 with a crosshead speed of 100 mm/min and a force of 1 kN at room temperature. All the film samples were cut into rectangular shapes with a length of 30±0.3 mm, a width of 6.80±0.7 mm, and a thickness of 0.07 mm for the 2% film and a thickness of 0.16 mm for the 5% film.

### **2.3.7. Scanning electron microscopy**

Scanning electron microscopy (SEM) studies were carried out using a Quanta 650 FEG equipped X-ray microanalysis with low-vacuum capabilities at a voltage of 10 keV. Film samples were cut into small pieces and attached to slab surfaces with double-sided adhesive tape.

## 2.4. Statistical analysis

Data are presented as mean  $\pm$  standard deviation (SD). The n-value refers to number of replicates performed for each study. One-way ANOVA was performed on all results, with  $P < 0.05$  considered to be significant.

## 2.5. Results

The storage and loss modulus of various 2% and 5% PVA film formulations were determined (Figure 2.1). Based on the results, the storage modulus for both 2% and 5% blank films were slightly higher than their counterpart films loaded with NP. The storage modulus of 2% blank film varied between  $22.3 \pm 5$  to  $13.9 \pm 3$  MPa for a temperature ramp from 30°C to 60°C and  $143.24 \pm 14.18$  to  $82.63 \pm 5.43$  MPa for 5% blank film at the same temperature ramp. Furthermore, the storage modulus for films containing 3 mg of NP was also higher than the ones containing 5 mg of NP. PVA films containing 3 mg and 5 mg of NPs vary between  $15.67 \pm 2.08$  to  $10.07 \pm 1.35$  MPa and  $12.72 \pm 5.29$  to  $8.15 \pm 3.70$  MPa, respectively. The storage modulus decreased gradually as the temperature increased. The mean storage and loss modulus are presented in Figures 2.2A and 2B, respectively. The sharpest slope of the storage modulus (detected by TA Instrument Universal Analysis 2000 software) was used to determine the glass transition temperature where the film began the transition from a glassy state to a more rubbery state. The mean glass transition temperatures for each film as determined using the storage modulus is presented in Figure 2.2A. As can be seen in Table 2.1, 2% PVA films loaded with either 3 mg ( $53.25 \pm 2.86$  °C) or 5 mg ( $54.10 \pm 7.63$  °C) NP exhibited higher mean glass transition temperatures compared to 5% PVA films with 3 mg ( $40.05 \pm 2.09$  °C) or 5 mg ( $42.07 \pm 2.21$  °C) NP, respectively (Table 2.1), when using

the storage modulus for determination. In contrast, no significant differences were observed in any of the film groups when determining glass transition temperature using the loss modulus (Table 2.1B).

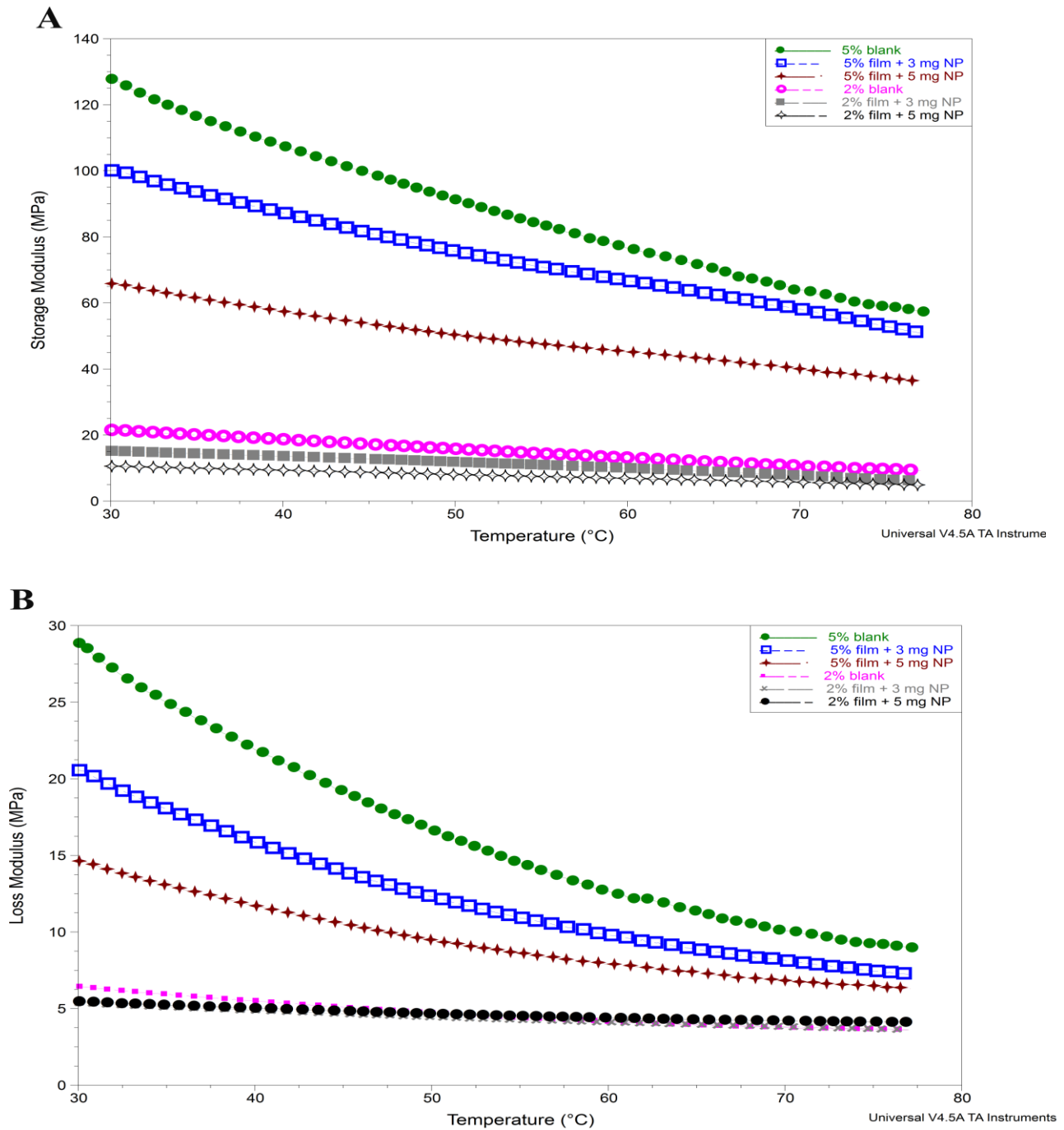


**Figure 2.1: Determination of storage and loss modulus of film samples (Plot from DMA analysis software).** Variation in (A) storage and (B) loss modulus for 2 and 5% PVA blank films or films containing 3 mg or 5 mg of NP. Data were plotted using TA Instrument Universal Analysis 2000 software.

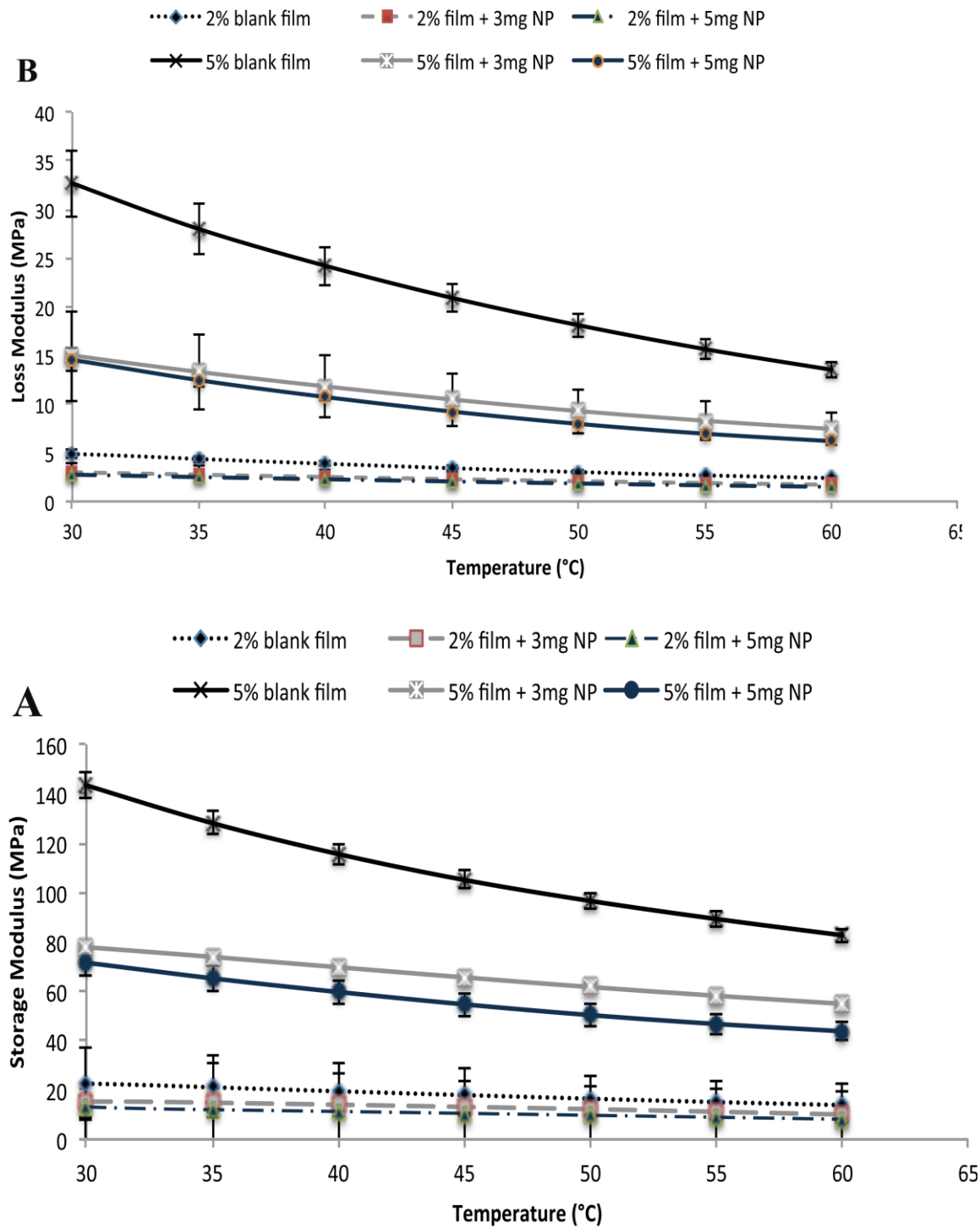


**Figure 2.2: Determination of storage and loss modulus of film samples.** (A) storage modulus and (B) loss modulus of 2% and 5% PVA films loaded with 3 mg or 5 mg NPs. Data represent the mean  $\pm$  SD (N=3)

**Table 2.1: Glass transition temperature determined using two different parameters**

(A) storage modulus and (B) loss modulus. Data represent mean± SD (N=3).

**A**

Glass Transition (°C)	Blank Film	3 mg NP loading	5 mg NP loading
2% PVA film	39.61 ±2.76	53.25±2.86	54.10±7.63
5% PVA film	37.57±0.28	40.05±2.09	42.07±2.21

**B**

Glass Transition (°C)	Blank Film	3mg NP loading	5mg NP loading
2% PVA film	37.94 ±0.1	36.89±3.48	40.14±4.01
5% PVA film	36.88±1.4	37.81±0.12	37.7±0.32

Disintegration studies were performed on blank PVA films and films loaded with 3 or 5 mg of NP. 50 mg of each film was immersed in 3 mL of PBS buffer and placed in an incubator shaker at 37°C and 100 rpm (Table 2.2). 2% PVA films with 3 or 5 mg loading disintegrated within 3 hr making the medium cloudy. The 5% PVA films containing 3 or 5 mg loading partially disintegrated even after 24 hours with no changes to the transparency of the medium.

**Table 2.2: Disintegration time for PVA films.**

PVA films	2% blank	2% film + 3mg NP	2% film + 5mg NP	5% blank	5% film + 3mg NP	5% film + 5mg NP
Disintegration time	3h	3h	3h	Partially after 24h	Partially after 24h	Partially after 24h

In vitro release studies were performed on different film preparations. The amount of fluorescent NPs released was evaluated using a microplate reader (Figure 2.3). Figure 2.3 represents the release obtained from 2% PVA films loaded with 3 mg or 5 mg of NPs and 5% films loaded with 3 mg or 5 mg. 2% films demonstrated a release of  $18.92 \pm 5.6 \mu\text{g}$  ( $8.7 \pm 0.7 \%$ ) for 5 mg NP loading and  $11.48 \pm 1.5 \mu\text{g}$  ( $9.8 \pm 0.5 \%$ ) for 3 mg NP loading after 4 hours followed by a slow and negligible release up to 24 hours. There was a slow release of NPs up to 24 hours with  $6.8 \pm 0.8 \mu\text{g}$  ( $3.25 \pm 0.39\%$ ) for 5% film formulation containing 5 mg NPs loading and  $4.13 \pm 0.36 \mu\text{g}$  ( $3.15 \pm 0.27\%$ ) for 3mg of NPs loading.



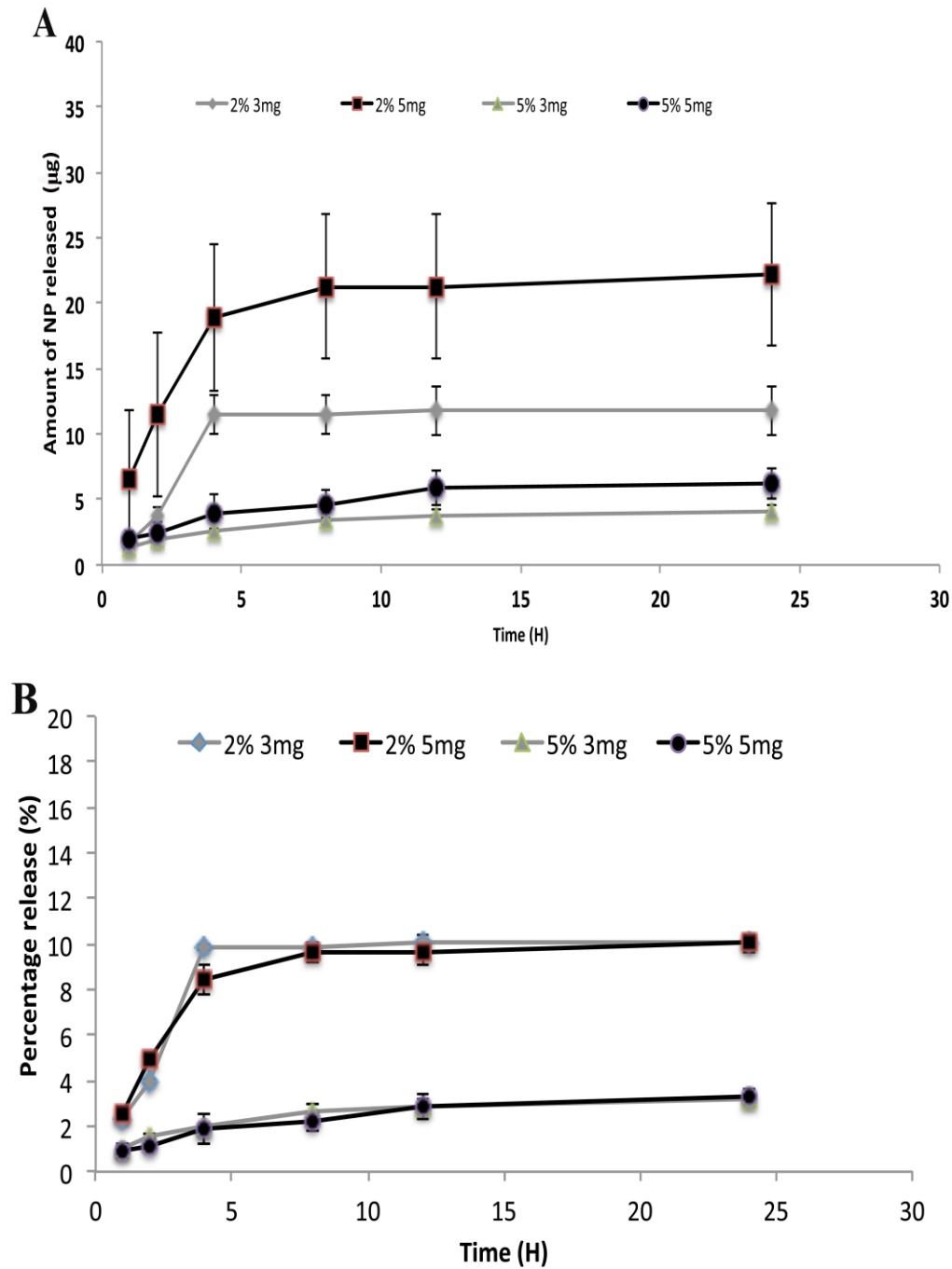


**Figure 2.3: In vitro cumulative release of 2% and 5% PVA films loaded with 3mg or 5mg fluorescent NPs. (A) Amount of NP released (B) Percentage of NPs released. Data represent mean  $\pm$  SD (N=3)**

Tensile properties such as Young’s modulus, maximum load at break, tensile strain at maximum load and tenacity (used to measure the overall strength) of the film at maximum load has been calculated from stress-strain curves (Table 2.3). 2% blank films have a tensile strain at maximum load of 0.162 mm/mm, and 0.151 mm/mm for films containing 3 mg NP loading and 0.134 mm/mm for films containing 5 mg NP loading. The 5% blank films demonstrated to have lower tensile strain and started to break at 0.037 and 0.043 mm/mm for the 3 mg and 5 mg NP loading, respectively. 2 % PVA films present more elasticity but start breaking at lower load, around 1N compared to 5% PVA film, which started to break around 7N. The 5% PVA film is less elastic, and broke at only 1 mm of the crosshead displacement distance compared to the 2% film which broke after 4 mm of extension.

**Table 2.3:** Mechanical properties measured at room temperature for 2% and 5% PVA films loaded with 3 mg or 5 mg NPs. Data represent mean± SD (N=3). N/Tex= Tenacity; Maximum Load in Newton (N)

	<b>Tensile strain (Extension) at Break (Standard) [%]</b>	<b>Maximum Load [N]</b>	<b>Modulus (Automatic Young's) [MPa]</b>	<b>Tensile strain at Maximum stress [%]</b>	<b>Tenacity at Maximum load [N/tex]</b>
<b>2% blank</b>	36.83±5.03	1.2±0.1	10.5±2.4	13.1±2.78	1.14±0.14
<b>2% film + 3mg NP</b>	41.03±5.36	0.86±0.15	7.36±0.77	16.23±2.5	1.16±0.2
<b>2% film + 5mg NP</b>	41.36±4.92	1±0.2	8.33±1.15	13.8±2.42	1.06±0.05
<b>5% film blank</b>	28.76±1.5	7.23±0.49	128.2±18.37	5.24±0.87	7.68±0.72
<b>5% film + 3mg NP</b>	28.03±5.46	6.1±1.1	153.66±15.97	4.63±0.86	6.61±0.98
<b>5% film + 5mg NP</b>	25.76±2.03	7.16±0.3	133.03±18.94	5.76±2.1	6.52±1.14

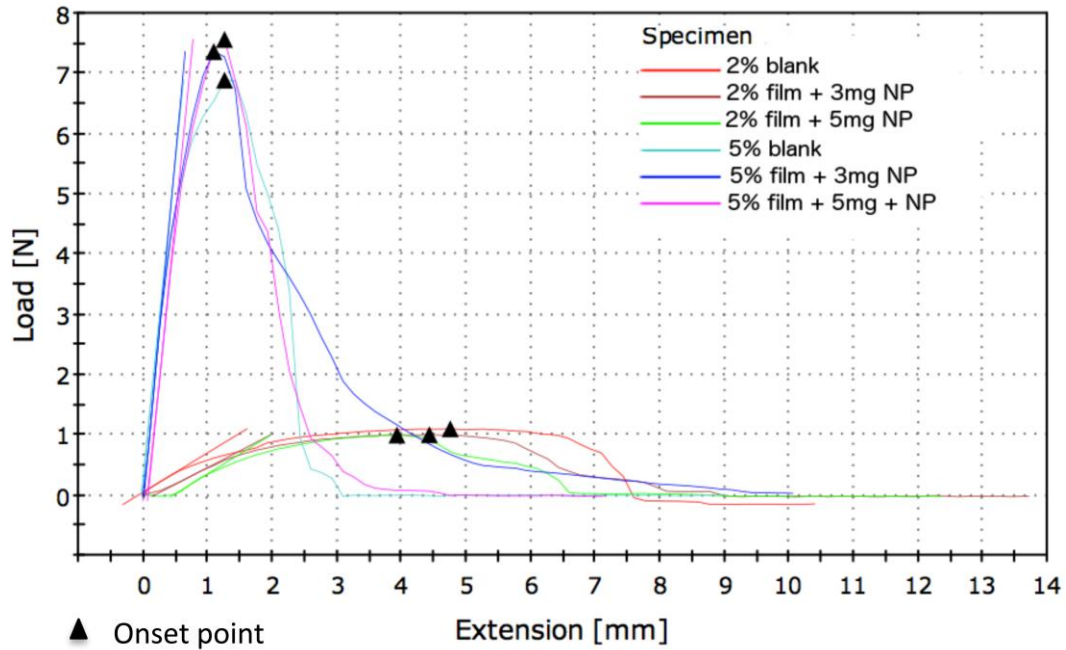


**Figure 2.4: Tensile strain of 2% and 5% PVA films loaded with 3 mg or 5 mg of NPs.** The onset point represents the moment the film started to tear. Load in Newton (N).

The surface morphology of each film was visualized by their SEM images. The 2% blank film presents some porous structure, which is less obvious on 3mg and 5 mg NP, loaded films. The 5% PVA films present a much compact structure with very few porous structures.

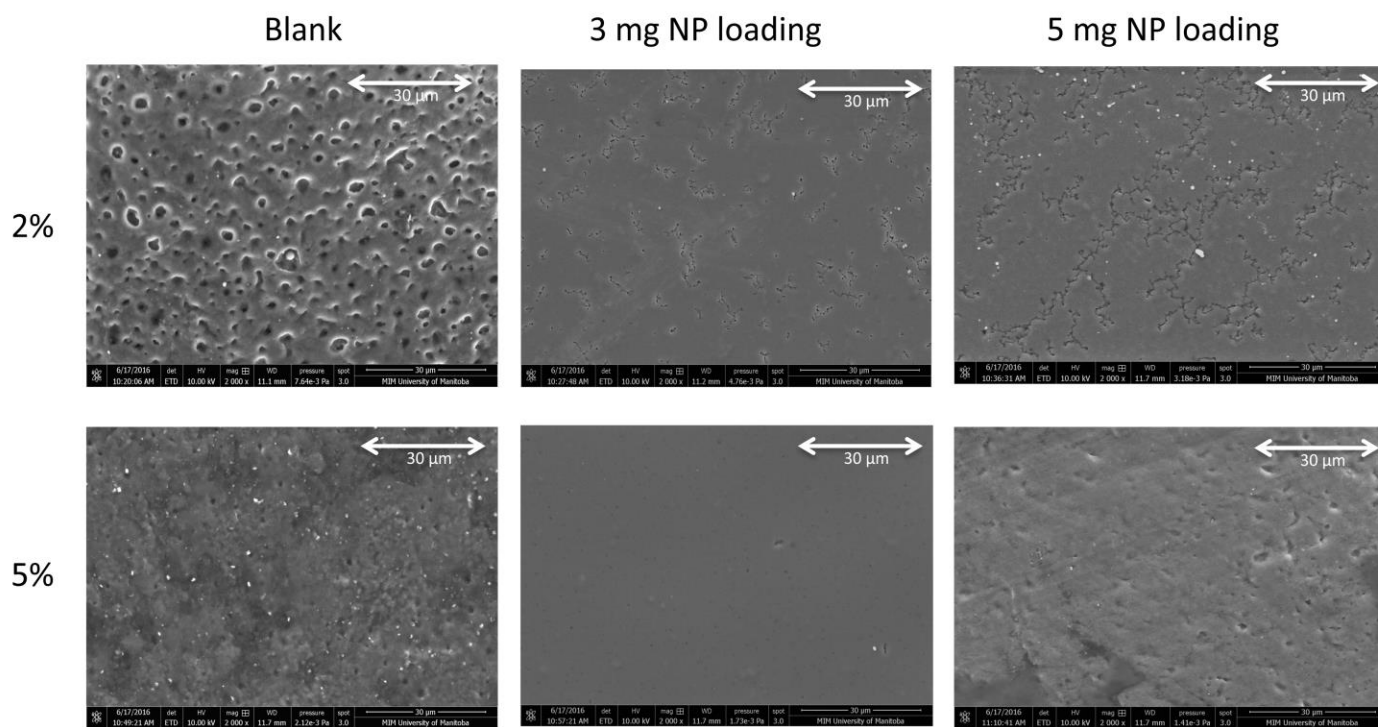


**Figure 2.5: SEM images of 2% and 5% PVA films containing 3 mg or 5 mg of NP loading (2000 X).**

## 2.6. Discussion

Vaginal films have been developed for multiple purposes and present many advantages, but the films must be designed in a specific way to be acceptable, usable, and stable [220]. For vaginal films, it must possess certain characteristics so that it will not cause irritation or toxicity, must be flexible enough to be easily handled by the patient and more importantly, must allow the active compound to be released at a given time frame for a therapeutic effect. In this study, we determined the mechanical properties of PVA films containing NPs as previously developed [205]. The film formulation using PVA and two different plasticisers (PEG 400 and glycerol) produce

films that are smooth and slightly transparent. Different percentages of PVA produced different film thicknesses, which can play an important role in the thermodynamic properties of a film. In this study, we maintained the quantity of plasticisers constant and changed the amount of PVA or NP loading and evaluated its effects on the mechanical properties of the films. The disintegration study presented in Table 2.2 showed that the 2% PVA film formulation broke down completely in 3 h. The amount of NPs loaded into the films appeared to have no impact on the rate of disintegration but in contrast, the ratio of PVA/plasticiser used had an influence. Jun-Seo et al (2000), reported that the plasticising effect of PEG400 on PVA will make the film more flexible, and disintegrate more easily [209]. The film formulation containing 5% PVA was composed of a lower ratio of plasticiser/PVA. These films were thicker, can swell and partially break down after 24 h. A release study using fluorescent NP as presented in Figure 2.3 correlated with the disintegration study. The 2% film formulation, which disintegrated faster, showed the highest concentration of NPs released after 4 h. This release increased slowly until 8 h and remained constant until 24 h. The higher NP released represents a very low percentage which can probably be explained by a rapid decay of the fluorophore used to fabricate the commercial PLGA NP during the film fabrication process and the release study. Films loaded with 5mg of NP exhibited higher release of NP compared to 2% and 5% PVA films loaded with 3mg NP. Films formulated using 5% PVA exhibited a lower NP release profile which appears to be related to the slower disintegration rate in comparison to 2% films. To further analyze the mechanical properties of the films, we used DMA to evaluate the storage modulus, which is a measurement of the elastic response of a material, and the loss modulus, which is the measurement of the viscous response of a material. Storage modulus and loss modulus are two parameters that we used to determine the transition temperature of the films. TA Instrument Universal Analysis 2000 software is used to

integrate all curves in order to determine the glass transition derived from the storage and loss modulus. From looking at Figure 2.1A the presence of NPs in the film matrix affect the physical properties of the film, in addition to plasticizers can reduce intermolecular forces, increasing the mobility of polymer chains. This can decrease the storage modulus of the film and also affect the glass transition temperature as described by Ding et al. [221]. Less plasticizer gave a higher storage modulus as seen in with the 5% PVA film formulation compared to 2%. Based on the results, it appears that as we incorporate more PLGA NPs into the matrix of PVA, it will tend to make the films less stiff. We also evaluated the loss modulus, which measures the energy dissipated as heat in order to determine the glass transition temperature of the polymeric film. Glass transition temperature determined using the storage modulus presents a transition state of blank films around 40°C. This transition state remained constant for 3 mg and 5 mg NP film loading in 5% PVA film formulation. A small increase in glass transition temperature was observed for 2% PVA films loaded with 3 and 5 mg of NPs, which is around 50°C. This means that the 2 % PVA films loaded with NPs became more amorphous (semi-crystalline polymer) at a slightly higher temperature than 5% films containing the same loading of NPs. This might be due to the restriction of the NPs on the mobility of matrix segments of the film [222]. We also determined the glass transition temperature using the loss modulus. All the transition temperatures using the loss modulus occurred around 38°C (Figure 2.2B). There was no significant difference between 2% and 5% PVA film formulations, either loaded with or without NPs. The amount of NPs loaded in the films did not have a significant impact on the glass transition temperature range. This shows that a transition takes place within the 38-50°C temperature range. A wide temperature range was chosen (up to 80 °C) to perform the thermal studies to mimic extreme conditions in which the film may potentially be subjected to e.g. countries with elevated ambient temperatures and inside a parked

car where the temperature can rise up to 80 °C [223]. Those conditions will affect the film stability and in some cases render them unusable. When looking at the mechanical properties of the films, 2% films, which are very elastic due to the ratio of plasticizer present, were very fragile and broke at a load of 1 N. On the other hand, 5% films were less elastic because of the lower ratio of plasticizer but more rigid, so they break at a load of around 7 N. Compared to 2 % films, they supported a load higher than 6.5 N before breaking. The presence of NPs in the matrix of the films appeared to have no major effects on their elasticity. As revealed in the SEM images (Figure 2.5), the blank 2% PVA films appeared to have a more porous structure while 3 mg and 5 mg NP loaded films did not display this property. The porous structures, as explained by Ping et al., are probably due to the shrinkage of the film due to rapid water evaporation while exposed to heat during the film formation [224]. They further explained that under heat, the molecular chains of PVA are inclined to rearrange to form crystalline regions. This may also explain why NP loaded films do not reveal obvious pores since the presence of the NPs in the polymer structure will interact with PVA molecules to prevent shrinkage. The porous morphology is less obvious in 5% films since the PVA ratio is higher but some small pores are visible. Vaginal Contraceptive Film<sup>®</sup> (VCF) (Apothecus Pharmaceutical) is a commercially available PVA based film containing glycerine as a plasticiser and N9 as a spermicide [225]. This film has been reported to have a relatively hard texture and having sharp edges [226]. Those sharp edges and hard texture can potentially cause trauma to the female genital tract before the film is dissolved. In an effort to make our product softer and more pleasant for the user, we added PEG400 to supplement glycerol. The VCF film on the other hand exhibits faster dissolution compared to our formulation, which suggest that the viscoelasticity of PEG400 affects the film disintegration time.

## **2.7. Conclusion**

The present study focused on the viscoelastic and mechanical behaviour of PVA films formulated along with NP for potential applications in vaginal drug delivery. The amount of PVA in the film formulation plays an important role on the film disintegration and the release of the NPs. The presence of the NPs in the film matrix did not alter much the mechanical behaviours. The presence of plasticisers, PEG 400 and glycerol enhance the films flexibility, which also play an important role in the rate of film disintegration and can influence the rate of NP release from the films. Hence, film formulations can be customized for the controlled release of NPs with the desired viscoelastic and mechanical properties suitable for vaginal drug delivery. 2% film formulation is ideal for a fast disintegration and drug release while 5% film formulation is ideal for slower and prolonged release time.



## **Chapter 3: Evaluating the impact of hydroxychloroquine-loaded polyurethane intravaginal rings on lactobacilli**

Adapted from the following research article:

Yannick Traore, Yufei Chen, Anne-Marie Bernier, and Emmanuel A. Ho  
*Antimicrob Agents Chemother* 59:7680 –7686. doi:10.1128/AAC.01819-15.

### **3.1. Abstract**

The use of polymeric devices for controlled, sustained delivery of drugs is a promising approach for the prevention of HIV-1 infection. Unfortunately, certain microbicides, when topically applied vaginally, may be cytotoxic to vaginal epithelial cells and the protective microflora present within the female genital tract. In this study, we evaluated the impact of hydroxychloroquine(HCQ)-loaded, reservoir-type, polyurethane intravaginal rings (IVRs) on the growth of *Lactobacillus crispatus* and *Lactobacillus jensenii* and on the viability of vaginal and ectocervical epithelial cells. The IVRs were fabricated using hot-melt injection molding and were capable of providing controlled release of HCQ for 24 days, with mean daily release rates of  $17.01 \pm 3.6 \mu\text{g/mL}$  in sodium acetate buffer (pH 4) and  $29.45 \pm 4.84 \mu\text{g/mL}$  in MRS broth (pH 6.2). Drug-free IVRs and the released HCQ had no significant effects on bacterial growth or the viability of vaginal or ectocervical epithelial cells. Furthermore, there was no significant impact on the integrity of vaginal epithelial cell monolayers, in comparison with controls, as measured by transepithelial electrical resistance. Overall, this is the first study to evaluate the effects of HCQ-loaded IVRs on the growth of vaginal flora and the integrity of vaginal epithelial cell monolayers.

### **3.2. Introduction**

Based on a study conducted on 3400 women in the United States by the National Health and Nutrition Examination Survey showed that 29% of women within the age of 14-49 live with bacterial vaginosis (BV), the most common bacterial infection of the female genital tract (FGT) [227, 228]. It has been estimated that in 2014, more than 36.9 million people globally are infected with human immunodeficiency virus (HIV) [13]. More than 50% of those infected with HIV are women with heterosexual transmission as the main route of infection [229]. Despite the fact that

BV, HIV, and other sexually transmitted infections occur via the FGT, conventional treatment strategies involve oral administration of drugs. Most of these therapeutic strategies have failed because orally administered drugs can be highly metabolized by the liver before being absorbed into the systemic circulation and reaching the FGT. Increasing the administered dose may not be possible since this can result in severe systemic toxicity. The ideal treatment for infections or diseases affecting the FGT would be to deliver drugs locally via the vagina to increase therapeutic effects while reducing systemic toxicity.

Numerous intravaginal products have been developed for the treatment of local infections including semi-solid ointments, creams, suppositories, and vaginal gels [230, 231]. Studies have shown that patient compliance with respect to semi-solid dosage forms is low [232]. Major drawbacks include the fact that it requires daily applications, can be messy, and there can be leakage of the product resulting in reduced therapeutic efficacy. To overcome some of these issues, specialized drug delivery systems such as intravaginal rings (IVR) have been developed [68]. IVRs can be designed to provide sustained and controlled drug release, ultimately resulting in increased patient adherence [233]. To date, IVRs have been approved by the FDA for contraception and hormone replacement therapy [234]. Recently, researchers have begun investigating the potential application of IVRs as microbicides (products applied topically vaginally for the treatment/prevention of sexually transmitted infections) and for the treatment of bacterial vaginosis [68, 235]. The major advantage of IVRs versus gels or tablets is the fact that IVRs can provide sustained release of drugs (>14 days) for long-term therapy, eliminating the need for daily drug administration [68, 236]. Once the IVR is self-inserted by the patient, it can remain within the FGT for prolonged periods of time and will not interfere with sexual intercourse [112]. Upon completion of the therapy cycle, patients can easily remove the IVR themselves. In order to develop an

effective IVR for therapeutic applications, it is important to take into consideration the nature of the drug and the chosen polymer used for IVR fabrication [67]. For example, IVRs must not have any significant effects on the normal flora of the FGT. Many microorganisms live in the FGT and protect the mucosal environment against pathogenic bacteria. Studies have shown that changes in the level of the lactobacillus family (most abundant flora in the vagina), will lead to the growth of pathogenic bacteria, resulting in inflammation of the FGT [237]. We have previously described the fabrication of a novel reservoir-type IVR for the controlled and sustained delivery of the immunomodulatory drug HCQ as a potential prevention strategy for HIV-1 [68]. The IVR demonstrated no significant impact on the viability of vaginal epithelial cells and on the production of pro-inflammatory cytokines in vitro. However, the effect of developed system on microflora and the integrity of vaginal epithelial cell monolayer were not addressed. Since these are critical parameters for the development of a biocompatible microbicide, the current study investigated the effects of drug-free IVRs and HCQ-loaded IVRs on vaginal lactobacilli, the main components of the normal vaginal flora, as well as the integrity of the vaginal epithelial cell monolayer. This is the first study to evaluate the effects of HCQ-loaded IVRs on the growth of vaginal flora.

### **3.3. Materials and Methods**

#### **3.3.1. Materials**

*Lactobacillus jensenii* (ATCC 55920) and *Lactobacillus crispatus* (ATCC 33820) were purchased from American Type Culture Collection (ATCC, Rockville, Maryland, USA). Lactobacilli MRS broth and agar were obtained from Thermo Fisher Scientific (Waltham, MA, USA). Medical grade non-biodegradable polyether urethane (PU) Tecophilic® HP-60D-35 and HP-93A-100 were purchased from Lubrizol (Wickliffe, OH, USA). HCQ was purchased from TCI

America (Portland, OR, USA). HPLC grade water, methanol, and acetonitrile were obtained from VWR International LLC (Batavia, IL, USA). Methocel™ K100M premium hydroxypropyl methylcellulose (HPMC) was kindly supplied by the Dow Chemical Company (New Milford, CT, USA). Human vaginal epithelial cell line VK2/E6E7 (ATCC CRL-2616), human ectocervical epithelial cell line Ect1/E6E7 (ATCC CRL2-614) and human CD4<sup>+</sup> T-cell line Sup-T1 (CRL-1942) were obtained from ATCC. Keratinocyte-serum free medium (K-SFM), recombinant human epidermal growth factor and bovine pituitary extract were obtained from Life Technologies (Carlsbad, CA, USA). Trypsin-EDTA, penicillin/streptomycin solution and fetal bovine serum (FBS) were purchased from Gibco® Life Technologies (Burlington, ON, Canada).

### **3.3.2. Fabrication of IVRs**

PU HP-60D-35 and PU-93A pellets were dried overnight at 80°C in an oven prior to the fabrication of IVRs. The pellets were melted using a hot-melt injection molder at 160°C for PU-60D and 140 °C for PU-93A and then directed into a pre-heated mold (Cardatech, Alexandria, VA, USA) for the fabrication of macaque and human size reservoir-type IVRs (Figure 3.1). The outer diameter for the macaque-size IVRs is 25 mm, and the cross-sectional diameter is 5 mm. The wall thickness of the IVRs is 0.75 mm. A digital caliper was used for all measurements.



**Figure 3.1: Aluminum mold for the fabrication of reservoir-type IVR segments.** The mold can produce segments for a large human size IVR (55 mm outer diameter and 5.5 mm cross-sectional diameter) and a small macaque size IVR (25 mm the outer diameter and 5 mm the cross-sectional diameter). The wall thickness for both IVRs is 0.75 mm. IVR segments were fabricated using hot-melt injection molding of HP-60D-35 PU and HP-93A-100.

### **3.3.3. HCQ/HPMC semi-solid preparation and HCQ extraction**

The lumen of the IVR segments (PU-60D and PU-93A) was filled with HCQ/HPMC semi-solid at a 1:1 ratio. Briefly, HCQ/HPMC was prepared by weighing 160 mg of HCQ and dissolving in 1.28 mL of distilled water. 160 mg of HPMC was then added to the dissolved HCQ and gently mixed with a spatula. The mixture was then transferred into a 5 mL syringe connected to a second syringe via tubing. The contents of the syringe were passed back and forth for 80 passes to allow homogenous mixing. Drug extraction was performed on random aliquots of the semi-solid mixture and analyzed using high-performance liquid chromatography (HPLC) to confirm homogeneity (See below for HPLC method). The HCQ/HPMC mixture ( $10 \pm 5$  mg) was then diluted with 1 mL of distilled water in a microcentrifuge tube and vortexed at 2000 rpm at 4°C overnight. The concentration of HCQ was then analyzed by HPLC. All downstream studies were done using the polymer presenting the best release profile.

### **3.3.4. HPLC Method**

Quantification of HCQ was determined using a reversed-phase HPLC method as previously described (8). Briefly, a Shimadzu LC-2010A HPLC machine was used with a Waters Nova-Pak C18 column (4  $\mu$ m, 3.9 x 150 mm) in isocratic condition. The mobile phase included methanol, acetonitrile and 58 mM sodium phosphate dibasic containing 15 mM heptanesulphonic acid (4:22:74, v/v). The pH was adjusted to 3.1 using concentrated phosphoric acid. The flow of the mobile phase was maintained at 1 mL/min and the column at 25°C for a run of 15 min with 40  $\mu$ L of sample injected. The peak for HCQ appeared around 13 min.

### **3.3.5. In vitro release studies**

HCQ-loaded IVR segments were sealed at both ends with silicone caps to prevent leakage and to mimic drug release from a “complete” IVR that does not have exposed ends. First, the release profiles of PU-60D and PU-93A were compared in sodium acetate buffer before choosing the suitable polymer for the rest of the studies. The segments were then sterilized using 70% isopropanol and dried in a biosafety cabinet overnight. The segments were placed in 5 mL of 25 mM of sodium acetate buffer (pH 4) and placed in an incubating shaker (37°C; 100 rpm). Every 24  $\pm$  0.5 h, a sample of the release buffer was collected and buffer was replenished to maintain sink conditions. HPLC was used to evaluate the concentration of HCQ in each sample. PU-60D presenting the suitable release profile, was used for the rest of the studies. To evaluate the system on bacteria, PU-60D segments were prepared and filled with HCQ semi-solid as described earlier and placed in 5 mL of MRS broth for a period of 24 days and placed in an incubating shaker (37°C; 100 rpm). The sampling and analysing were done as previously described.

### 3.3.6. Sensitivity test of HCQ on Lactobacilli, vaginal/ectocervical epithelial and immune cells

The microtitre broth dilution method was used to determine the minimum inhibitory concentration of HCQ on *Lactobacillus crispatus* and *Lactobacillus jensenii* as previously described with slight modifications [238, 239]. Briefly, bacteria were grown on MRS agar and one colony from the agar plates was transferred into 10 mL of MRS broth. The broth was incubated at 37°C under 5% CO<sub>2</sub> for 24 h. The culture medium was diluted to achieve a concentration of approximately 10<sup>5</sup> CFU/mL. 100 µL of 60 mg/mL of HCQ was added to each well in a 96 well plate and serially diluted to 1.8 mg/mL. Gentamicin (10 µg/ml) and blank MRS broth were used as controls. 5 µL of 10<sup>5</sup> CFU/mL of bacteria was dispensed in all the wells of the plate except one column containing blank MRS broth solution (sterility control and blank for the microplate reader). All plates were incubated at 37°C at 5% CO<sub>2</sub> for 24 h. Samples were analyzed at 580 nm using a microplate reader (Biotek, Winooski, USA).

Ect1/E6E7, VK2/E6E7 and Sup-T1 cells were seeded separately in 96-well plates at a density of 2.5 x 10<sup>5</sup> per well. After 2 h, 100 µL of HCQ or 200 µg/mL of N9 (N-9; positive control) were added into each well for 24 h. MTS reagent (40 µL) was added and the optical density of each well was analyzed at 490 nm after 1 h. Data were normalized and expressed as a percentage of the mean value of the negative control (untreated cells).



### 3.3.7. Cytotoxicity evaluation of IVR segments on lactobacilli and vaginal/ectocervical cell lines

An elution assay was used to evaluate the cytotoxicity of drug-free IVR segments on bacteria. Briefly,  $100 \pm 0.5$  mm IVR segments were sterilized in 70% isopropanol for 10 sec and dried in a sterile biosafety cabinet. The segments were transferred aseptically into 10 mL of sterile PBS and incubated at 37°C for 1, 7, 15, and 30 days at 100 rpm in an orbital shaker. The supernatant was collected aseptically and filtered through 0.2  $\mu$ m syringe filters and stored at -80°C in 15 mL tubes until further analysis. 5  $\mu$ L ( $10^5$  CFU/mL) of the diluted *Lactobacillus crispatus* and *Lactobacillus jensenii* were seeded in 96 well plates containing 100  $\mu$ L of medium at a ratio of 1:3 elution medium to growth medium (18). 100  $\mu$ L of the positive control (gentamicin 10  $\mu$ g/mL) and blank MRS broth solution were added as well. All plates were incubated at 37°C at 5% CO<sub>2</sub> for 24 h and samples were analyzed using a microplate reader at 580 nm.

IVR segments loaded with HCQ/HPMC were immersed in isopropanol for 10 min to prevent any contamination from external bacteria, and dried overnight in a biosafety cabinet. The segments were then placed in 5 mL of MRS broth for different time points (1, 3 and 7 days) at 37°C and shaken at 100 rpm in an orbital shaker. 100  $\mu$ L of broth containing elution media from HCQ-loaded IVR segments were distributed in a 96-well plate for different time points. 5  $\mu$ L of  $10^5$  CFU/mL of *Lactobacillus jensenii* or *crispatus* were added to each well. Sterile MRS broth and MRS broth containing gentamicin (10  $\mu$ g/mL) were used as controls. The 96-well plates were incubated at 37 °C under 5% CO<sub>2</sub> for 24 h and analyzed at 580 nm using a microplate reader.

IVR segments ( $150 \pm 5$  mg) were incubated in 10 mL of K-SFM medium for 30 days. 1 M acrylamide in K-SFM was used as positive control for inducing cell death while plain K-SFM medium was used as a negative control [68]. 100  $\mu$ L of elution medium was used to treat

Ect1/E6E7 or VK2/E6E7 cells ( $2.5 \times 10^5$  cells per well) for 24 h followed by the addition of MTS reagent for 2 h. Optical density of each well was read at 490 nm and data was normalized to the negative control.

### **3.3.8. In vitro evaluation of IVR segments on vaginal epithelial cell layer integrity**

VK2/E6E7 were grown in K-SFM supplemented with 0.1 ng/mL of recombinant human epidermal growth factor, 0.05 mg/mL bovine pituitary extract, 44.1 mg/L calcium chloride and 1% penicillin-streptomycin under 5% CO<sub>2</sub> at 37°C. The cells were transferred onto a cell culture polycarbonate membrane insert (pore size 1 µm) at a density of  $2 \times 10^5$  cells/insert. The cells were seeded in 0.3 mL of culture medium and the inserts were placed in 6-well plates containing 1 mL of medium. The cells were grown on the inserts for 3 days and the cell monolayer integrity was evaluated by measuring changes in trans-epithelial electric resistance (TEER) using a voltohmmeter (Millicell<sup>®</sup> ERS-2, Millipore). After reaching a TEER value of around 30 Ω cm<sup>2</sup> cells were exposed to HCQ-free IVR segments, HCQ-loaded IVR segments, and 50 µg/mL of free HCQ for 2 days. Untreated cells and cells treated with N-9 were used as controls.

#### **Statistical analysis.**

Data are presented as the mean ± standard deviation (SD). The n values refer to the numbers of replicates performed for each study. One-way analysis of variance was performed with all results, with P values of <0.05 considered to be significant.

### 3.4. Results

#### 3.4.1. In vitro release studies

HCQ/HPMC (1:1 wt/wt) loaded PU-93A IVR segments incubated in sodium acetate buffer (pH 4) at 37°C shaken at 100 rpm, demonstrated a high burst release for the first three days and a decreasing release for the remaining days with ~ 3.8 mg of HCQ released in seven days ( $R^2$  value of 0.84). PU-60D presented a sustained release of HCQ over 24 days (Figure 3.3) and was used for the rest of the studies. The daily mean release of HCQ was approximately  $17.01 \pm 3.6$   $\mu\text{g/mL}$  ( $39.19$   $\mu\text{M}$ ) of the initial 4 mg loading, with a cumulative release of  $2041.80 \pm 180.21$   $\mu\text{g/mL}$  ( $4703.30$   $\mu\text{M}$ ) at day 24 (near zero-order release profile with a  $R^2$  value of 0.999). HCQ sulfate has a high water solubility ( $>20$  mg/mL as reported by Sigma Aldrich). We are releasing around 17  $\mu\text{g/mL}$  per day which is 1000x less than the saturation limit. Release studies were also conducted in MRS broth at a pH of 6.2 (Figure 3.3). The release rate in MRS broth was significantly higher than in sodium acetate buffer (P-value  $<0.05$ ) with a daily mean release rate of  $29.45 \pm 4.84$   $\mu\text{g/mL}$  ( $67.86$   $\mu\text{M}$ ) and a cumulative release of  $3534.52 \pm 30.32$   $\mu\text{g/mL}$  ( $8143.79$   $\mu\text{M}$ ) at day 24 (near zero order release profile with a  $R^2$  value of 0.996).

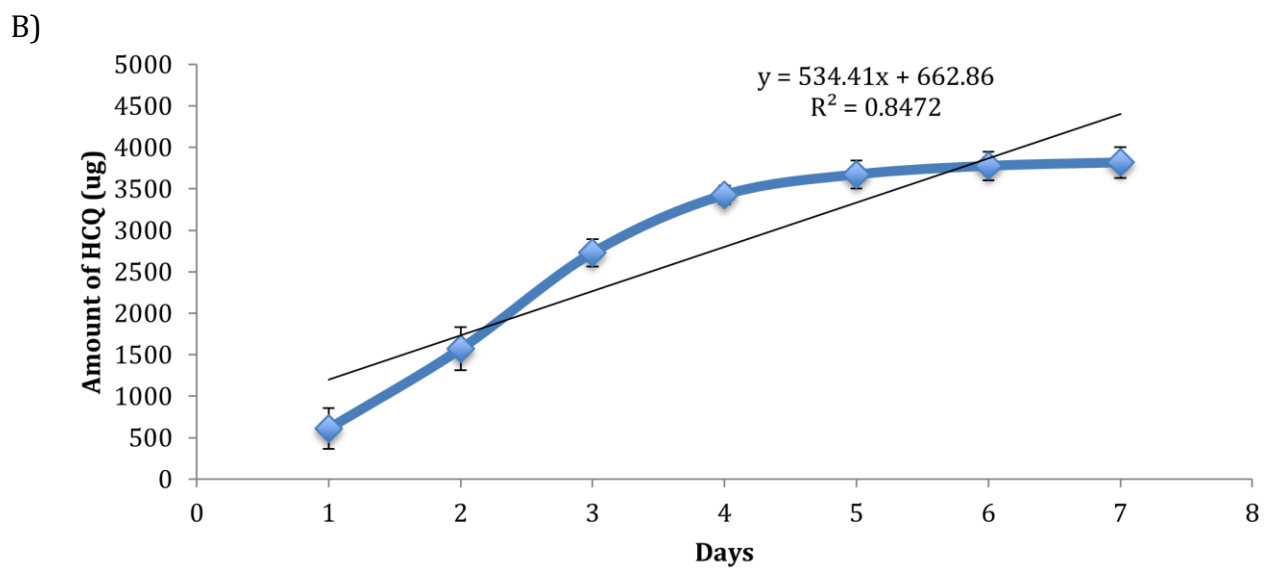
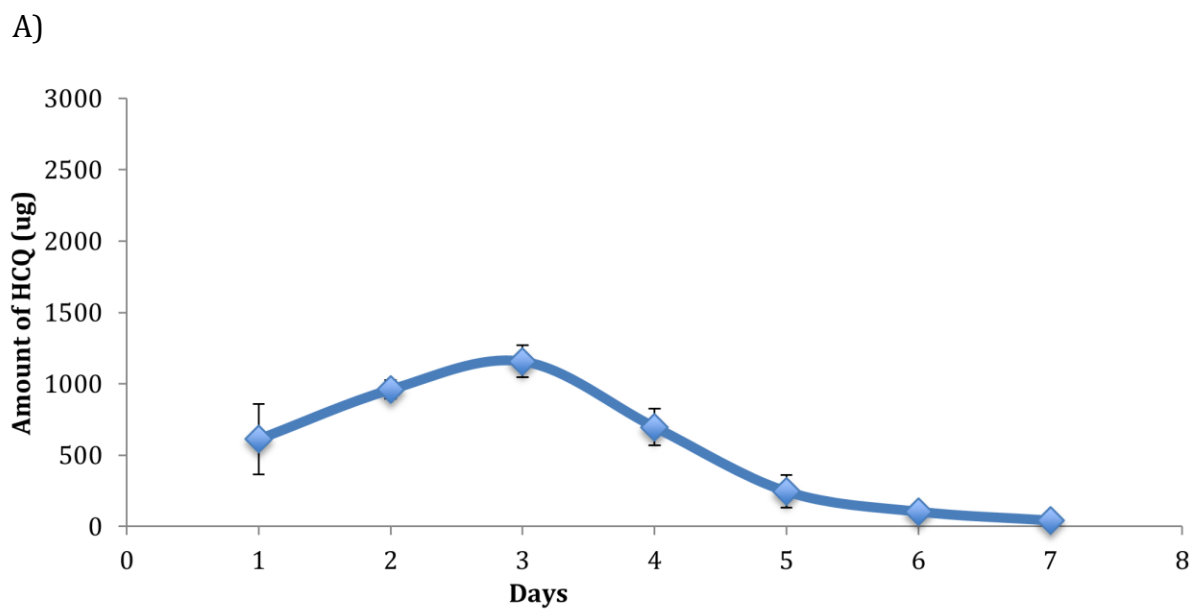


**Figure 3.2: Release study of HCQ in sodium acetate from PU-93A.** (A). Daily release of HCQ from HCQ/K100M (ratio 1:1 wt/wt). Release studies were performed in 5 mL of 25 mM sodium acetate buffer (pH 4). (B) Cumulative release of HCQ from HCQ/K100M (ratio 1:1 wt/wt) IVR segments. Data represent mean +/- S.D. ; N=4

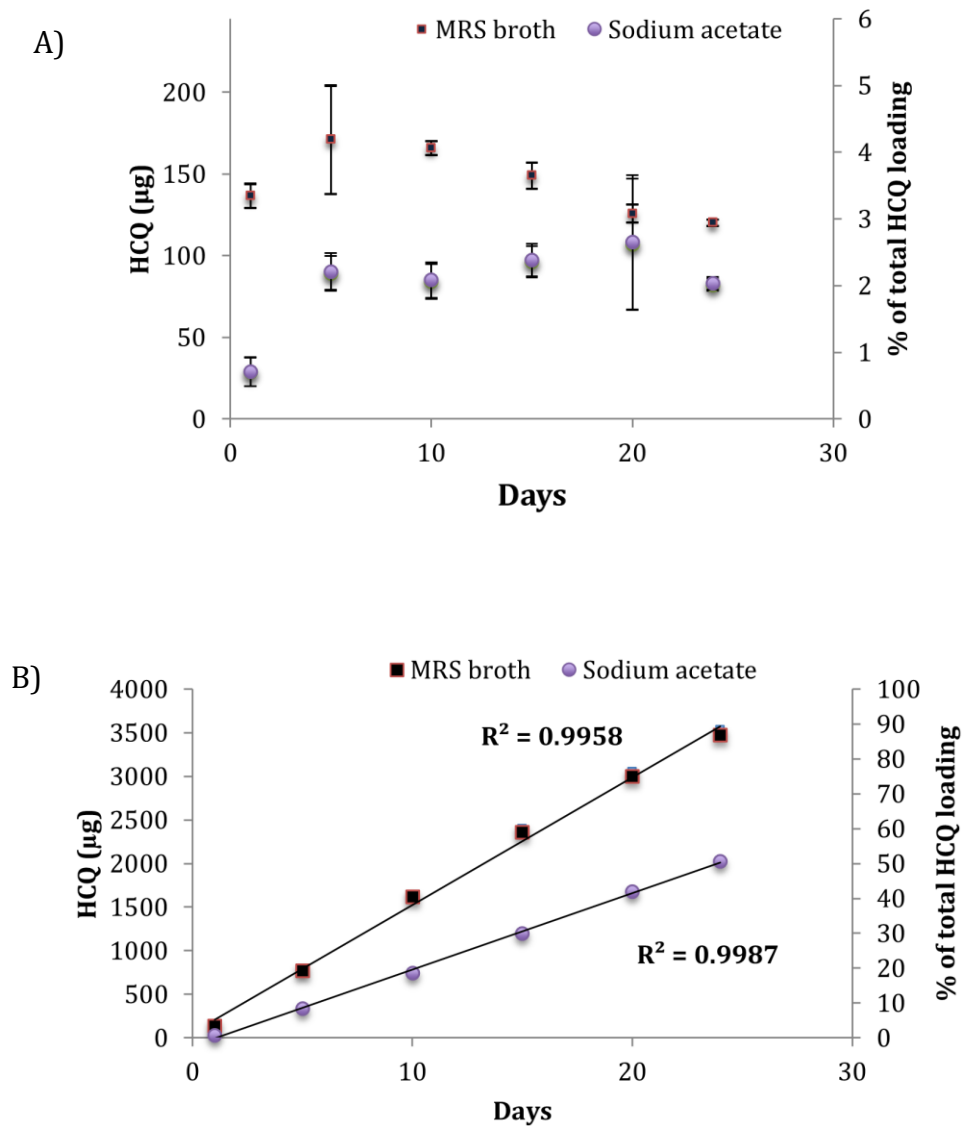


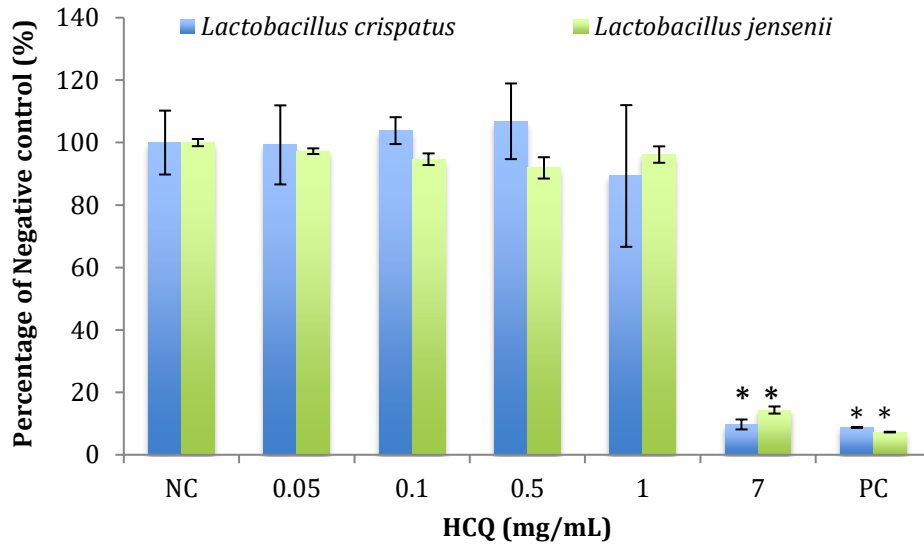
**Figure 3.3: Release study of HCQ in sodium acetate and MRS broth.** (A). Daily release of HCQ from HCQ/K100M (ratio 1:1 wt/wt) IVR segments for 24 days. Release studies were performed in 5 mL of 25 mM sodium acetate buffer (pH 4) or MRS broth (pH 6.2) and shaken on an orbital shaker at 37 °C, 100 rpm. (B) Cumulative release of HCQ from HCQ/K100M (ratio 1:1 wt/wt) IVR segments for 24 days. Data represent mean +/- S.D. ; N=4

### **3.4.2. Sensitivity test of HCQ on Lactobacilli, vaginal/ectocervical epithelial and immune cells**

As shown in Figure 3.4A, 0.05 mg/mL of HCQ (approximately the amount of HCQ released daily from the segment) had no significant impact on the growth of *lactobacillus jensenii* or *crispatus*. Only at a concentration of 7 mg/mL of HCQ (which is more than 100-fold the concentration released daily) was there significant inhibition in growth of both bacteria. The positive control gentamicin (10 µg/mL) inhibited 100% of bacterial growth.

Different concentrations of free HCQ were evaluated on the vaginal and ectocervical epithelial cell lines VK2/E6E7 and Ect1/E6E7, respectively, and on CD4<sup>+</sup> Sup-T1 cells (Figure 3.4B). HCQ concentrations up to 0.01 mM did not elicit any significant cytotoxicity effects. Concentrations of 0.1 mM significantly reduced Sup-T1 viability and concentrations  $\geq 1$  mM significantly reduced cell viability of all three cell lines.

A)



B)

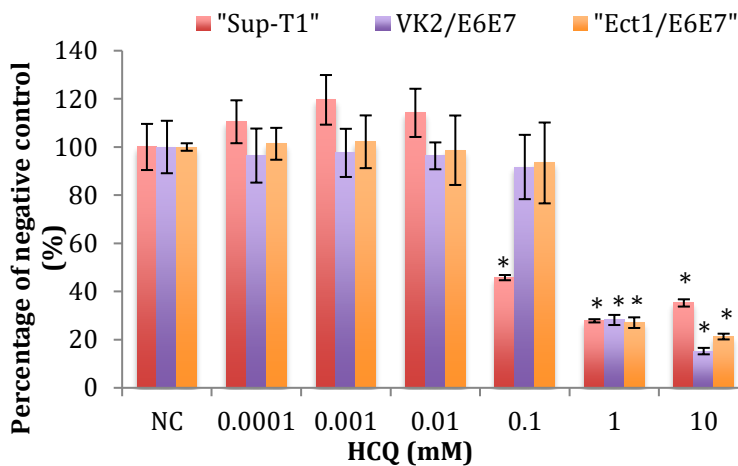


**Figure 3.4: The effects of 24 h HCQ treatment on vaginal normal flora, vaginal ecto-cervical and epithelial cells and CD4+ immune cells.** (A) *Lactobacillus crispatus* and *jensenii*.

Bacterial growth was measured using a microplate reader set at 580 nm. The negative control (NC) was drug-free medium containing bacteria and positive control (PC) was medium containing gentamicin (10  $\mu\text{g}/\text{mL}$ ). Data represent mean  $\pm$  S.D.; N=4; \*P<0.05 vs NC. (B)

Vaginal epithelial cells VK2/E6E7, ectocervical epithelial cells Ect1/E6E7, and CD4+ T-cells Sup-T1. NC consists of cells cultured in drug-free medium and PC consists of 200  $\mu\text{g}/\text{mL}$  N-9.

Data represents mean  $\pm$  S.D.; N=6; \*P<0.05 vs NC

### **3.4.3. Cytotoxicity evaluation of IVR segments on lactobacilli and vaginal/ectocervical epithelial cell lines**

Drug-free IVR segments had no significant impact on the growth of *Lactobacillus jensenii* and *crispatus* after incubation for 30 days (Figure 3.5A) and on the viability of VK2/E6E7 and Ect1/E6E7 cells after 30 days when compared to controls (Figure 3.5B).

HCQ released from the IVR segments significantly reduced the growth of *Lactobacillus crispatus* after day 3 and 7 but no significant changes in the growth of *Lactobacillus jensenii* was observed (Figure 3.6).



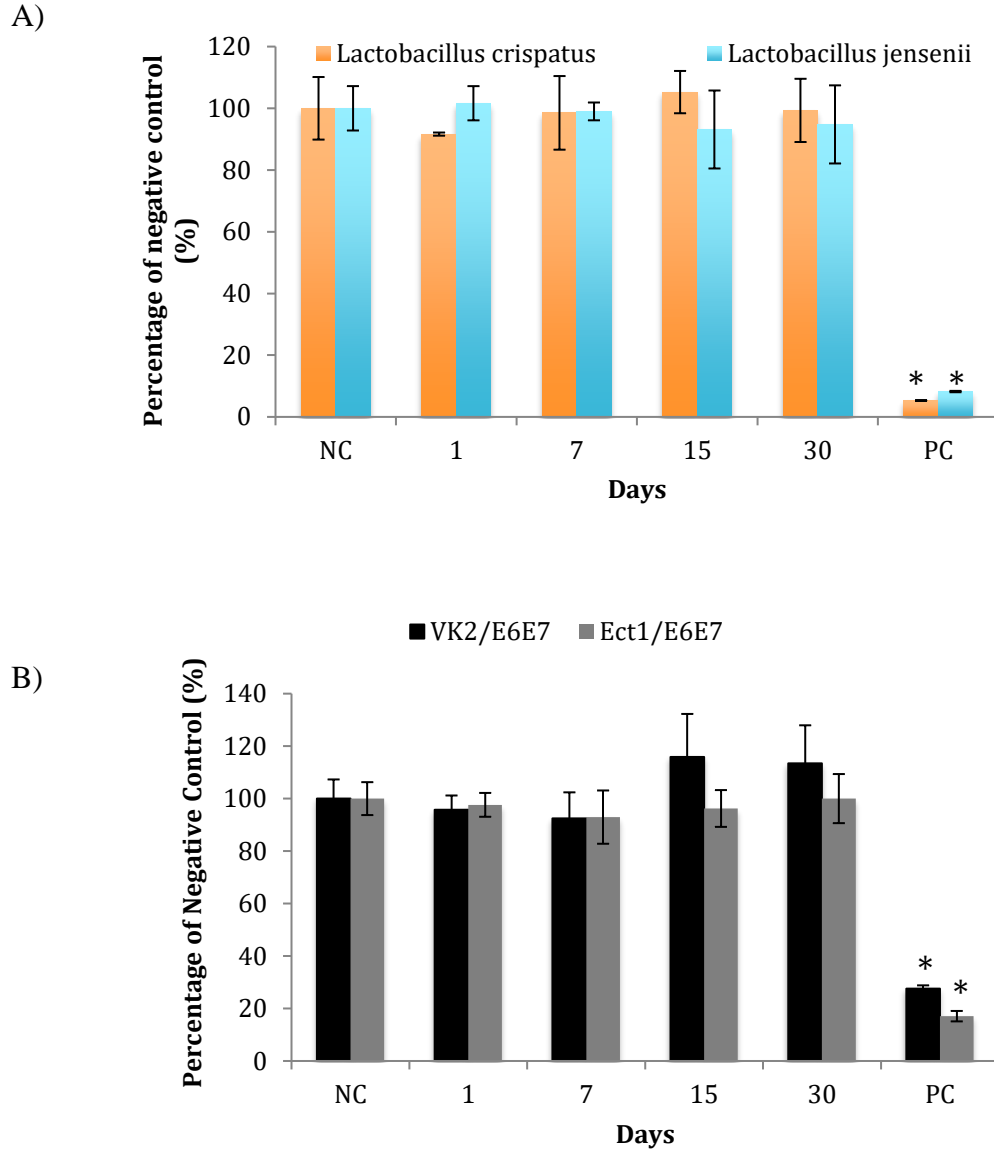


**Figure 3.5: Elution assay on *Lactobacillus crispatus* and *jensenii* and vaginal cells VK2/E6E7 and Ect1/E6E7 .** (A) *Lactobacillus crispatus* and *jensenii* treated with elution media from drug-free IVR segments incubated in culture medium (ratio 1:3 v/v) for 24 h. Bacterial growth was measured using a microplate reader set at 580 nm. The negative control (NC) consists of culture medium containing bacteria and positive control (PC) consists of medium containing gentamicin (10 $\mu$ g/ml). Data represents mean  $\pm$  S.D.; N=3; \* $P$ <0.05 vs NC (B) Cell viability evaluation of VK2/E6E7 and Ect1/E6E7 after treatment with drug-free elution media. NC consists of cells treated with blank cell culture medium and PC consists of 1M acrylamide prepared in culture medium. Data was normalized to the NC and represents the mean  $\pm$  S.D.; N=6; \* $P$ <0.05 vs NC.

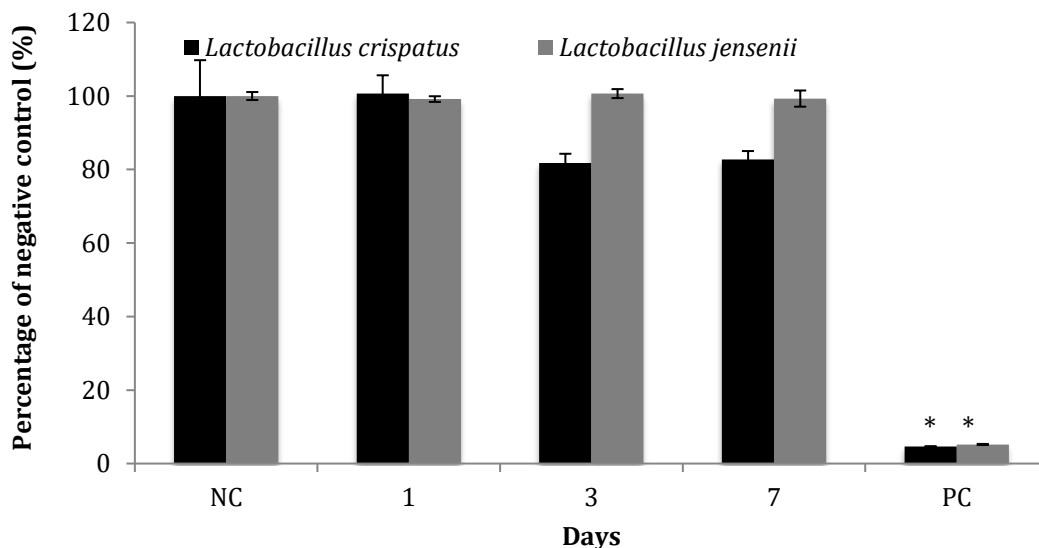


**Figure 3.6: Cytotoxicity study from HCQ released from IVR segment on *Lactobacillus crispatus* and *jensenii*.** *Lactobacillus crispatus* and *jensenii* treated with media for 24 h containing HCQ released from drug-loaded IVR segments at various time points. Bacterial growth was measured using a microplate reader set at 580 nm. The negative control (NC) consists of bacteria treated with drug-free medium and the positive control (PC) consists of bacteria treated with medium containing gentamicin. Data represents the mean  $\pm$  S.D.; N=4; \* $P < 0.05$  vs NC.

#### 3.4.4. Assessment of transepithelial electrical resistance (TEER) of VK2/E6E7

The mean TEER value of an intact monolayer of VK2/E6E7 cells was approximately  $30.55 \pm 1.7 \Omega \text{ cm}^2$ , which is comparable to previously reported values [240]. Figure 3.7 reports the TEER values after treatment with free HCQ (50  $\mu\text{g/mL}$ ), drug-free IVR and HCQ-loaded IVR containing 1 mg/mL of HCQ. No significant differences in TEER were observed with any of the treatment groups in comparison to the negative control after 48 h. The positive control (N-9) decreased TEER by  $37.59 \pm 5.97\%$  after 48 h.

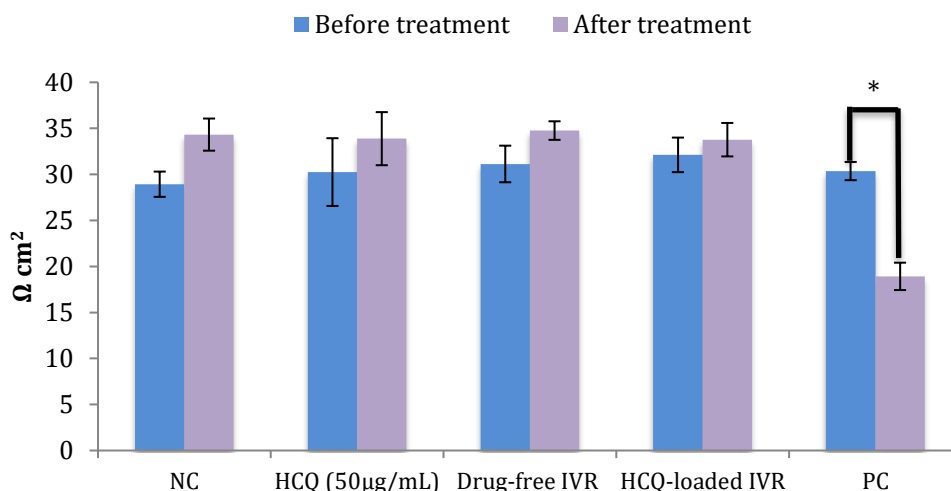


**Figure 3.7: Evaluation of TEER on a monolayer of VK2/E6E7 cells.** The cells were treated with free HCQ (50 μg/mL; 115.2 μM), drug free IVR segments and HCQ eluted from an IVR segment for 48 h. Drug-free medium was used as negative control (NC) and N-9 (1 mg/mL) was used as a positive control (PC). Data represents the mean +/- S.D.; N=3; \* $P < 0.05$  vs before treatment.

### 3.5. Discussion

The FGT is becoming an important site for both local and systemic drug delivery particularly for the prevention of sexually transmitted infections eg. intravaginal microbicides. Benefits of intravaginal delivery include higher drug concentrations locally and a reduction in systemic toxicity. As a result, there is an urgent need to develop an effective and safe microbicide that can prevent HIV-1 infection. Damage to the vaginal epithelial surface due to certain chemicals and drug carriers can cause inflammation of the FGT [241, 242]. Numerous studies have shown that inflammation within the FGT can increase the risk of HIV acquisition, an issue observed with several failed microbicide trials [243, 244]. Furthermore, the majority of in vitro studies evaluating

microbicides have focused on the induction of inflammation in vaginal epithelial and immune cells [245]. There is currently a lack of studies evaluating the impact of microbicides on the natural flora present in the FGT. Among the normal flora that will protect the FGT, lactobacilli are the main type of bacteria that set the balance between pathogenic bacteria and the normal flora. A decrease in lactobacilli encourages an overgrowth of pathogenic bacteria and can lead to inflammation [121, 246, 247]. For example, studies have shown an increased risk of HIV infection in women with vaginitis and susceptibility to various sexually transmitted diseases [243-246]. Therefore, it is very important to assess the toxicity effects of microbicides on lactobacilli as well as their effects on vaginal epithelial cell monolayer integrity, to ensure that the microbicides do not disrupt the complex microenvironment.

HCQ is approved for the treatment of malaria, systemic lupus erythematosus, and rheumatoid arthritis. A number of studies have also demonstrated the direct anti-viral activity of HCQ against HIV [186, 190]. Furthermore, HCQ is capable of decreasing the activation of T-cells, reducing the number of target cells for HIV infection [184]. Two different medical grade polymers were evaluated for their release profiles. PU-93A which has 100% percent water swellibility released almost 100% of HCQ loaded in 7 days. The PU-93A presented a burst release for the first 3 days due to high water infiltration into the polymer causing the polymer to swell and release the payload (Figure 3.2). We were able to obtain sustained release of HCQ from PU-60D IVR segments for up to 24 days in sodium acetate buffer and in MRS broth. The greater release observed in MRS broth versus sodium acetate buffer may be due to the high protein-binding capacity of HCQ itself [248]. The protein and lipid components present in MRS broth could act as a sink for HCQ during the release studies [248]. A study has shown that 4.34  $\mu\text{g}/\text{mL}$  (10  $\mu\text{M}$ ) is capable of suppressing early T-cell activation [186]. In the same study, a higher concentration of

up to 100 $\mu$ M (43.4 $\mu$ g/ml) has been used to induce the IQ state in T-cells and was found to be safe [186]. The daily concentration released (Figure 3.3 A) from our IVR system was within the necessary therapeutic concentration range (4.34  $\mu$ g/mL) [249] to induce IQ. To evaluate the safety of HCQ on lactobacilli, we treated the most common type of lactobacillus found in the FGT with different concentrations of HCQ. *Lactobacillus crispatus* and *jensenii* are the main strains of vaginal flora that produce hydrogen peroxide with a respective production of 95% and 94% according to a study conducted by Antonio and colleagues [250]. The lactobacillus family also uses the glycogen present in the vaginal tract to produce lactic acid to maintain an acidic vaginal environment (pH 4.2 – 5) [238]. The highest daily concentration of HCQ released in MRS broth from our reservoir IVR segment was nearly 35-fold lower than the highest concentration tested in the current study (1 mg/mL), which had no significant impact on bacterial growth (figure 3.4A). Concentrations higher than 1 mg/mL significantly inhibited the growth of both strains, which could be attributable to the bacteriostatic effects of HCQ [251]. Therefore, the level of HCQ released from our device is significantly lower than the levels that inhibit the growth of lactobacilli but is high enough to elicit a therapeutic effect within the FGT.

We have also evaluated the impact of drug-free IVR on bacterial growth. This is important to ensure that there is no degradation or unreacted polymer products leaching out of the IVR with time. Based on our results, drug-free IVRs had no significant impact on the growth of lactobacilli (Figure 3.5A). Although we have shown that free HCQ and drug-free IVRs have no significant impact on the growth of lactobacilli individually, it is unknown whether HCQ released from IVRs may have a significant effect. In our studies, HCQ-loaded IVR segments that were immersed in MRS broth for up to 7 days had no significant impact on *Lactobacillus jensenii* but there was a slight decrease in the growth of *Lactobacillus crispatus* with 3-day- and 7-day-immersed samples.

One possible reason for this observation may involve the higher levels of HCQ accumulated within the 3-day and 7-day MRS broth samples [251]. In the current study, IVR segments were incubated in broth medium for up to 7 days without changes in the broth medium. As a result, HCQ released from the IVR segments accumulated in the MRS broth during the entire 7-day study period (except when samples were collected on days 1, 3, and 7). Since normal FGTs produce vaginal secretions at 2 to 10 ml/day [252], HCQ released from the IVRs can be “washed out” of the FGT, resulting in lower vaginal HCQ concentrations.

Furthermore, it was important to determine whether our IVR system would be cytotoxic to the surrounding epithelial tissues and the underlying mucosal immune cells of the FGT. Therefore, we evaluated the impact of our IVR system on the viability of vaginal and ectocervical epithelial cell lines and in a CD4<sup>+</sup> T-cell line. HCQ concentrations of up to 4.34µg/mL showed no significant effects ( $P < 0.05$ ) on the viability of VK2/E6E7 vaginal epithelial cells, Ect1/E6E7 ectocervical epithelial cells, or Sup-T1 immune cells, compared to the negative control. Drug-free IVR segments also demonstrated no significant impact on the viability of these three cell lines over a period of 30 days.

Although we have shown that our HCQ-loaded IVR segments have no significant impact on the viability of vaginal/ectocervical epithelial cell lines, CD4<sup>+</sup> T-cell line, and lactobacilli, it was not known whether there were any changes in the tight junctions of vaginal epithelial cells, which is a concern since this may increase the opportunities for viruses to penetrate the vaginal mucosal layer and to infect underlying immune cells [253]. As a result, we evaluated TEER values for VK2/E6E7 cell monolayers before and after exposure to HCQ alone, drug-free IVR segments, or HCQ-loaded IVR segments. All of the treatment groups demonstrated no significant effects on

TEER values after 48 h, compared to the negative control, suggesting that the vaginal epithelial cell monolayers were still intact.

This is the first study to evaluate the impact of HCQ-loaded IVRs on the growth of major strains of lactobacilli commonly found in the FGT. The amount of HCQ released daily was within the therapeutic concentration range necessary to induce T-cell IQ. The IVR system had no significant effects on the growth of *Lactobacillus crispatus* and *jensenii*, the viability of vaginal/ectocervical epithelial cells or immune cells, or the integrity of vaginal epithelial cell monolayers. These promising results support further investigation into the effectiveness of this new platform as a microbicide for the prevention of HIV-1 infection and other sexually transmitted infections.

**Chapter 4: Segmented intravaginal ring for the combination  
delivery of hydroxychloroquine and anti-CCR5 siRNA  
nanoparticles as a potential strategy for preventing HIV infection**

Adapted from the following research article:

Yannick Leandre Traore, Yufei Chen, Fernanda Padilla and Emmanuel A. Ho,

Drug Delivery and Translational Research 2021 doi: 10.1007/s13346-021-00983-w

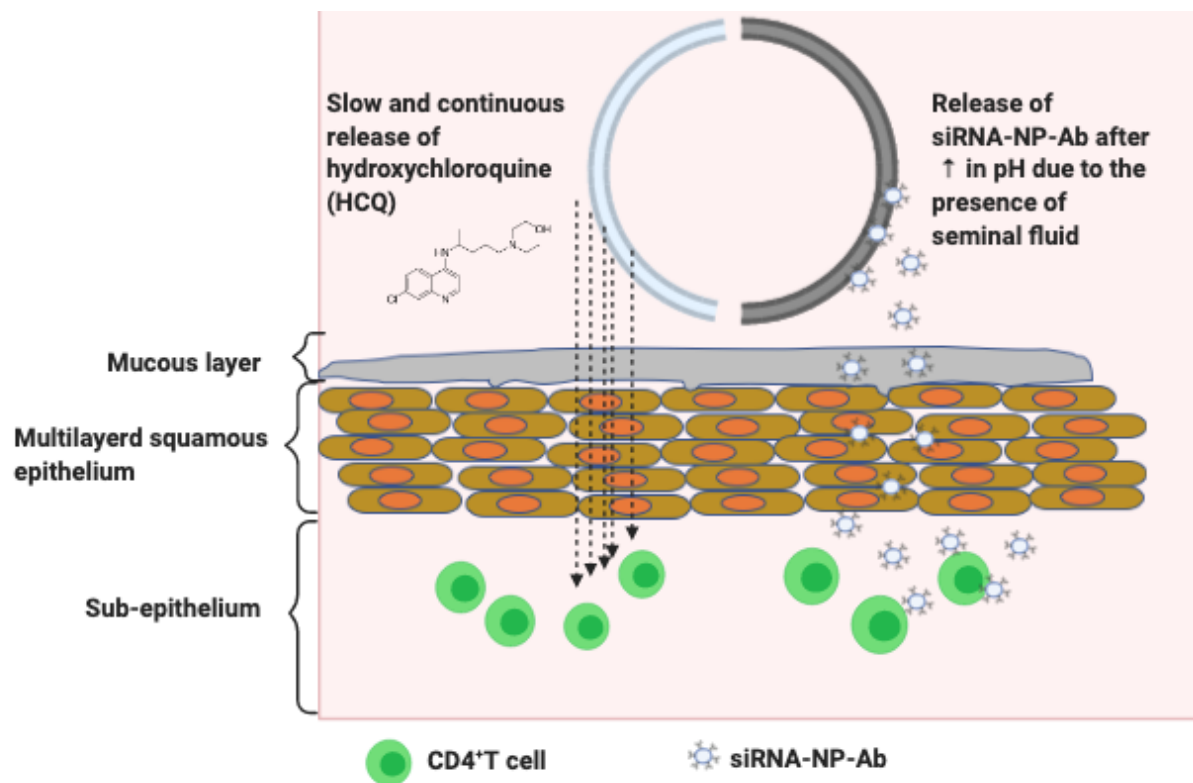


#### **4.1. Abstract**

Vaginal drug delivery has been shown to be a promising strategy for the prevention of sexually transmitted infections. Therapy delivered at the site of infection has many advantages including improved therapeutic efficacy, reduction in systemic toxicity and reduced potential for development of drug resistance. We developed a “smart” combination intravaginal ring (IVR) that will: 1) provide continuous release of HCQ to induce T-cell immune quiescence as the first-line of defense and 2) release nanoparticles containing anti-CCR5 siRNA only during sexual intercourse when triggered by the presence of seminal fluid as the second-line of defense. The IVR was capable of releasing HCQ over 25 days with a mean daily release of  $31.17 \pm 3.06$   $\mu\text{g/mL}$ . In the presence of vaginal fluid simulant plus seminal fluid simulant, over 12x more nanoparticles ( $5.12 \pm 0.9$  mg) were released over a 4 hr period in comparison to IVR segments that were incubated in the presence of vaginal fluid simulant alone ( $0.42 \pm 0.19$  mg). Anti-CCR5 siRNA nanoparticles were able to knockdown  $83 \pm 5.1\%$  of CCR5 gene expression in vitro in the CD4<sup>+</sup> T-cell line Sup-T1. The IVR system also demonstrated to be non-cytotoxic to VK2/E6E7 vaginal epithelial cells.

**KEYWORDS: HIV, Intravaginal ring, pH-responsive polymer, Anti-CCR5 siRNA, Solid lipid nanoparticles.**

## Graphical Abstract



## 4.2. Introduction

Despite the efforts that have been made to date, HIV is still one of the leading causes of death in developing countries. More than 38 million people globally are living with HIV at the end of 2019 with women being more vulnerable due to biological and social-cultural factors. Reasons include the larger surface area of the female genital tract (FGT) in comparison to the male genital tract and the fact that after sexual intercourse, semen remains within the FGT for prolonged periods, increasing exposure to HIV [12, 254, 255]. Condoms remain as the best method for preventing HIV infection during heterosexual intercourse but unfortunately, in certain developing countries, women are not able to negotiate condom usage with their partners [256]. Furthermore,

due to the high rate of mutation by HIV, most conventional drugs are not effective due to the development of drug resistance. To reduce the development of multidrug resistance, therapy involving different classes of antiretrovirals is necessary [257]. However, this multidrug therapy can pose as a burden for patients especially when it must be taken daily. As one example, pre-exposure prophylaxis (PrEP) consisting of tenofovir and emtricitabine, both reverse transcriptase inhibitors and marketed as Truvada<sup>®</sup>, demonstrated high efficacy against HIV-1 [258]. Interestingly, a study has reported that low patient compliance to Truvada may result in the development of antiviral drug resistance [259, 260]. Hence, the necessity to develop an easy and effective therapy against HIV that does not require daily drug administration is required. A great strategy is to develop microbicides (self-administrated topical PrEP) that do not require much effort from the user [62]. An ideal microbicide would be one that is long-acting and is capable of delivering high dose of drug to the target site demonstrating therapeutic efficacy and low toxicity. A common challenge with microbicide development as observed in clinical trials is low patient adherence [261]. In addition, some microbicides have also elicited inflammation within the FGT resulting in increased HIV infection rates [243, 262, 263]. Different microbicides have been developed in the past several decades including vaginal gels, creams, suppositories, bio-adhesives and intravaginal ring [62, 264]. Intravaginal rings (IVRs) are an excellent alternative that can provide controlled and sustained release of an active ingredient within the FGT for an extended period [68]. IVRs have high acceptability amongst users and can be designed to deliver different active ingredients using the same ring [265, 266]. Furthermore, in a recent clinical trial, it was reported that placebo IVRs did not significantly induce an inflammatory response within the FGT of women suggesting that IVRs are safe for long-term use e.g. 28 days. [267]. In this study, we developed a dual-combination IVR system designed to prevent HIV infection by incorporating

two distinct approaches. The first strategy will be to induce an immune quiescent state using HCQ to reduce the number of HIV target cells within the FGT. Secondly, our IVR system will utilize gene therapy to knockdown the expression of CCR5 using small interfering RNA (siRNA) to reduce HIV binding to target cells.

It has been shown that high CD4<sup>+</sup> T-cell immune activation strongly correlates with HIV infection [268]. CD4<sup>+</sup>CCR5<sup>+</sup> immune cells are the primary target cells for HIV. While activated, there will be an increase expression of cell surface markers such as HLA-DR, CD69, and CD38 resulting in an increase in the susceptibility for HIV infection [188]. Studies have shown that HIV-exposed seronegative women exhibit a unique immune phenotype called IQ whereby they exhibit a lower baseline of T-cell immune activation when compared to people that are at a greater risk of contracting HIV [188, 269]. HCQ, a widely available FDA approved immunomodulatory drug used for the treatment of malaria, systemic lupus erythematosus and rheumatoid arthritis, has been shown to reduce HIV viral loads and induce T-cell IQ [186, 270, 271]. By using an IVR to deliver HCQ in a sustained and controlled manner at the site of infection e.g. FGT, it will greatly reduce viral infection during sexual intercourse. The immunomodulatory properties of HCQ is a result of its ability to increase the pH of lysosomes within T-cells, interfering with the association of the invariant chain of the major histocompatibility complex class II molecule leading to their reduced ability to process antigens [272, 273]

The second strategy will be to use siRNA directed against the CCR5 receptor expressed at the surface of T-cells. HIV will bind to CD4 and CCR5 receptors at the surface of T-cells to become internalized. Studies have shown that knocking down the CCR5 gene will prevent HIV-1 infection. For example, the first patient to be completely “cured” from HIV received a bone marrow transplant from a donor who had a rare stem cell mutation that prevented the expression

of CCR5 on T-cells. Three months after the transplant, the patient was completely cured of HIV [274]. Recently, a second case of another patient following the same treatment using CCR5 knockout stem cell transplant received from a donor was also cured of HIV [275]. Since it will be challenging to find sufficient donors for all HIV patients, using gene therapy to knockdown the CCR5 expression is a promising approach. In our study, we plan to deliver siRNA to target the CCR5 gene as a strategy for reducing HIV infection [276, 277]. siRNA being negatively charged cannot cross the cell membrane, and as a result, requires a carrier system such as solid lipid nanoparticles (SLN) to deliver siRNA into T-cells. SLNs were used due to its demonstrated biocompatibility and simplicity in terms of customization. For active targeted delivery to immune cells, SLNs were functionalized with anti-CD4 antibody. The attached CD4 antibody will facilitate binding of SLNs to the CD4 receptor on the surface of T-cells resulting in improved internalization.

Our study aims to develop and characterize a segmented combination IVR delivery system consisting of one-half of the IVR loaded with HCQ and the second-half of the IVR to be coated with a pH-responsive film loaded with siRNA-encapsulated SLNs. It is expected that at normal vaginal pH (3.5-4.3) there will be no release of siRNA-loaded nanoparticles. During heterosexual intercourse, the vaginal pH becomes elevated (>6.2) due to the presence of seminal fluid [191]. As a result, it is expected that at pH>6.2, the IVR will provide rapid release of siRNA-nanoparticles while HCQ will be released continuously over time at both acidic and neutral pH to prevent immune activation of T-cells. This novel dual combination microbicide has the potential to improve patient compliance and reduce HIV infection.

### 4.3. Materials and Methods

#### 4.3.1. Materials

Hydrophilic thermoplastic polyurethane (Tecophilic™ HP-60D-35) was purchased from Lubrizol Advanced Materials (Cleveland, OH, USA). Eudragit L100 (methacrylic acid-methyl acrylate copolymer; anionic pH-sensitive polymer) was kindly donated by Evonik Industries (Essen, Germany). Hydroxypropyl methylcellulose (HPMC) K100M was donated by Dow Chemical Company (New Milford, CT, USA). Polyethylene glycol 400, NF (PEG-8) was acquired from Medisca (Saint-Laurent, QC, Canada). HCQ was purchased from Thermo Fisher Scientific (Burlington, ON, Canada). CellTiter 96® Aqueous One Solution Cell Proliferation Assay (MTS) was purchased from Promega (Madison, USA). Glyceryl monostearate (molecular weight 358.56) was purchased from Sigma-Aldrich (Ontario, Canada). L- $\alpha$ -phosphatidylcholine (Soy-95%) (molecular weight 770.123 g/ mol) and 1,2-distearoyl-sn-glycero-3-phosphoethanolamine-N-[amino(polyethylene glycol)-2000] (DSPE PEG 2000) were purchased from Avanti Polar Lipids (AL, USA). Polyvinyl alcohol (PVA; 31–50 kDa) and polyethyleneimine (branched, MW 25K) were obtained from Sigma-Aldrich (Ontario, Canada). Tris-EDTA was purchased from ThermoFisher Scientific (Ontario, Canada). 2-(N-morpholino) ethanesulfonic acid (MES) was purchased from Sigma-Aldrich (Ontario, Canada). 1-ethyl-3-(3-dimethylaminopropyl) carbodiimide (EDC; 200 mg/mL) N-hydroxysuccinimide (NHS; 275 mg/mL) were purchased from G-Biosciences (Missouri, USA). Anti-Human CCR5 siRNA (sense: 5'-GUUCAGAAACUACCUCUUAdTdT-3' ; antisense: 3'-dTdTCAAGUVUUUGAUGGAGAAU-5') was purchase from Dharmacon (ON, Canada). Human CCR5 primers (Forward: 5'-TTCATCATCCTCCTGACAATCG-3'; Reverse: 5'-GCCACCACCCAAGTGATCAC-3') and human GAPDH primer (Forward: 5'-AAGAAGGTGGTGAAGCAGGCG-3'; Reverse: 5'-

AGACAACCTGGTCCTCAGTGTAGC-3') were purchased from Thermo Fisher (ON, Canada). E.Z.N.A.<sup>®</sup> RNA isolation kit was purchased from Sigma Aldrich (ON, Canada). PercCTa SYBR Green SuperMix and qScript<sup>™</sup> cDNA were purchased from Quanta (ON, Canada). Anti-CD4 antibody was purchased from Abcam (ON, Canada).

#### **4.3.2. IVR fabrication**

“Reservoir-type” and “matrix-type” IVR segments were fabricated from medical grade polyurethane (PU) HP-60-D-35 pellets using hot-melt injection molding (Medium Machinery, LLC, Woodbridge, VA, USA). Briefly, the pellets were dried overnight at 80°C and loaded into a hot-melt injection molding. The PU was then melted inside the injection molder and injected into a custom-fabricated, pre-heated aluminum mold for the reservoir-type or matrix-type segment. The mold produced IVR segments with a 25 mm outer diameter and 5 mm cross-sectional diameter for the matrix type IVR. The reservoir type IVR had a wall thickness of 0.75 mm (Figure 4.1), 25 mm outer diameter and 5 mm cross-sectional diameter. The reservoir segment containing HCQ in the lumen was joined to the matrix segment using a butt-welding kit.

#### **4.3.3. HCQ loading in reservoir-type IVR**

HCQ was mixed with HPMC K100M to create a semisolid as described previously [69]. Briefly, 160 mg of HCQ was added to 1.28 mL of distilled water and mixed using the two-syringe method. 160 mg of HPMC K100M was added to the HCQ solution and mixed using the two-syringe method. The semisolid was passed through the syringes 40 times to ensure homogeneity. The mixture was loaded into a reservoir-type IVR segment and both ends were sealed with resin caps pre-made using Smooth-Cast 300.

#### **4.3.4. Nanoparticle fabrication.**

SLNs encapsulated with siRNA (siRNA-NP) were prepared using a double-emulsion solvent evaporation technique as previously described with slight modifications [278]. We added 50  $\mu$ L of 0.372 mg/mL PEI to a solution containing 45  $\mu$ L of Tris-EDTA buffer and 5  $\mu$ L of 25  $\mu$ g siRNA. The mixture was incubated at room temperature for 15 min and mixed periodically. This aqueous solution was added slowly to 1.4 mL solution of glyceryl monostearate and L- $\alpha$ -phosphatidylcholine dissolved in acetone and ethanol and sonicated for 30 s on ice using a probe sonicator. The double emulsion was formed by adding this mixture to 8 mL of 2% (w/v) PVA solution. We added 100 $\mu$ l of DSPE-PEG COOH from a 1.5mg/mL stock solution to the dispersion and stirred overnight. The organic solvents were then evaporated, and the siRNA-NPs were washed, and the encapsulation efficiency was determined. Anti-CD4 antibody was conjugated to the siRNA-NP by activating the carboxyl group on the nanoparticle's surface by the addition of EDC and NHS at pH 6 for 60 min. The pellet was resuspended in 4.8 mL of 100mM of MES buffer and 100  $\mu$ l of 27mg/mL of NHS and 100  $\mu$ l of 10mg/mL of EDC were added. SLNs were vortexed and placed on an orbital shaker for 20min. SLNs were collected by centrifugation at 20,000g for 40 min and the supernatant was discarded. The SLNs were resuspended in 1 mL of PBS and 100 $\mu$ l of 0.5 $\mu$ g/mL of anti-CD4 antibody was added to the suspension. The SLNs were placed on the orbital shaker for another 2 hours. The antibody-conjugated nanoparticles (siRNA-NP-Ab) were washed with distilled water, lyophilized, and stored at -20°C until further analysis. Nanoparticle size and net surface charge were determined by light scattering using Zetasizer (Malvern). The antibody conjugation efficiency was performed following a method previously published by our lab [279]. Briefly, unconjugated antibodies from the supernatant were quantified using QuantiPro™ BCA assay (Sigma-Aldrich, USA). A volume ratio of 1:1 of BCA reagent and the



supernatant were mixed and incubate at 60°C for 1 hour. The sample was allowed to cool to room temperature and the reading was done at 505 nm on the microplate reader using BSA as standard.

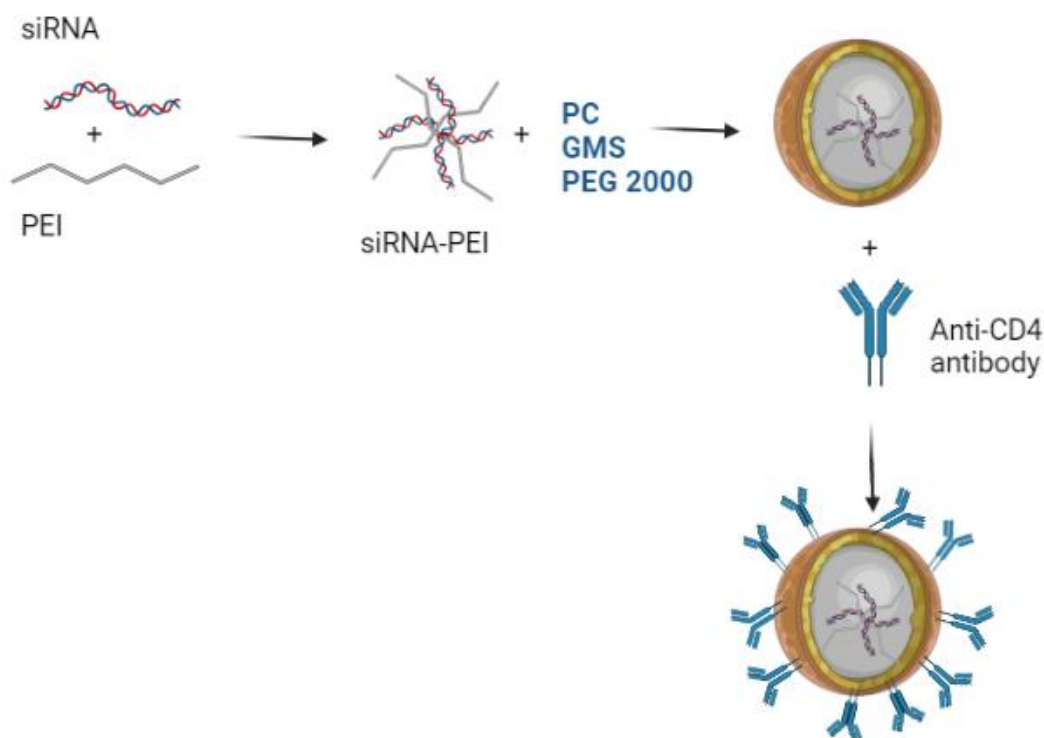


**Figure 4.1: SLN preparation and conjugation to anti-CD4 antibody:** PEI: Polyethylenimine, PC: L- $\alpha$ -phosphatidylcholine; GMS: Glyceryl monostearate

#### 4.3.5. pH-responsive coating preparation

An optimised film formulation is necessary to achieve a uniform coating on the surface of the IVR. The coating should be able to stick to the IVR matrix when dried and not crumble or peel off when the IVR is compressed. For these reasons, we first evaluated the film forming capacity of Eudragit L100 and optimized the formulation that will work best for our IVR segments. Briefly, different percentages of Eudragit were dissolved in various organic solvents and evaluated for its film-forming properties. The solvents include isopropanol, dichloromethane, methanol,

dichloromethane:ethanol (50:50 v/v), and methanol:water (50:50 v/v). The mixture of organic solvent and Eudragit L100 was stirred at room temperature for at least 3 hr. After the complete dissolution of the polymer, PEG400 was added at different ratios (Table 2) and stirred for another 10 min. In order to choose the best film formulation for the IVR coating, we performed a disintegration study to determine the rate of film disintegration. Briefly, 15 mg of Eudragit L100 films containing PEG were incubated in PBS buffer (pH 7.2) for 20 min. Afterward, the remaining film was removed, dried in an oven at 37°C and weighed. For the complete disintegration time, we monitored the film until there was complete dissolution with no visible particles in the buffer. Next, after deciding on the formulation that gave the best adherence and the fastest disintegration time, siRNA-NP-Ab was added to the formulation (3% Eudragit L100 plus 0.2 mL PEG 400), mixed and sonicated for 30 min without heat to obtain an aqueous dispersion and to remove air bubbles. A matrix IVR segment was coated with the mixture and dried at 40°C for 15 min.

#### **4.3.6. In vitro release studies from the reservoir-type and matrix-type IVR segment**

Release studies were performed using reservoir-type IVR segments ( $19.6 \pm 0.7$ mm) containing HCQ and K100M in the lumen as previously described [69] in vaginal fluid simulant (VFS; pH 4.2) following the recipe proposed by Owen et al. [252]. Briefly, IVR segments ( $19.6 \pm 0.7$  mm) were placed in 5 mL of VFS at 100 rpm speed and 37°C. The amount of drug released was quantified using a reverse-phase HPLC method. Isocratic conditions were used with a Waters Nopak<sup>®</sup> C18 column (4 $\mu$ m, 3.9x150 mm) on Shimadzu LC-2010A HPLC system. The mobile phase consisted of 58 mM sodium phosphate dibasic buffer containing 15 mM of heptanesulfonic acid, acetonitrile and methanol at a volume ratio of 74:22:4 and the pH was adjusted to 3.1 with ortho-phosphoric acid. The flow rate was set at 1 mL/min and the wavelength of the detector was

set at 343 nm. The column was kept at room temperature and the HCQ retention time was approximately 8.4 min. We aim to achieve a targeted HCQ release of at least 4.3  $\mu\text{g/mL}$  which is the minimum concentration required to induce T-cell IQ [249].

Separately, the pH-responsive coated matrix-type IVR segments were placed in two different release buffers. The first release buffer was VFS (pH 4.2) and the second buffer was a seminal fluid simulant (SFS; pH 8.2) prepared using a modified recipe of Rastogi et al. [280]. SLN containing coumarin 6 (C6) was prepared to help track NP release from the IVR segments. Briefly, a set of segments coated with Eudragit L100 containing C6 -SLN were placed in 4 mL of VFS. The volume of ejaculated seminal fluid is between 0.1 to 11 mL [281, 282]. Ejaculation volume less than 1 mL is considered hypospermia and more than 6 mL is considered hyperspermia. In this study we decided to evaluate the lowest normal ejaculation volume capable of changing the vaginal tract pH. Accordingly, another set of IVR segments were placed in 4 mL of VFS + 1 mL of SFS to simulate the presence of seminal fluid during sexual intercourse and placed inside a rotary shaker at 37°C and set at 100 rpm. The data was analyzed using a fluorescent microplate reader (SpectraMax M5).

#### **4.3.7. In vitro cytotoxicity studies of IVR containing NPs**

In vitro cytotoxicity was evaluated using the CellTiter 96<sup>®</sup> Aqueous One Solution Cell Proliferation assay. Briefly, vaginal epithelial cells VK2/E6E7 cells were cultured in K-SFM containing 0.1 ng/mL recombinant human epidermal growth factor, 44.1 mg/L calcium, 0.05 mg/mL bovine pituitary extract and 1% penicillin-streptomycin. The cells were incubated at 37°C with 5% CO<sub>2</sub>. Separately, this medium was used to incubate a matrix IVR segment coated with a pH-responsive polymer. The segment in the medium was incubated at 37°C for 24 hrs at 100 rpm


in an orbital shaker. After almost reaching confluency, the cells were seeded onto 96-well plates at a density of  $2.5 \times 10^5$  cells per well. The cells were then incubated for another 24 hrs and the medium in each well were replaced with the elution medium collected previously. 1M acrylamide was used as positive control and plain medium was used as negative control. The cells were incubated back for another 24 hrs followed by the addition of 20  $\mu$ L of CellTiter 96<sup>®</sup> Aqueous One Solution Cell Proliferation assay reagent and incubated for another 2 hrs. The optical density of the wells was read using a microplate reader (SpectraMax M5) at 490 nm and data were normalized to the negative control value. Previously, we have shown that HCQ-loaded reservoir segments were non-cytotoxic [69].

#### **4.3.8. In vitro CCR5 gene knockdown study**

In order to evaluate the efficacy on our SLN to deliver siRNA inside the cells and to know the minimum amount of siRNA needed to induce gene knockdown, we treated Sup-T1 cells in a 96-well plate with only different concentrations of siRNA-NP-Ab. Briefly, SupT-1 cells were cultured in RPMI medium supplemented with 10% fetal bovine serum and 1% penicillin-streptomycin incubated at 37°C with 5% CO<sub>2</sub>. The cells were seeded in 96 well-plate at a density of  $2 \times 10^4$  cells/well. Each well was treated with 1.4 mg, 0.7 mg or 0.35 mg of siRNA-NP-Ab. The cells were incubated for 48 hrs at 37°C with 5% CO<sub>2</sub>. After incubation, the cells were washed with PBS and processed for mRNA extraction using the E.Z.N.A.<sup>®</sup> Total RNA Kit I. 1  $\mu$ L of 100 ng of mRNA were mixed to 4  $\mu$ L of cDNA supermix and 15  $\mu$ L of RNase/DNase free water to make cDNA using qScript<sup>™</sup> cDNA SuperMix in a thermal cycler (Bio-Rad C1000<sup>™</sup> Thermal Cycler). The parameters for the thermal cycler used were 25°C for 5 min, 42°C for 30 min, 85 °C for 5min and hold at 4°C. RT-PCR was performed using a mix of 10  $\mu$ L of PerfeCTa SYBR Green

SuperMix, 2  $\mu$ L of cDNA template, 2  $\mu$ L of CCR5 forward and reverse primers (3 $\mu$ M). GAPDH gene was used as endogenous control following the the same preparation as our gene of interest. The RT-PCR was using the Applied Biosystems StepOnePlus using the incubation times as presented below:

95 °C for 5 min  
95 °C for 15 seconds  
60 °C for 30 seconds  
72 °C for 30 seconds  
72 °C for 15 seconds



30 repeats

For the next study, Sup-T1 cells were seeded in a 24-well plate at a density of  $0.8 \times 10^5$  cells per well. An insert was placed into each well and an IVR segment coated with a pH-responsive polymer containing siRNA-NP-Ab (sterilized using ultraviolet light for 1 hr) was placed into the insert. The IVR segments were suspended above the insert using a custom-designed holder made out of stainless steel wire (Fig. 1B). Negative control had an insert containing an IVR segment coated with blank NPs and another well with nothing but cells. The plate was placed on a shaker inside an incubator set at 2 rpm to allow the dissolution of the coating for 48 hrs at 37°C with 5% CO<sub>2</sub>. After incubation, we proceeded to the mRNA extraction and gene analysis as described above.

### **Statistical analysis.**

Data are presented as the mean  $\pm$  standard deviation (SD). The n values refer to the numbers of replicates performed for each study. One-way analysis of variance was performed with all results, with P values of  $<0.05$  considered to be significant.

## 4.4. Results

### 4.4.1. IVR fabrication.

A photo of the matrix and reservoir type IVR joined together is shown in Figure 4.1. A complete macaque-size IVR has a diameter of 25 mm, and a cross-sectional diameter of 5 mm. The reservoir-type IVR segment has a wall thickness of  $\sim 0.7$  mm and a length of  $19.6 \pm 0.7$  mm. The lumen of the reservoir was filled with HCQ mixed with K100M. The matrix IVR was coated with the modified pH-responsive polymer containing siRNA-NP-Ab. Both segments were joined together by applying heat to partially melt both ends of the different segments.

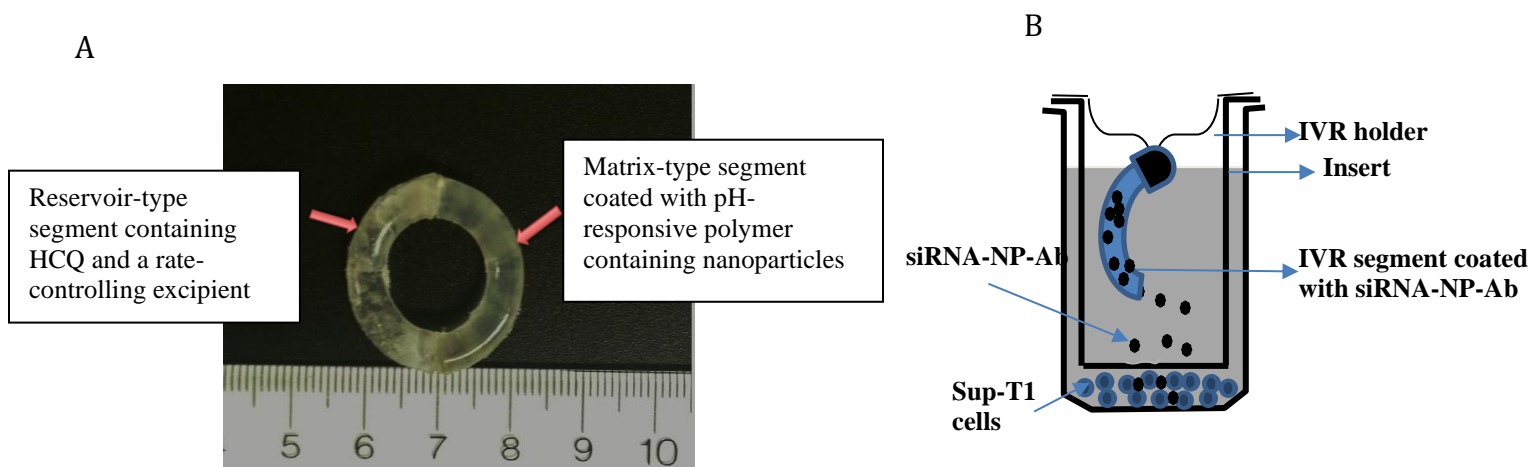


**Figure 4.2: Segmented intravaginal ring (IVR).** (A) The picture depicts a segmented intravaginal ring (IVR) formed by combining a reservoir-type segment with a matrix-type segment. The size of the IVR (25 mm x 5 mm) is designed for implantation into the female genital tract of non-human primates. IVR segments were fabricated using hot-melt injection molding of HP-60-D-35 polyurethane pellets and joined by butt-welding. (B) schematic representation of the IVR segment in a cell culture insert incubated with Sup-T1 cells.

#### 4.4.2. NP fabrication.

Table 4.1 summarizes the SLN size, net surface charge, and drug encapsulation efficiency. The mean size of siRNA-NP-Ab was around  $265.3 \pm 15.7$  nm with a polydispersity of around 0.2. The siRNA encapsulation efficiency was  $79.63 \pm 7.3\%$  and the net surface charge was around  $-26 \pm 3.4$  mV. Drug-free SLN had an average size of  $210.5 \pm 20.8$  nm with a polydispersity of 0.2. The antibody conjugation efficiency was  $26.35 \pm 4.41\%$ .

**Table 4.1: CCR5 siRNA-encapsulated SLN size, zeta potential, and encapsulation efficiency.**

	Size (nm)	Encapsulation Efficiency (%)	Zeta potential (mV)	PDI
siRNA-NP-Ab	$265.3 \pm 15.7$	$79.63 \pm 7.3\%$	$-26 \pm 3.5$	0.2
Drug-Free SLN	$210.5 \pm 20.8$	—	$-15 \pm 4.3$	0.2

#### 4.4.3. pH-responsive coating preparation

It is important to determine whether or not the selected solvent was capable of dissolving Eudragit L100. Table 4.2 lists the different solvents that were evaluated for their ability to dissolve Eudragit L100 and their film-forming properties. Dichloromethane and dichloromethane:ethanol (50:50 v/v) were able to dissolve Eudragit L100 completely, but they also partially dissolved the polyurethane HP-60D-35. Isopropanol was able to dissolve Eudragit L100 and did not have any effects on the polyurethane. Table 4.3 summarizes the effects of varying amounts of Eudragit L100 and PEG 400 dissolved in isopropanol on film formation properties. The usage of low amounts of

Eudragit L100 (3%) with low amounts of PEG 400 (0.1 mL) resulted in the formation of fragile and easy-to-break films. Too much PEG 400 (0.5 mL) hindered the film-forming capacity of Eudragit L100 resulting in a gel-like mixture. As a result, 3% Eudragit L100 dissolved in isopropanol supplemented with 0.2 mL of PEG 400 was used for all downstream studies since it produced the most uniform film with the fastest disintegration time. We observed rapid disintegration within the first 20 min (42%) followed by a reduced rate of disintegration for the next 2.5 h. Complete film dissolution was achieved in 3 h (Table 4.4). Only the formulations capable of forming a uniform and flexible film were considered in Table 4.4 for the disintegration study. The use of higher amounts of Eudragit L100 (>3%) resulted in films with longer disintegration times (>5 h).

**Table 4.2: Eudragit L100 properties in different organic solvents and their impact on polyurethane.**

Solvents	Percentage of Eudragit L100			Film forming properties	Effects on polyurethane
	1%	3%	5%		
Methanol:Water (50:50 v/v)	Insoluble	Insoluble	Insoluble	No	None
Methanol	Partially soluble	Insoluble	Insoluble	No	None
Dichloromethane	Soluble	Soluble	Soluble	Yes	Dissolved
Dichloromethane:Ethanol (50:50 v/v)	Soluble	Soluble	Soluble	Yes	Partially dissolved
Isopropanol	Soluble	Soluble	Soluble	Yes	None



**Table 4.3: Impact of varying amounts of Eudragit L100 and PEG 400 dissolved in isopropanol on film formation.**

<b>FILM FORMATION</b>						
			PEG 400			
			(mL)			
EUDRAGIT	0	0.1	0.2	0.3	0.4	0.5
(%)						
3	Rigid film	Rigid film	<b>Flexible</b>	Gel state	Gel state	Gel state
4	Rigid film	Rigid film	Rigid film	<b>Flexible</b>	Gel state	Gel state
5	Rigid film	Rigid film	Rigid film	<b>Flexible</b>	Gel state	Gel state
7	Rigid film	Rigid film	Rigid film	Rigid film	<b>Flexible</b>	Gel state

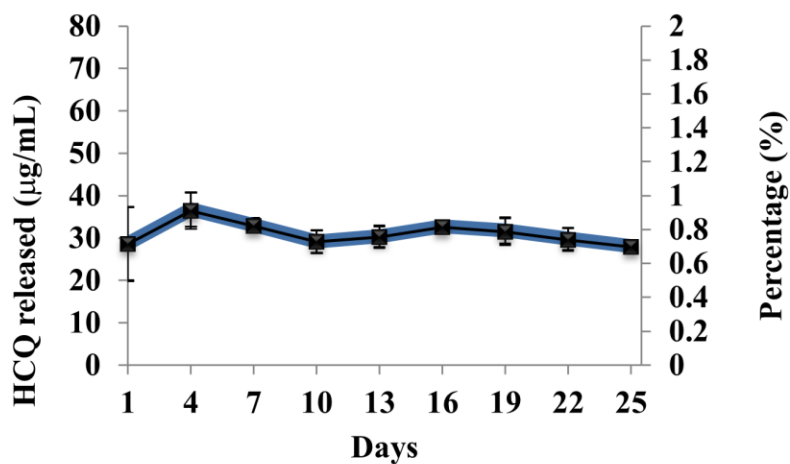
**Table 4.4: Eudragit L100 film disintegration time**

<b>Eudragit/PEG</b>	<b>PBS pH 4</b>	<b>PBS pH 7.2</b>
	<b>Disintegration time</b>	
<b>3%/0.2mL</b>	None	<3 hours
<b>4%/0.3mL</b>	None	>5 hours
<b>5%/0.3mL</b>	None	>5 hours
<b>7%/0.4mL</b>	None	>6 hours
<b>7%/0.5mL</b>	None	>6 hours

#### 4.4.4. In vitro release

Release studies were performed on reservoir-type IVR segments containing HCQ/K100M in VFS separately from the matrix type IVR. We previously published a study evaluating the release of HCQ from HP-60D-35 IVR segments in sodium acetate buffer [68]. In this study, release was evaluated in VFS which more closely represents the physiological environment. HCQ released from the IVR segment was sustained over 25 days with a mean daily release of  $31.17 \pm 3.06$   $\mu\text{g/mL}$  following a near-zero release kinetic profile ( $R^2=0.998$ ) (Figure 4.2). Over the period of 25 days,  $19.81 \pm 1.3$  % of the total amount loaded was released. The matrix-type IVR coated with the pH-responsive polymer containing C6-SLN was introduced in two different buffers for the release study. After 4 h, the segment placed in VFS released  $0.42 \pm 0.19$  mg of C6-SLN while the IVR segment that was incubated in VFS supplemented with SFS buffer released 12x higher amounts of C6-SLN ( $5.12 \pm 0.9$  mg) (Figure 4.3).

A)



B)

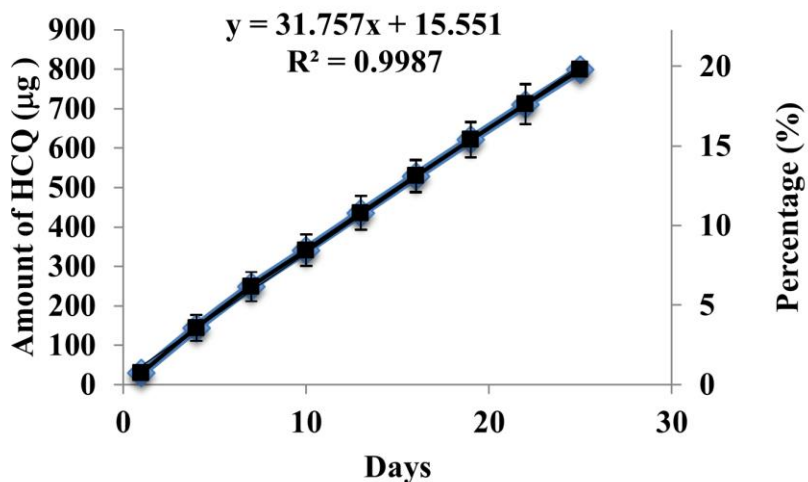


**Figure 4.3: HCQ release in VFS.** (A) Daily release of HCQ from HCQ/HPMC-loaded (ratio 1:1 wt/wt) IVR segments for 25 days. Release studies were performed in 5 mL of VFS (pH 4.2) and shaken on an orbital shaker at 37°C, 100 rpm. Data represents mean  $\pm$  S.D.; N=4. (B) Cumulative release of HCQ from HCQ/HPMC-loaded (ratio 1:1 wt/wt) IVR segments for 25 days. Data represents mean  $\pm$  S.D.; N=4

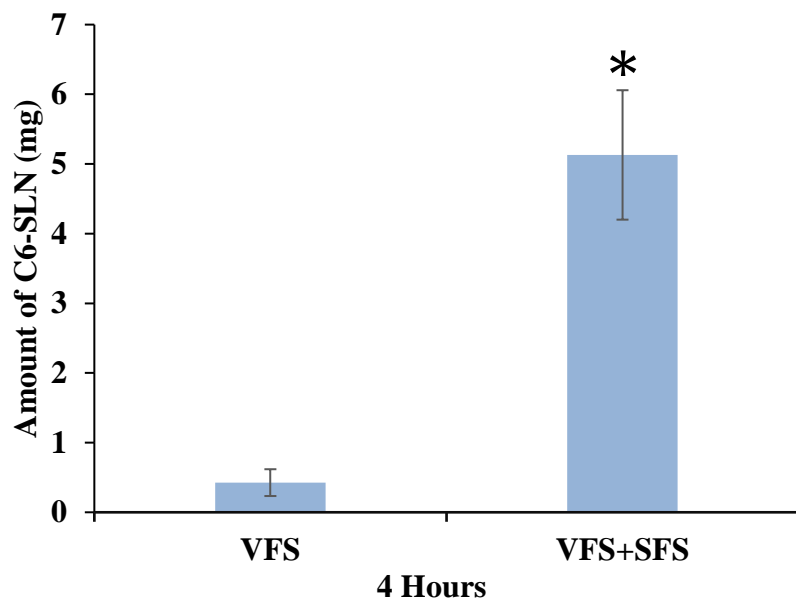


**Figure 4.4: Release of C6-SLNs in VFS and SFS.** Release study of C6-SLNs in VFS only and in VFS plus SFS to simulate the presence of seminal fluid during sexual intercourse. Data represent the mean  $\pm$  SD (n = 4). \*P < 0.05 versus VFS. C6: coumarin-6; VFS: Vaginal fluid simulant; SFS: Seminal fluid simulant.

#### 4.4.5. Determination of the in vitro cytotoxicity of IVR containing SLNs

The safety profile of the reservoir-type IVR segment containing HCQ/K100M was previously evaluated and published [69]. As a result, we focused only on the second half of the IVR in this study. As shown in Figure 4.4, no significant cytotoxicity was observed in VK2/E6E7 cells incubated with matrix-type IVR segments coated with the SLN-loaded pH-responsive coating in comparison to the control.

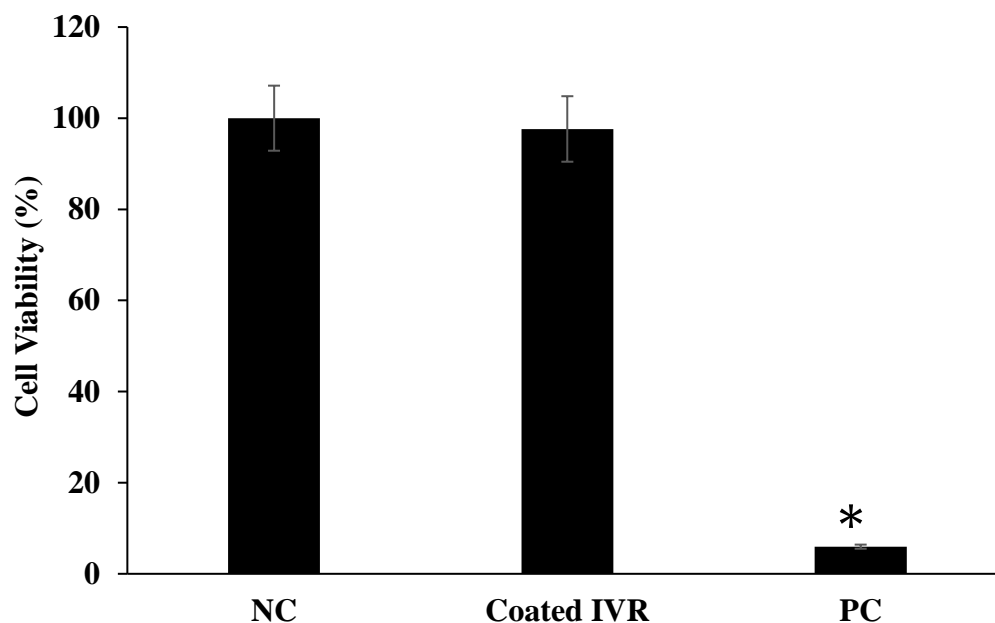


**Figure 4.5: Cytotoxicity evaluation of IVR coated with Eudragit L100 on VK2/E6E7 epithelial vaginal cells.** The IVR segment was coated with 15 mg of Eudragit L100 film. PC: Positive control (1M acrylamide); NC: Negative control (cell media). Data represents mean  $\pm$  S.D.; N=4. \*P < 0.05 versus NC

#### 4.4.6. In vitro CCR5 downregulation study

To evaluate the gene knockdown efficiency of the SLN containing siRNA, siRNA-NP-Ab were incubated directly with SupT-1 cells. Cells treated with 1.4 mg of siRNA-NP-Ab for 48 hours (containing approximately 5  $\mu$ g of siRNA) were able to achieve close to 60% CCR5 gene knockdown in 96-well plate (Figure 4.5). IVR segments coated with 7 mg of siRNA-NP-Ab (containing around 21.25  $\mu$ g of siRNA) was able to release enough SLNs to significantly reduce CCR5 gene expression by  $83 \pm 5.1\%$  in comparison to controls after 48 hours of incubation in SupT-1 cells in a 24-well plate (Figure 4.6).

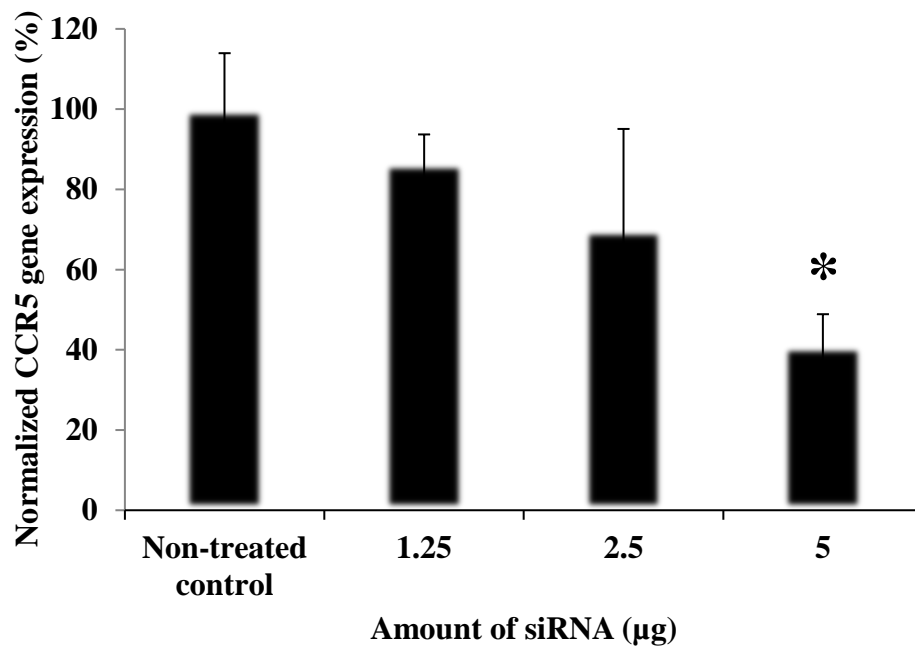


**Figure 4.6 Evaluation of CCR5 gene expression using real-time PCR.** The T-cell line (Sup-T1) was treated with various concentrations of siRNA-NP-Ab for 48 hr. Data represents mean  $\pm$  S.D.; N=3. \*P < 0.05 versus non-treated control

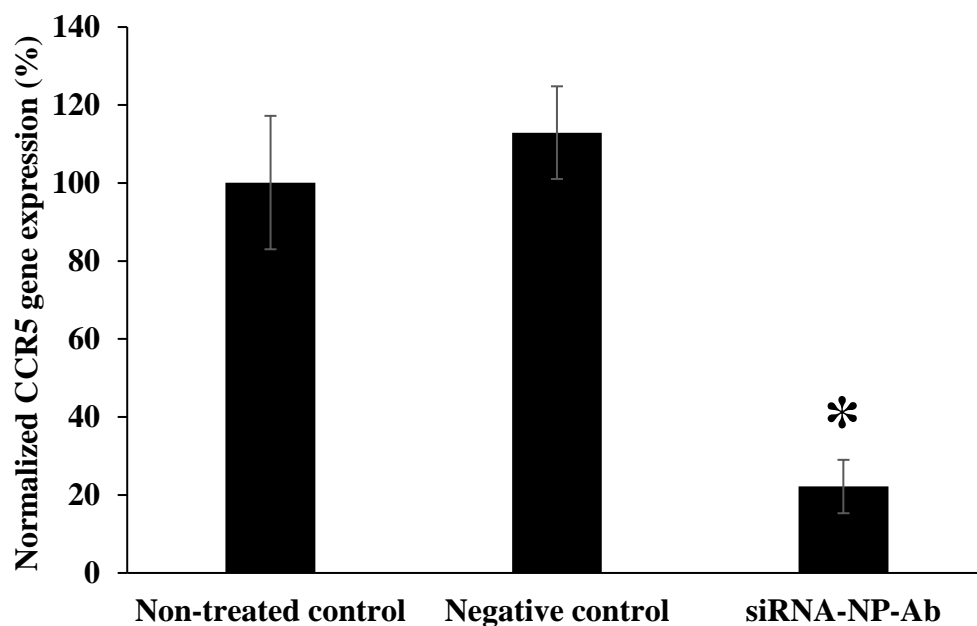


**Figure 4.7: Evaluation of coated IVR segment on CCR5 knockdown.** CCR5 gene knockdown in Sup-T1 cells incubated with IVR segments coated with pH-responsive Eudragit L100/PEG containing siRNA-NP-Ab (~19.09  $\mu$ g of anti-CCR5 siRNA). Blank: Sup-T1 cells alone; Negative control: consists of the IVR segment coated with the pH-responsive polymer but with drug-free SLNs. Data represents mean  $\pm$  S.D.; N=3. \*P < 0.05 versus negative control.

#### 4.5. Discussion

HIV continues to be a major global health concern particularly for women, who are disproportionately impacted due to biological and socio-cultural factors. Many of the current therapies fail due to low patient compliance and the development of drug resistance [283]. An IVR system that can provide prolonged drug release and is easily administered without the assistance of a healthcare practitioner, will increase patient adherence [117]. Furthermore, using two different strategies that prevent HIV access to its target cells will greatly reduce infectivity and the potential to develop drug resistance. Our system is designed to deliver HCQ continuously for over 3 wks to

induce a T-cell immune quiescent state within the FGT as the first-line of defense. During heterosexual intercourse, the second half of the IVR will rapidly release anti-CCR5 siRNA-NP-Ab to reduce the expression of CCR5 as the second-line of defense. However, further evaluation of our IVR system is required to determine whether or not drug resistance will develop.

HIV-exposed seronegative sex workers exhibit a low baseline of immune activation within the FGT [269]. It is believed that this immune quiescent state plays an important role in protecting against HIV infection. We decided to induce T-cell IQ using the immunomodulatory drug HCQ. It has been shown that HIV-exposed seronegative people exhibit low baseline immune activation with reduced expression of HLA-DR, CD38, CD69, and CCR5 on T-cells [188, 284, 285]. In our study, HCQ was able to cross the hydrophilic PU wall of the IVR segments while immersed in buffer. The PU HP-60D-35 has a water swellability of 35% of its mass. The influx of water inside the polymer will aid in the diffusion of HCQ. To further control the diffusion of HCQ, a rate-controlling excipient HPMC was used. The concentration needed to induce IQ in vitro is ~4.3  $\mu\text{g}/\text{mL}$  [186, 286]. The IVR segment is capable of releasing at least 7 folds more than the required concentration to induce IQ. We demonstrated in previous studies that HCQ released from HP-60D-35 was safe in a rabbit model, in the presence of vaginal (VK2/E6E7) and cervical (ECT-1/E6E7) epithelial cells, and in the presence of normal flora *Lactobacillus jensenii* and *crispatus* [69, 287]. The concentration of HCQ released in this study is significantly lower than the concentration reported that can induce cytotoxicity in vaginal cells (433.96  $\mu\text{g}/\text{mL}$ ) and *Lactobacillus jensenii* and *crispatus* (7  $\text{mg}/\text{mL}$ ) [69].

The second half of the IVR segment was fabricated to release anti-CCR5 siRNA-NP-Ab at high pH. The anti-CCR5 siRNA was mixed with PEI prior to encapsulation into SLNs. We believe once, inside the cells, the siRNA can escape endosomal degradation via the proton sponge



effect imparted by the positively charged PEI [288]. PEI has been shown to aid in the condensation of siRNA improving its encapsulation efficiency and assisting in the proton sponge effect by rupturing endosomes due to osmotic swelling.

To avoid unnecessary gene knockdown when it is not required, well-timed release of SLN is important. The release of SLNs can be triggered during sexual intercourse by the presence of seminal fluid inside the FGT. This can be achieved by using Eudragit L100 that will react with the change in pH environment due to the presence of seminal fluid. Eudragit L100 made of poly(methacrylic acid-co-methacrylate) is protonated and uncharged at acidic pH. At basic pH, it will become deprotonated and the negative charges repel themselves causing the polymer to swell [289, 290]. The swelling of the polymer leads to its disintegration and the release of the SLNs. For the fabrication of the pH-responsive film, we evaluated different solvents capable of dissolving Eudragit L100 (Table 1). The aim of this experiment was to find the most suitable solvent capable of dissolving only Eudragit L100 but not the PU matrix that it is coated on. Isopropanol appeared to completely dissolve Eudragit L100 and not have any visible effects on the PU HP-60D-35. Disintegration time of the pH-responsive film is also important since the rate of SLN release needs to be rapid during sexual intercourse. Since HCQ is continuously released to maintain T-cell IQ, it is assumed that this will provide sufficient time for the SLNs to be released, enter CD4<sup>+</sup> T-cells and silence CCR5 gene expression to prevent infection. In a non-human primate study, the authors have shown that sufficient infection was established only after 4 days [291]. Studies have shown that cervicovaginal mucus within the FGT may hinder nanoparticles from reaching the underlying submucosa [292]. As a result, the SLNs we prepared were coated with PEG that will potentially enhance the mucus penetration ability of the particles as described by others [293]. Assuming there is no mechanical tearing of the vaginal epithelium during sexual intercourse, we expect our SLNs

to enter the target cells and knockdown CCR5 gene expression in less than 4 days. For the SLN release studies, C6, a hydrophobic fluorescent dye was used to monitor the SLNs. As expected, in VFS alone, very low amounts of SLN was released. To simulate sexual intercourse, 1 mL of SFS was added to the VFS. In a study by Fox et al., the authors measured changes in vaginal pH during sexual intercourse using radio-telemetry and found that low volumes of semen (1.5 mL) was capable of raising vaginal pH from 3.5 to 5.5 within 15 sec [294]. At higher volumes of semen (5 to 6 mL) the vaginal pH can be raised from 4.3 to 7.2 in 8 sec [294]. For our studies, we used 1 mL of SFS which was capable of raising the pH of VFS from 4.2 to 7.3. This volume was selected to mimic the lower range of ejaculated seminal fluid, which was sufficient in removing almost the entire pH-responsive coating on the IVR segment. Human seminal fluid has a high buffering capacity and can easily change the vaginal tract pH from acidic to neutral and basic [295, 296].

In our studies, we determined that as low as 5  $\mu$ g of siRNA was capable of knocking down gene expression by around 50%. This study also confirmed that there was sufficient uptake of SLN by Sup-T1 cells to significantly reduce CCR5 mRNA expression. It took 48 hrs for the siRNA to be released from the SLNs to induce gene knockdown. However further studies must be performed in vivo to evaluate how fast the SLNs will reach the submucosa and to determine its efficiency in preventing HIV infection [291]. For in vivo studies, it is possible that other surrounding cells e.g. vaginal epithelial cells, may uptake the SLN, as a result, functionalizing the SLN with anti-CD4 antibody will improve targeted delivery to CD4<sup>+</sup> T-cells. Lastly, we determined that the coated IVR segments were non-cytotoxic to VK2/E6E7 vaginal epithelial cells. We have previously shown that PU HP-60D-35 is stable under accelerated stressed conditions of 40°C and 75% relative humidity [68], but further studies are needed to confirm the stability of the pH-responsive coating

under the same conditions. Although room temperature may not affect the coating, it is unknown what impact countries with elevated climates and humidity may have.

#### **4.6. Conclusion**

To the best of our knowledge, this is the first study to combine the delivery of HCQ and gene therapy as a novel strategy for preventing HIV infection. We were able to deliver HCQ continuously for over 3 weeks and also rapidly deliver siRNA-NP-Ab only at elevated pH environments such as those simulating the presence of seminal fluid. We were able to achieve significant CCR5 gene knockdown in comparison to controls and the IVR segment was non-cytotoxic towards vaginal epithelial cells. Overall, combining chemotherapy and gene therapy into a single IVR is a promising platform that should be further explored for its potential as a microbicide.

#### **Acknowledgements**

This study was funded in part by a Canadian Institutes of Health Research Project Grant (PJT166153) and a Natural Sciences and Engineering Research Council of Canada Discovery Grant (RGPIN-20156-06008) awarded to Emmanuel A. Ho. The authors would like to thank Vincent Jimenez, Gabriel Luo and Sidi Yang for their technical help.

**Conflicts of interest/Competing interests:**

Yannick L. Traore, Yufei Chen, Fernanda Padilla, Emmanuel A. Ho declare that there is no conflict of interest.

**Chapter 5: Thermo-responsive hydrogels for reducing biofilm formation on chronic wounds.**

## 5.1. Introduction

Chronic wounds are often associated with ulcers (diabetic, pressure, venous) and non-healing infections [297]. They present a substantial economic burden to the healthcare system significantly reducing the quality of life and potentially leading to serious events such as limb amputations or premature deaths [297]. Unfortunately, this burden is also subjected to increase as the population ages and lifestyle diseases such as diabetes and obesity become increasingly prevalent. Currently, treatment of chronic wounds involves regular replacement of wound dressings and constant monitoring from a healthcare professional. Therefore, an ideal wound dressing would require infrequent changes providing wound-healing properties for a long duration of time. It would also be expected to be non-toxic, maintain a moist environment, protect the wound bed, and promote tissue proliferation [298].

Covering the entire surface area of the body, the skin is the largest organ in the human body approximately comprising one-tenth of the body mass [299]. As the body's only barrier to the external environment, it protects it against exogenous factors and pathogenic microorganisms [300]. Normally, the skin is able to restore its integrity after injury through a process involving hemostasis, inflammation, proliferation, and remodeling [301]. Wound healing is a complex process that can be interrupted by both local (oxygenation, infections, biofilms) and systemic factors (age, gender, ischemia, diseases, medication, alcoholism, smoking, immunocompromised conditions, nutrition) [301]. When certain conditions are not met, wounds that generally heal in between 4-6 weeks enter and remain in a pathogenic, inflammatory stage failing to progress through the normal healing process resulting in a chronic wound [302]. The inflammation stage is an important stage of the wound healing process playing an important role in removing infectious microorganisms. However, incomplete microbial clearance in chronic wounds can cause

prolonged inflammation that leads to elevated levels of pro-inflammatory cytokines and matrix metalloproteinases that degrade the ECM [301]. Thus, an imbalance of proteases and growth factors puts the wound in a chronic state leading to a wound that fails to heal.

Bacterial biofilms also arise as a potential factor hindering proper wound healing. With over 90% of chronic wounds containing biofilms, the microenvironment of chronic wounds is optimal for bacterial growth [303]. Biofilms are characterized by bacteria encased in an extracellular polymeric substance (EPS) matrix with an altered phenotype in regard to growth, gene expression, and protein production. Biofilm formation is a multistep process involving surface adherence, attachment and accumulation [166]. Clinically, biofilm has been proven to delay healing in different types of chronic wounds. Being less metabolically active than other bacteria, biofilms hinder chronic wounds from being susceptible to antibiotic treatment, resistant to host immune responses and therefore slow tissue repair by stimulating chronic inflammation [304]. Therefore, the presence of biofilms in wounds is crucial to take into consideration when formulating a treatment plan. In this paper, biofilms of *Staphylococcus aureus*, a ubiquitous Gram-positive bacterium was studied. *S. aureus* is a major bacterial human pathogen that causes a wide variety of clinical manifestation, and are often found on skin, mucous membranes. As well, it is also one of the most prevalent bacterial species identified in chronic wounds causing prolonged inflammation and healing failure [305].

Various wound dressing materials such as hydrogels, hydrocolloids, foams, and alginates are available [298]. Of all the different materials, hydrogels are the most attractive due to fluid absorbency, ability to form a protective barrier and provide a moist environment for skin regeneration. However, most hydrogels are limited with poor mechanical properties [306]. Thus, in an attempt to increase the attractive features and overcome the limiting properties, the hydrogel

was lyophilized (Xerogel), resulting in a scaffold with effective exudate absorbency, physical stability and prolonged protection barrier via slow degradability. The proposed hydrogel is composed of gelatin, chitosan and ascorbic acid and aims to meet all the needs for proper wound healing and fast recovery.

Gelatin is a polymer derived from collagen; an abundant protein found in human connective tissue. It is commonly used in tissue engineering due to high abundance, low cost, biocompatibility, biodegradability and low antigenicity [307]. As wound dressing materials, gelatin contains peptide sequences recognized by cell integrin receptors for cell adhesion and the ability to form a nanofibrous structure biomimics the extracellular matrix essential for skin regeneration [307]. Although gelatin is not a replacement for the new collagen production in wound tissue, it can still form an environment attracting critical cells for wound healing and provide an alternative substrate for negative effectors such as free radicals and proteases [308]. A structural transition occurs from a helix to a coil at temperatures above 35°C, undergoing a solid to liquid phase change [309]. With an average skin surface temperature of an individual at room temperature being around 33°C, the hydrogel is able to slowly transform into liquid form [310]. Compared to traditional dry gauze wound dressings that may cause further injury upon removal, dressings composed of gelatin being thermosensitive will liquify into a gel and allow convenient removal or wash off without causing further harm to the wound bed.

Chitosan a  $\beta$ -1,4-linked polymer of glucosamine and a derivative of chitin was used as a crosslinker to improve the physical stability of the hydrogel [311]. In order to convert chitosan into liquid form, it was dissolved in 1M of ascorbic acid. Several studies have shown the efficacy of ascorbic acid inhibits the formation of *S. aureus* biofilms in chronic wounds [312]. Being a biocompatible hydrophilic cationic biopolymer makes chitosan suitable to deliver drugs [313]. As



well, its antimicrobial effects against a broad range of both gram-positive and negative bacteria as well as fungi can prevent wound contamination. Moreover, previous in vitro studies have demonstrated the antibacterial properties of chitosan NPs [313].

Various wound dressings that have been developed each have distinct features that protect the wound and promote healing. However, as chronic wounds are multifactorial in etiology, in this article we investigated to create a multifunctional dressing ideal for wound healing. This dressing functions as a foam-like dressing that moderately absorbs wound exudate. Moreover, the film-like thickness provides flexibility, and the designed dressing will allow patients to place it in difficult areas. Upon contact with wound fluid and skin surface temperature of 33 degrees Celsius, the dressing transforms itself into a hydrogel capable of rehydrating dry wounds and allowing painless removal from the wound bed.

## **5.2. Materials and Methods**

### **5.2.1. Materials**

The gelatin from bovine skin, chitosan, ascorbic acid, Resazurin sodium salt, coumarin 6, Tryptic Soy Broth and sodium chloride were purchased from Sigma-Aldrich (Ontario, Canada). Glycerol monostearate (molecular weight 358.56) was purchased from Sigma-Aldrich (Ontario, Canada).  $\alpha$ -L-phosphatidylcholine (Soy-95%) (molecular weight 770.123 g/ mol) was purchased from Avanti Polar Lipids (AL, USA). Polyvinyl alcohol (PVA; 31–50 kDa) was purchased from Sigma-Aldrich (Ontario, Canada). *Staphylococcus aureus* (ATCC 25923) subsp. *aureus* Rosenbach was purchased from ATCC (Virginia, USA). D-glucose monohydrate was purchased from Thermo Fisher Scientific (Burlington, ON, Canada),

### **5.2.2. Solid lipid nanoparticles preparation.**

SLNs containing either our drug of interest (LL37 and vancomycin) or C6 were prepared using a double-emulsion solvent evaporation technique described previously with modification [278]. Briefly, 10mg of L-phosphatidylcholine and 5mg of glyceryl monostearate and were dissolved in 700 $\mu$ L of acetone and 700 $\mu$ L of ethanol at 55°C. 100 $\mu$ L of 0.05mg/mL of C6 or 100  $\mu$ L of the drug mixture (200  $\mu$ g of LL37 and 400  $\mu$ g of vancomycin) solution was added into the lipid mixture. A primary sonication was performed for 20 seconds by a microtip probe sonicator at amplitude 5. The resultant emulsion was then emulsified with an aqueous phase solution containing 10mL of chilled 2% poly vinyl alcohol (PVA) and sonicated for another 60 seconds. The SLNs were stirred overnight to evaporate the organic solvent. They were collected by centrifugation (20,000g, 40min, 4°C) and washed twice with autoclaved Milli-Q water to remove excess emulsifier and free drug. SLNs were added to 30mg of perlitol dissolved in 1mL of autoclaved Milli-Q water and frozen overnight at -75°C. Then SLNs were lyophilized for 24hr. NP size and net surface charges were determined by light scattering using ZetaPALS (Brookhaven).

### **5.2.3. Hydrogel preparation**

The fluid absorbing capacity of the hydrogel is one of the important criteria for maintaining a moist environment over the wound bed. For the preparation of the hydrogel, we used a method already published with slight modification [314]. Briefly, to make 6% gelatin hydrogel, 0.6g of gelatin Type-A powder was dissolved in distilled water heated at 30°C until the solution becomes clear (about 30min). For the hydrogel to be stable, we must introduce a cross-linking agent such as Chitosan. The amount of chitosan was carefully added to present a UCST of around 33°C.

To make the chitosan solution, 10mL of autoclaved milli-Q water was used to dissolve 1.7612g of ascorbic acid powder and continuously stirred for 30 min at room temperature to produce a solution of clear 1M of ascorbic acid. 0.2g of chitosan was added to the solution and stirred at room temperature for overnight to ensure complete dissolution. 1:1 ratio of 6% gelatin and 2% chitosan were mixed to form the hydrogel. NPs suspension is added to the mixture to have the hydrogel NP formulation. Hydrogels were frozen overnight at -75°C then lyophilized for 24hrs.

#### **5.2.4. C6 SLNs release study from hydrogel.**

Release study was conducted on PermeGear Franz cells, and 6 hydrogels were tested at once. In the Franz cells, Whatman cellulose acetate membrane filter (1.2µm, diameter 47mm) was installed between the donor and the receiver compartment. The lyophilized hydrogel were place in the donor chamber and cover with parafilm to prevent moisture from the air to be in contact with the sample. The receiver chamber was filled with distilled water. Three hydrogels were tested at 33°C and the other three were tested at room temperature 23°C. A sampling volume of 5mL every 20minutes was withdrawn for a total of 2 hours, after every sampling, the receptor chamber was replenished with fresh autoclaved milli-Q water. 200µL of the collected sample was dispensed in a 96-well plate, and a standard was made using lyophilized C6 SLN. Fluorescence was measured at the excitation wavelength of 485nm, emission wavelength of 538nm, and cut-off wavelength at 530nm.

#### **5.2.5. Preparation of microtiter plate-based biofilm model**

The microtiter plate-based (MTP) systems are frequently used for biofilm model systems [315, 316]. This is a cheap and easy model to study biofilm and allowed to perform many tests simultaneously [317]. *S. Aureus* was used in our study to form the biofilm model. To be able to

form the biofilm the Tryptic Soy Broth (TSB) was supplemented with 2% Glucose and 4% NaCl. One colony of *S. Aureus* was inoculated in 10mL of fresh both and incubated at 37°C and shake at 100 rpm for 24 hours. From that, 100µl of a dilution to generate 10<sup>8</sup> CFU was transfer in tissue-treated 96 wells microtiter plate. The plate was then incubated at 37°C for 24 hours. The supernatant was then removed and the biofilm was rinsed to remove unbound cells.

#### **5.2.6. Quantification of the biofilm using crystal violet and resazurin assays**

The total amount of biofilm biomass formed can be assessed using the crystal violet (CV) assay. CV binds to negatively charged surface molecules and polysaccharides in the extracellular matrix. Briefly, after 24h incubation, the content of the microtiter plate was discarded and the wells were washed to eliminate non-adherent cells. Biofilm was fixed with 96% ethanol and stained with 200µl of 0.05% CV for 5 min. The content of the plate was discarded again and the bound CV was solubilized with acetic acid before reading the absorbance using the microplate reader at 570nm.

Resazurin assay was used to determine the metabolic activities of the biofilm. It is a blue redox dye that can be reduced by viable bacteria in the biofilm. Briefly, non-adherent cells will be discarded from the microplate. 1 mg/mL of resazurin was in PBS. The solution was protected from light and stores at 4°C. 100 µl of 10µg/mL of resazurin was added into each well and blank resazurin was added to non-treated wells as blank control. The plate was then incubated at 37°C for 20 min. The fluorescence was read using a microplate reader (SpectraMax M5) with excitation set at 530nm and emission at 590nm.

### **5.2.7. Biofilm treatment with SLNs containing LL37 and vancomycin**

The bacteria were diluted to a concentration of  $10^7$  CFU and dispense in 96-well plate. The plate was incubated for 24h at 37°C to allow the formation of a mature biofilm. The biofilm was treated with 1, 3, and 6mg/mL of SLNs containing LL37/Vancomycin. The plate was incubated for 24h at 37°C. After the plate was rinsed gently in PBS to remove unattached and loosely attached bacteria and we proceeded with the biofilm evaluation using CV as described above.

### **Statistical analysis.**

Data are presented as the mean  $\pm$  standard deviation (SD). The n values refer to the numbers of replicates performed for each study. One-way analysis of variance or student t-test were performed on all results, with P values of  $<0.05$  considered to be significant.

## **5.3. Results**

### **5.3.1. Solid lipid nanoparticles preparation.**

Table 5.1 summarized the particle sizes of the SLNs containing LL37 and vancomycin, and also the encapsulation efficiency and the zeta potential. The mean particle size is  $237.8 \pm 13.3$  for loaded SLN and  $207.3 \pm 13.7$  for drug-free SLN. The encapsulation efficiency for LL37 is  $67.45 \pm 6.7$  and for the vancomycin is  $59.1 \pm 7.4$ . The zeta potential for blank SLNs were  $-20 \pm 3.2$  mV and for the drug-loaded particles were  $-18 \pm 2.1$  mV.

**Table 5.1: LL37-Vancomycin SLN characterisation.**

	Size (nm)	Encapsulation Efficiency (%)	Zeta potential (mV)	PDI
<b>Drug loaded</b>	237.8±13.3	LL37 :67.45±6.7	-18±2.1	0.21
		Vancomycin: 59.1±7.4		
<b>Drug Free</b>	207.3±13.7		-20±3.2	0.23

### 5.3.2. Hydrogel preparation

For the hydrogel preparation, we used gelatin type-A. First, we evaluated the phase transition of gelatin alone. As reported in Table 5.2, 3% of gelatin will take approximately 25 min at 33°C to completely liquify. Increasing the gelatin percentage also increases the liquefaction time. For example, 10% gelatin took up to 39 min to liquify. To have a better texture of the hydrogel and better control on the liquefaction, we formulated the gelatin mixed with Chitosan. Increasing the percentage of chitosan increase the liquefaction time. 0.6% chitosan formulated with 6% gelatin took 30 min to completely liquify, but 1% chitosan with 6% gelatin took twice the time, 60 min for complete liquefaction (Table 5.3). As noticed with gelatin alone, increasing the percentage of gelatin with chitosan also increases the liquefaction time. 9% gelatin formulated with 1% chitosan failed to completely liquefy even after 5 hours.

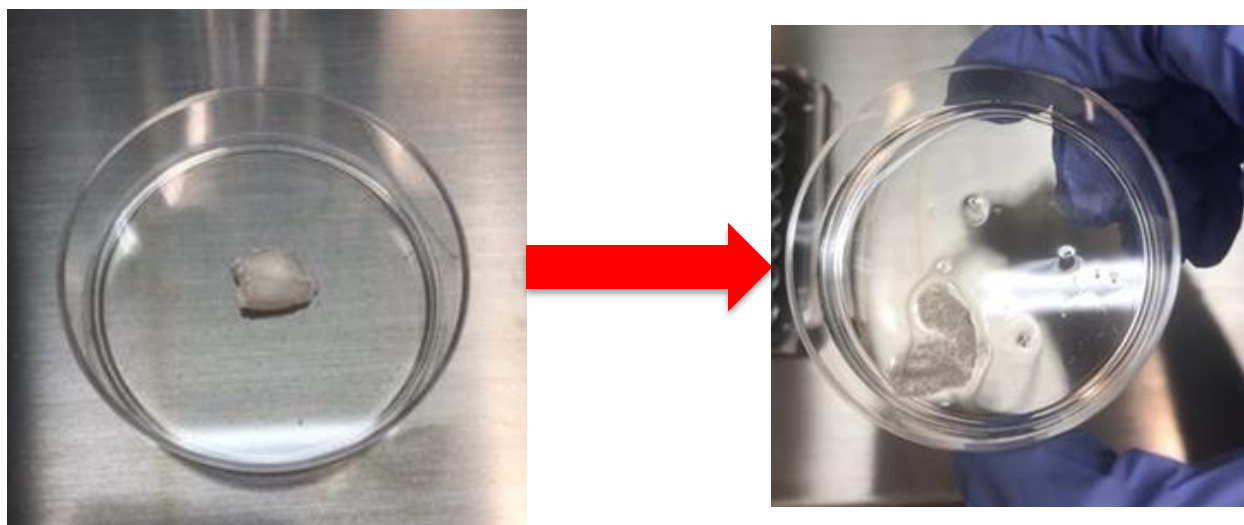


**Figure 5.1: Picture of lyophilised 3% gelatin at 25°C and at 33°C after 25 min.**

**Table 5.2: Gelatin hydrogel phase transition.**

	3% Gelatin	5% Gelatin	10% Gelatin
Time required to liquefy at 33°C	25 min	28 min	39 min

**Table 5.3: Liquefaction time of different ratio of gelatin/chitosan.**

Chelatin/Chitosan	6% Gelatin 0.6% Chitosan	6% Gelatin 1% Chitosan	9% Gelatin 0.6% Chitosan	9% Gelatin 1% Chitosan
Time required to liquefy at 33°C	Viscous liquid (15 min) Completely liquid (30 min)	Liquid at 60 min	Liquid at 30 min	Stay jelly after 5 hours

### 5.3.3. C6 SLNs release study from the gelatin-chitosan formulation.

We performed the release study of SLN from the hydrogel at room temperature and also 33°C which is the mean temperature of human skin. To be able to track the SLN and quantify them, coumarin 6 was encapsulated with SLN. C6-SLNs were mixed with the hydrogel, lyophilized before performing the release using Franz diffusion cell. Figure 5.1 shows the release at 23°C and 33°C for two hours. At both temperatures, the hydrogel will start releasing after been moisturized by the wound fluid. A higher release at 33°C is observable with a total of 78.62% released compare to 23°C with 65.24% released (Figure 5.2).

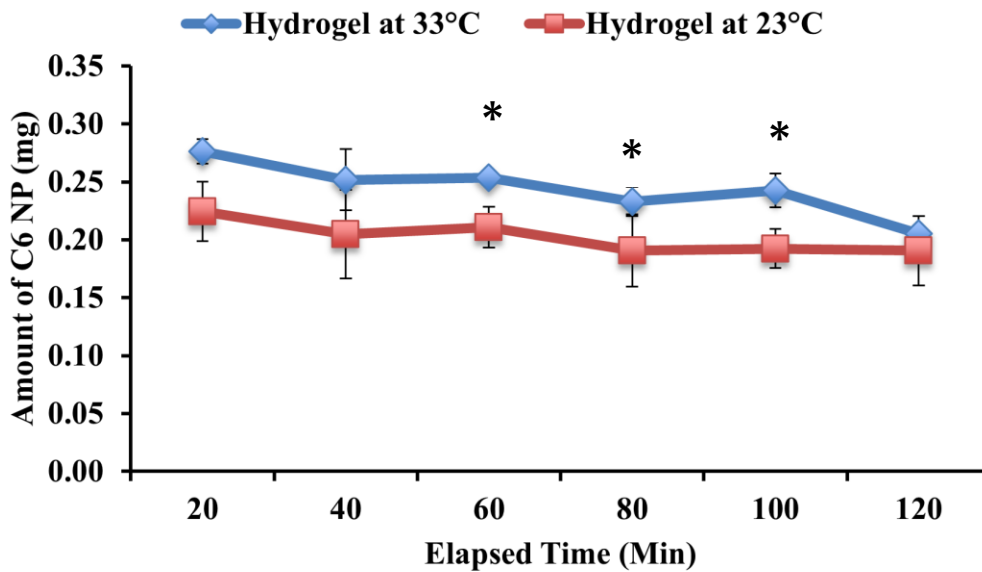


**Figure 5.2: Amount of C6 NP Released Over Time.** Data represent the mean  $\pm$  SD.; N=3 , P-value < 0.05 compared to 23°C.



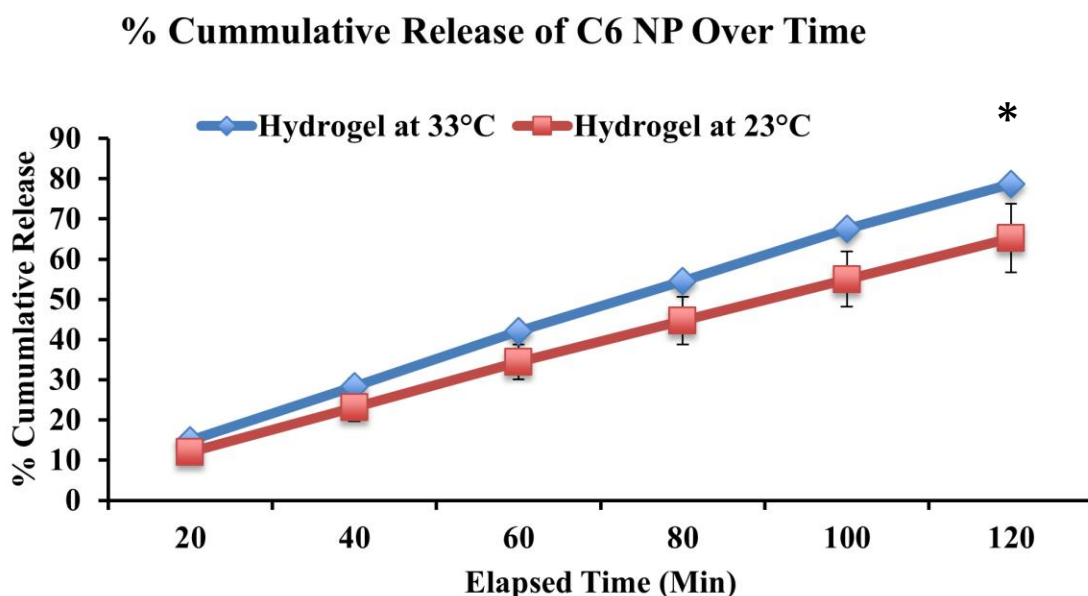


**Figure 5.3: Percentage cumulative release of C6-SLN over time.** Data represent the mean  $\pm$  SD.; N=3, P-value < 0.05 compared to 23°C.

#### 5.3.4. Quantification of the biofilm using crystal violet and resazurin assays

We prepared a microtiter plate-based biofilm (MTP)-base model. First, we evaluated the concentration of bacteria needed in each well to form a sticky biofilm. Using crystal violet to quantify the biomass, Figure 5.3 shows  $10^7$  CFU/mL was an optimum concentration to form the biofilm.  $10^8$  CFU seems to be too much for the bacteria to form a proper biofilm.

In order to evaluate the living bacteria inside the biofilm, we treated each well with Resazurin (Figure 5.4).  $10^7$  CFU was kept as the optimum amount of bacteria.

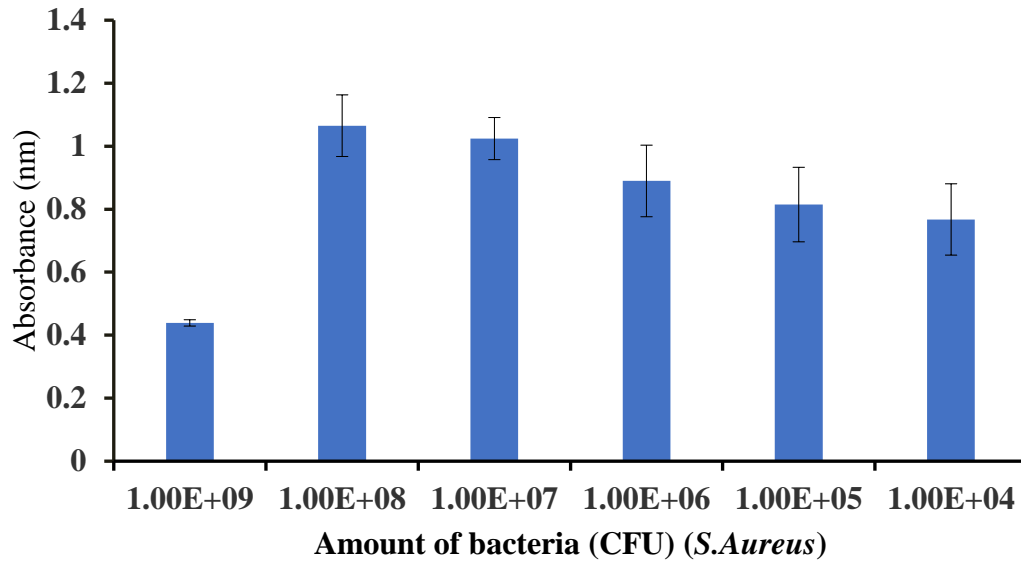


**Figure 5.4: Assessment of *S. aureus* biomass using 0.05% crystal violet in a 96-well plate.**  
Data represents the mean  $\pm$  S.D.; N=3.

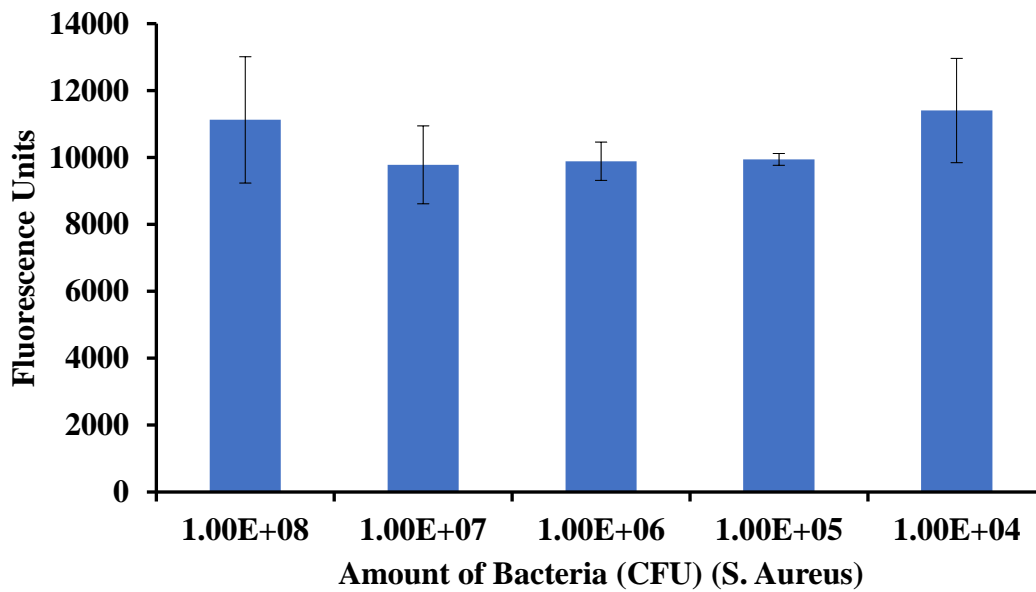


**Figure 5.5: Evaluation of living *S.Aureus* bacteria present in the biofilm using resazurin.** Data represent the mean  $\pm$  S.D.; N=3.

### 5.3.5. Biofilm treatment with SLNs containing LL37 and Vancomycin

Prepared LL37/vancomycin-SLN was used to treat biofilm formed using  $10^7$  CFU/mL of *S. Aureus* in a 96-well plate. Figure 5.5 shows different concentrations of SLNs used to treat the biofilm included negative control which is only blank medium and positive control consisted of penicillin-streptomycin. The different concentrations of SLNs used slightly reduce the amount of biofilm but lesser than the positive control. Three different concentrations 1, 3, and 6 mg/mL with were used to treat the biofilms. 1 and 2 mg/mL slightly reduced the biofilm with a significant reduction observed with 6 mg/mL. The positive control significantly reduced the biofilm formation compared to the highest concentration of SLN used (6 mg/mL).

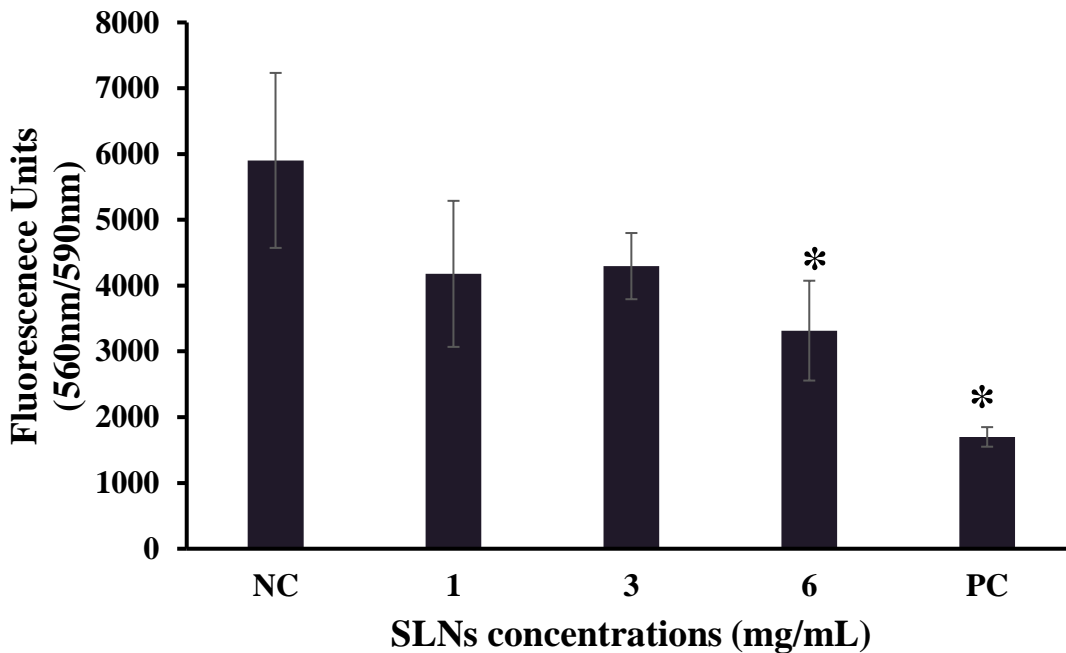


**Figure 5.6: Biofilm treatment with LL37/vancomycin-SLNs.** Blank medium as negative control and penicillin-streptomycin as positive control. NC: Negative control=Broth only, PC: positive control= 400 units of penicillin/400 ug of streptomycin. Data represent the mean  $\pm$  S.D.; N=3. \*P-value < 0.05 compared to blank.

#### **5.4. Discussion:**

The wound dressing plays an important role in the wound healing process. Currently available dressings still present some challenges in helping with wound healing. An ideal wound dressing will consider some important points such as maintaining a moist environment for the wound bed and having the possibility to remove the excess fluid. Also, it is very important to have a dressing that is easy to remove, non-toxic, and can be applied for a long period of time [192]. Gelatin appears to be an ideal biomaterial, which depending on its formulation, can be used to maintain a moist environment for the wound, can be used as a scaffold for tissue reconstitution, is non-toxic and, can be easily removed since it will liquefy at high temperatures. More importantly, gelatin can be used as a drug delivery vehicle to help remove the bacterial infection commonly seen with chronic wounds [318]. The biofilm present in chronic wounds prevents them from healing, it is of the utmost importance to remove the bacterial infection for immunocompromised patients mostly to expect a skin regeneration [319]. The biofilm presence in chronic wounds plays a critical role by prolonging the inflammatory phase, such as the excessive release of cytokines, the extended presence of neutrophils and macrophages, the changes in oxygen concentration, and the pH in the wound [166]. In this study, we developed a thermo-responsive hydrogel as a wound dressing capable of delivering SLN containing a combination of LL37 and vancomycin in an effort to remove the bioburden from chronic wounds to improve wound healing.

We formulated a hydrogel using only gelatin and we evaluated how long different percentages of gelatin will take to liquefy at 33°C. As expected, increasing the percentage of gelatin from 3% to 10% also increased the liquefaction time from 25 min to 39 min (Table 2).

Gelatin has a triple helix configuration at room temperature and lower. Gelatin chains become disordered (coiled structure) while heated above 30 °C and becomes more liquid [320]. The transition between helix and coil depends on the temperature, pH, concentration, stress, solvent used, and the presence of cross-linking agents [320-322]. Unfortunately, gelatin alone has poor mechanical properties [323]. To improve the physical stability of gelatin, we introduced chitosan as a cross-linking agent. The cross-linking agent increases the time needed for a complete transition from gel to liquid (Table 3). Lyophilizing the final formulation gave the gelatin-chitosan a more spongy-like characteristic that improved the exudate absorbency and physical stability. The primary role of our formulation is to protect the wound surface, deliver drugs that will eradicate biofilm formation in chronic wounds, and allow easy removal of the dressing without re-opening the wound. LL37 is a member of the cathelicidin family and is a peptide that has been shown to play a major role in host defense and has been successfully used against *S. aureus*, one of the major bacteria constituting biofilms in chronic wounds [324, 325]. LL37 alongside the antibiotic vancomycin have been shown to exhibit synergistic antibacterial effects against *S. aureus* [326]. LL37 is a peptide and vancomycin is a glycopeptide, both of which may be prone to degradation. As a result, encapsulating the drugs into SLN will protect the drugs and offer slow prolonged release. Furthermore, the nanoparticle will help penetrate the biomass and deliver the drug to the bacteria encased in the extracellular matrix [327]. The LL37-vancomycin SLN was loaded into the hydrogel and lyophilized. By lyophilizing the hydrogel, it became more absorbent and can quickly absorb massive amounts of water and trigger the release of SLN present within the matrix. Figures 1 and 2 show a higher release of C6-SLN (C6 was used to fluorescently track SLN release) at 33°C compared to room temperature due to the thermo-responsive behaviour of the hydrogel. The higher release of C6-

SLN at room temperature might somewhat hide the thermo-responsiveness of the dressing suggesting a not adapted release experiment setup. Instead of using a Franz diffusion cell that content 5 mL of liquid in the receiver chamber which is in contact with the release membrane and the lyophilized hydrogel, a dryer environment would have been more adapted. The lyophilization dries the hydrogel by sublimation, removing the frozen water crystal under high pressure leaving enough pores in the hydrogel structure, thus the high water absorption capacity [328, 329]. Although we have a release at both temperatures, we still have a significant difference in the release up to 100 min. The overall cumulative amount of C6-SLN released at 33°C was significantly different (P-value<0.05) from room temperature. A dryer environment should be used in the future for testing the thermo-responsiveness.

In order to evaluate the efficiency of our SLN to break down the biofilm formation using *S. aureus*, was evaluated in 96-well plate (Figure 3 and 4) and LL37-vancomycin SLNs were used to treat the biofilm. Figure 6 shows the different concentrations of SLNs used to treat the biofilm and the quantification of the biomass after treatment. 1mg/mL and 3mg/mL of SLNs have no significant impact on biofilm formation. 6 mg/mL significantly reduced the biomass compared to the negative control (blank medium). In one SLN preparation, approximately 134.9 µg of LL37 and 236.4 µg of vancomycin were encapsulated into the nanoparticles. Shurko et al., showed that 32 µg/mL of LL37 and 256 µg/mL of vancomycin was enough to inhibit the growth of ATCC *S. aureus* 25923 [194]. It is possible in our study that the slow release of the drug from SLN is not sufficient to break down the biofilm in 24 hours. The limitation of the in vitro design makes it difficult to study longer periods since the bacteria will begin to die naturally due to a lack of nutrient replenishment. An increased amount of drug encapsulated will probably allow more drug release in 24 hours to have a major impact.

Those limitations will not necessarily reflect in vivo conditions since higher amounts of SLN can be used in the dressing and the release can be sustained for a longer period of time. A biofilm testing system with a continuous flow of medium would be more appropriate for longer duration experiments such as the flow displacement biofilm model system [317]. It is also possible that the small amount of LL37 released from the SLN was quickly degraded by aureolysin and V8 protease produced by *S. aureus* [330]. This suggests higher concentrations of LL37 might be necessary to have a bactericidal effect.

## **5.5. Conclusion**

This study aimed to develop a thermo-responsive dressing containing LL37-vancomycin SLN to help break down the biofilm formation on chronic wounds. We successfully fabricated a gelatin-chitosan hydrogel and improve its physical characteristic by lyophilization. As expected, was very absorbent and also liquefy at higher temperature hence an easy removal process from the wound without reopening the wound. Future studies are needed to better test the thermo-responsiveness of the system and complete characterisation of the system. We developed a microplate biofilm model and tested SLN containing LL37 and vancomycin on the system. The SLNs were able to reduce the biofilm formed but not to the extent expected. This study allows us to learn many limitations of our in vitro system and also revealed the opportunities to make the system better in future studies. Overall, we have a system that is capable of releasing SLN at high temperature and the SLNs containing LL37 and vancomycin was able to decrease the biofilm formation compared to the negative control.

## **Chapter 6: Conclusion**



## 6.1 Significance of the study

Drug delivery systems have been developed to administer a pharmaceutical compound in a controlled manner to achieve an optimized therapeutic effect. Topical drug delivery as opposed to parenteral route offer more opportunity to deliver different types of drugs and use different routes. For example, protein drugs have always been challenging to deliver because of their size and fast degradation. Using NPs the protein can be protected and delivered to the targeted organ. Drug delivery devices have been used for vaginal and anal drug delivery, skin permeation, nasal and pulmonary delivery. Topical drug delivery systems have been largely developed as microbicides for HIV prevention and also as a component of chronic wound dressings. Unfortunately, even with many efforts made in developing different microbicides to fight HIV infection, many fail due to toxicity issues or lack of efficacy. A lot of research must still be done to understand how the drug delivery systems work and how we can optimize them to achieve the aspired goal. For that reason, we took a different approach to understand the different mechanical behaviors of vaginal films containing NPs used to prevent HIV. We explored how the presence of NPs within the matrix of the film can affect the film structure. We also fabricated and characterized IVRs, especially the safety of polyurethane on vaginal cells and vaginal normal flora. In an effort to improve therapeutic efficacy and potentially prevent drug resistance, we developed a dual-segmented IVR system to deliver a chemotherapeutic agent along with siRNA. For the last half of the thesis, we investigated the usage of stimuli-responsive polymers to fine-tune how composition and delivery time can help minimize unnecessary drug release and toxicity when not needed. We used a pH-responsive polymer coating on the second half of our dual IVR system to deliver siRNA-encapsulated-NPs only when the pH of the FGT changed from acid to basic during sexual intercourse due to the presence of seminal fluid. Most of the post-exposure or pre-exposure

therapies existing nowadays are still non-affordable in developing countries. For example, the brand name Truvada, one of the well-known pre-exposure and also post-exposure prophylaxis cost around USD \$1,258 without any subvention from the government for one month of therapy for a single person [331]. More efforts have been made to develop cheaper generics of Truvada. For example, Canada has a more affordable generic under the name of Emtricitabine-Tenofovir that costs around CAD \$250 for 30 tablets. Those prices are very high for people living in developing countries where there are more people infected by HIV. The goal of this study was to design a more affordable therapy with high patient compliance. The design of the IVR is a good idea to empower women to protect themselves especially in regions where they cannot negotiate for safer sexual intercourse. HCQ is a good choice of drug to help protect people but also to reduce the price of the overall therapy since widely available at a lower price. With the purpose to develop a more potent therapy to protect against HIV infection and prevent drug resistance, gene therapy was introduced into the IVR design. Although siRNA is more expensive now, gene therapy is a fast-developing area of research and a cost-effective alternative will soon be developed. Although more studies must be done, if successful, this new platform might save a lot of lives and money for people living in developing areas.

Lastly, we explored another stimuli-responsive polymer for the development of a thermo-responsive wound dressing capable of delivering NPs containing drugs only when applied on the skin to eradicate biofilm formation on chronic wounds for immunocompromised patients. As previously stated, the current chronic wound dressing design and therapies have their flaws. Today, the most effective way to treat chronic wounds in immunocompromised patients is by surgery. Chronic wound is a huge burden for all communities and requires high financial inputs. The goal of this study was to create an easy-to-use wound dressing that can be applied on the wound to

protect it and also to deliver drugs that can eliminate the bioburden and speed up the wound healing process. This is aiming to create a therapy less invasive than surgery but with high effectiveness and hopefully improve the overall patient life conditions.

## **6.2 Summary of results**

We evaluated how the presence of NPs in the matrix of vaginal films composed of PVA can affect its mechanical properties. PVA films for drug delivery are usually formulated with plasticizers that affect the mechanical properties of the film to make it more flexible. The introduction of NPs into the matrix of the film may affect the film properties in terms of molecular crosslinking within the matrix. The objective of this study was to evaluate the physico-mechanical properties of PVA films containing plasticizers and in the presence of different concentrations of NPs. We found that the amount of PVA used in a film formulation and the ratio of PVA and plasticiser greatly affect the film disintegration time. The NPs within the film matrix did not significantly alter the film's mechanical behavior. From this study, we learned how we can fine-tune a film formulation to expect the desire NPs profile through the film disintegration. In this study, the fast decay of the fluorescence from the NPs during the release study explains the low cumulative release. A stable fluorophore must be used to obtain a better evaluation of the amount of particles released. Commercially available controls like N9 can be used for comparison.

Vaginal films are good drug delivery systems but they cannot provide controlled and sustained drug release for prolonged periods of time e.g. >1 week. In fact, the fast disintegration time of the film suggests a more rapid release of the active ingredient. IVRs can be designed to provide sustained and controlled drug release, ultimately resulting in increased patient adherence [233]. We developed a reservoir-type IVR that released HCQ in a controlled manner for >14 days.

We focused on the safety of the device and drug not only on vaginal cells but also on vaginal flora that is crucial for the protection of FGT. Damage to the vaginal surface due to the drug delivery device can cause inflammation of the FGT resulting in an increase in HIV infection [243]. We were able to achieve a daily release higher than the minimum concentration needed to induce IQ(4.3 $\mu$ g/ml) and 35-fold lower than the highest safe concentration tested (1 mg/ml). This study demonstrated the safety of the polyurethane HP-60D-35 used to fabricate the IVRs and HCQ toward vaginal and ectocervical cell lines Vk2/E6E7 and ECT1/E6E7 and also on the normal vaginal flora *Lactobacillus jensenii* and *Lactobacillus crispatus*. This chapter resumes promising results about the safety of IVR segment containing HCQ, but further in vivo studies must be done to evaluate its potentials as microbicide to prevent HIV infection.

In the following chapter, we designed a segmented IVR system capable of delivering two different therapies to prevent HIV infection. Using different therapies creates multiple obstacles to HIV replication and reduces the possibilities of mutations [332]. The IVR designed had two segments, the first segment is a reservoir-type segment containing HCQ and a rate-controlling excipient as discussed previously, and the second segment is a matrix-type IVR that is coated with a pH-responsive polymer containing siRNA encapsulated SLN. In this study, we are taking advantage of the design of a stimuli-responsive polymer for the right time delivery of the gene therapy. We were able to continuously HCQ for over 24 days. The second half of the IVR coated with a pH-responsive polymer released C6-SLNs only at high pH when SFS to the low pH VFS to simulate sexual intercourse. The siRNA-SLN-Ab released from the segment was able to knockdown the CCR5 gene expression in comparison to the negative control using drug-free SLN. As a control in future studies, scramble siRNA can be used to evaluate the effect of non-specific siRNA itself on the safety of cells and their potential implication in gene expression. We found

that the coated segment was non-cytotoxic to vaginal epithelial cell VK2/E6E7. We demonstrated here a system that can potentially prevent HIV infection and reduce the virus mutation rate.

The last project in this thesis was to develop a thermo-responsive wound dressing to help improve the healing of chronic wounds of immunocompromised patients by delivering drugs to eliminate biofilm formation. The main feature of this hydrogel dressing is its capacity to liquefy at a high temperature (33°C temperature of the skin) compared to room temperature. We found that hydrogels composed of gelatine alone liquefied faster than gelatin crosslinked with chitosan. We found that the formulation started to release C6-SLN upon absorbing the release buffer but more release was observed at 33 °C compared to room temperature. We found that the highest concentration of LL37/vancomycin-SLN (6mg/mL) used to treat the biofilm was able to significantly decrease the biomass compared to the negative control. However, we also observed that the positive control consisting of penicillin-streptomycin was more efficient due to its rapid contact with the bacteria. In conclusion, we developed a thermo-responsive system capable of release SLNs at high temperatures and our LL37/vancomycin was able to decrease the biofilm formation. Further characterizations are needed for this system and animal studies are required to evaluate the efficacy.

### **6.3 Future directions.**

Patient compliance and therapeutic efficacy should be the priority when developing a drug delivery system. Even if a drug delivery system is therapeutically performant, low user acceptability will hinder its effectiveness. While the intravaginal film is capable of rapid delivery of active compounds within the FGT, the design of an IVR is more appealing and more advantages. Studies have been done on user acceptability of some specific type of IVRs. To the best of our

knowledge, we still do not have such data for IVRs made from polyurethane HP-60D-35. Future studies have to look at the physical and mechanical properties of the IVR to make sure it is not too rigid causing injury to the FGT or easily expelled from the FGT. Although the three weeks release period makes sense taking into consideration the menstrual cycle, it would be ideal to have a long-acting drug delivery device (>6 months) as we are seeing now with the development of patches and injectables to protect against HIV infection. In this thesis, we used hot-melt extrusion to make the IVRs. This technique is fast and can produce consistent IVRs. But every time we have to change the design, it will require the fabrication of new molds. The aluminum mold needs to be created by a machine shop and requires high precision. Furthermore, lots of polymers are lost in the void space during the hot-melt injection process. In the future, using three-dimensional printing (3DP) will grant the possibility of producing different sizes and shapes of IVRs on the spot while generating minimal waste. The computer aid design (CAD) file used to 3DP the IVR can be easily modified in-house as necessary.

Although we observed interesting in vitro gene knockdown data, in vivo studies must be performed on lab-adapted animal models. Unfortunately, it is challenging to develop a rodent animal model that has an acidic FGT to evaluate our pH-responsive polymer. In the future, we can potentially use for example a Human microbiota-associated (HMA) mice of women normal flora developed by Wolfarth et al [333]. This model colonises the mouse genital tract with human normal microflora. We can take advantage of this acidic environment to test our pH-responsive coated IVR segments. It will be interesting if this mouse model can be humanized and we can challenge with HIV to evaluate the efficacy of our system in vivo.

We had many limitations while evaluating the thermo-responsive wound dressing. The thermo-responsiveness should have been tested in a less moist environment that is more similar to

human skin since the lyophilised hydrogel absorbed high quantities of release medium and triggered the release of NPs. The release study can be done using the thermo-responsive valve-based delivery device with two valves describe by Dinarvand et al [334]. Also, the flow displacement biofilm model system can be used in the future for a more optimized biofilm susceptibility study. In this system, the medium flows continuously and nutrients are constantly replenished, and wastes are removed. This system will allow to better characterize the adherence of the biofilm and extends the antimicrobial testing period which will give more time to the NPs to deliver their cargo to act on the bacteria.

Overall, in this thesis, I developed and characterised various drug delivery systems and demonstrated how they can be used as a microbicide to prevent HIV infection and as a wound dressing for eliminating biofilms and improving chronic wound healing. Further studies are required before these technology platforms can be approved for human use.

## References

1. Yang, D., RNA Viruses : Host Gene Resonnes to Infections. World Scientific Publishing Co. Pte. Ltd., 2009.
2. Shokouh, M.-N. and R.-J. Sarah, How does the humoral response to HIV-2 infection differ from HIV-1 and can this explain the distinct natural history of infection with these two human retroviruses? Immunology Letters, 2015. **163**(1): p. 69-75.
3. Hu, D.J., et al., The emerging genetic diversity of HIV. The importance of global surveillance for diagnostics, research, and prevention. JAMA, 1996. **275**(3): p. 210-216.
4. Martine, P., T.-K. Coumba, and N.N. John, Genetic diversity of HIV in Africa: impact on diagnosis, treatment, vaccine development and trials. AIDS (London, England), 2003. **17**(18): p. 2547-2560.
5. Sarah, L.R.-J. and C.W. Hilton, Out of Africa: what can we learn from HIV-2 about protective immunity to HIV-1? Nature Immunology, 2007. **8**(4): p. 329.
6. Marlink, R., et al., Reduced rate of disease development after HIV-2 infection as compared to HIV-1. Science (New York, N.Y.), 1994. **265**(5178): p. 1587-1590.
7. Ana, E.S., et al., CD4 T cell depletion is linked directly to immune activation in the pathogenesis of HIV-1 and HIV-2 but only indirectly to the viral load. Journal of immunology (Baltimore, Md. : 1950), 2002. **169**(6): p. 3400-3406.
8. David, M., J.D.N. Stuart, and M. Áine, Human immunodeficiency virus types 1 and 2 have different replication kinetics in human primary macrophage culture. Journal of General Virology, 2006. **87**(2): p. 411-418.
9. Feng, G., et al., Origin of HIV-1 in the chimpanzee Pan troglodytes troglodytes. Nature, 1999. **397**(6718): p. 436-441.



10. Paul, M.S. and H.H. Beatrice, Origins of HIV and the AIDS Pandemic. Cold Spring Harbor Perspectives in Medicine, 2011. **1**(1).
11. Florian, H. and J.H. Thomas, HIV infection of the genital mucosa in women. Current HIV/AIDS Reports, 2009. **6**(1): p. 20-28.
12. Unaids, Global HIV & AIDS statistics — 2020 fact sheet. 2020.
13. Unaids, J., UNAIDS report on the global AIDS epidemic. UNAIDS report on the global AIDS epidemic, 2013.
14. George, M.S. and H. Eric, HIV Transmission. Cold Spring Harbor Perspectives in Medicine, 2012. **2**(11).
15. Florian, H. and M.J. McElrath, Setting the stage: host invasion by HIV. Nature Reviews Immunology, 2008. **8**(6).
16. Diane, M., et al., HIV binding, penetration, and primary infection in human cervicovaginal tissue. Proceedings of the National Academy of Sciences of the United States of America, 2005. **102**(32): p. 11504-11509.
17. Bomsel, M., Transcytosis of infectious human immunodeficiency virus across a tight human epithelial cell line barrier. Nature medicine, 1997. **3**(1): p. 42-47.
18. Hu, J., M.B. Gardner, and C.J. Miller, Simian immunodeficiency virus rapidly penetrates the cervicovaginal mucosa after intravaginal inoculation and infects intraepithelial dendritic cells. Journal of virology, 2000. **74**(13): p. 6087-6095.
19. Richard, A.C., et al., Vaginal microbicides: detecting toxicities in vivo that paradoxically increase pathogen transmission. BMC Infectious Diseases, 2006. **6**(1): p. 90.

20. Andrea, M.W., et al., Genital Ulcers Facilitate Rapid Viral Entry and Dissemination following Intravaginal Inoculation with Cell-Associated Simian Immunodeficiency Virus SIVmac239. *Journal of Virology*, 2008. **82**(8): p. 4154-4158.
21. Anderson, D., Politch, J.A. and Pudney, J. (2011), HIV Infection and Immune Defense of the Penis. *American Journal of Reproductive Immunology*, 65: 220-229
22. Hideki, H., et al., Proliferative activation up-regulates expression of CD4 and HIV-1 co-receptors on NK cells and induces their infection with HIV-1. *European Journal of Immunology*, 2007. **37**(8): p. 2148-2155.
23. Ombere, S., E. Nyambedha, and S. Bukachi, Wimbo: implications for risk of HIV infection among circumcised fishermen in Western Kenya. *Culture, Health & Sexuality*, 2015. **17**(9): p. 1147-1154.
24. Howe, R.S., Circumcision as a primary HIV preventive: Extrapolating from the available data. *Global public health*, 2015: p. 1-19.
25. Collins, K.B., et al., Development of an in vitro organ culture model to study transmission of HIV-1 in the female genital tract. *Nature medicine*, 2000. **6**(4): p. 475-479.
26. Maher, D., et al., HIV binding, penetration, and primary infection in human cervicovaginal tissue. *Proceedings of the National Academy of Sciences of the United States of America*, 2005. **102**(32): p. 11504-11509.
27. Melikyan, G.B., Common principles and intermediates of viral protein-mediated fusion: the HIV-1 paradigm. *Retrovirology*, 2007. **5**: p. 111.

28. Zaitseva, M., et al., Expression and function of CCR5 and CXCR4 on human Langerhans cells and macrophages: implications for HIV primary infection. *Nature medicine*, 1997. **3**(12): p. 1369-1375.
29. Geijtenbeek, T.B., et al., DC-SIGN, a dendritic cell-specific HIV-1-binding protein that enhances trans-infection of T cells. *Cell*, 2000. **100**(5): p. 587-597.
30. Prakash, M., et al., Higher levels of activation markers and chemokine receptors on T lymphocytes in the cervix than peripheral blood of normal healthy women. *Journal of reproductive immunology*, 2000. **52**(1-2): p. 101-111.
31. Hladik, F., et al., Initial events in establishing vaginal entry and infection by human immunodeficiency virus type-1. *Immunity*, 2007. **26**(2): p. 257-270.
32. Zhang, Z.-Q.Q., et al., Roles of substrate availability and infection of resting and activated CD4+ T cells in transmission and acute simian immunodeficiency virus infection. *Proceedings of the National Academy of Sciences of the United States of America*, 2004. **101**(15): p. 5640-5645.
33. Karageorgos, L., P. Li, and C. Burrell, Characterization of HIV replication complexes early after cell-to-cell infection. *AIDS research and human retroviruses*, 1993. **9**(9): p. 817-823.
34. Munro, J.B. and W. Mothes, Structure and dynamics of the native HIV-1 Env trimer. *Journal of virology*, 2015. **89**(11):5752-5
35. de Goede, A.L., et al., Understanding HIV infection for the design of a therapeutic vaccine. Part I: Epidemiology and pathogenesis of HIV infection. *Annales pharmaceutiques francaises*, 2014. **73**(2):87-99

36. Brenchley, J.M., et al., CD4+ T Cell Depletion during all Stages of HIV Disease Occurs Predominantly in the Gastrointestinal Tract. *The Journal of Experimental Medicine*, 2004. **200**(6): p. 749-759.
37. Kinuthia, J., et al., A community-based assessment of correlates of facility delivery among HIV-infected women in western Kenya. *BMC pregnancy and childbirth*, 2015. **15**(1): p. 467.
38. Lim, S., et al., Violence against female sex workers in cameroon: accounts of violence, harm reduction, and potential solutions. *Journal of acquired immune deficiency syndromes (1999)*, 2015. **68 Suppl 2**: p. 7.
39. Grosso, A.L., et al., Structural determinants of health among women who started selling sex as minors in Burkina Faso. *Journal of acquired immune deficiency syndromes (1999)*, 2015. **68 Suppl 2**: p. 70.
40. UNAIDS, Fact sheet- Latest statistics on the status of the AIDS epidemic. 2017.
41. Robinson, H.L., New hope for an AIDS vaccine. *Nat Rev Immunol*, 2002. **2**(4): p. 239-50.
42. Weissenhorn, W., et al., Atomic structure of the ectodomain from HIV-1 gp41. *Nature*, 1997. **387**(6631): p. 426-30.
43. M. Tebit, D.N., Nicaise; Weinberg, Aaron; E. Quinones-Mateu, Miguel, Mucosal transmission of human immunodeficiency virus. *Current HIV Research*, 2012. **1**;10(1):3-8
44. Yang, S., et al., Novel intravaginal nanomedicine for the targeted delivery of saquinavir to CD4+ immune cells. *International journal of nanomedicine*, 2013. **8**: p. 2847-2858.

45. Card, C.M., T.B. Ball, and K.R. Fowke, Immune quiescence: a model of protection against HIV infection. *Retrovirology*, 2013. **10**: p. 141.
46. Cardo, D.M., et al., A case-control study of HIV seroconversion in health care workers after percutaneous exposure. Centers for Disease Control and Prevention Needlestick Surveillance Group. *N Engl J Med*, 1997. **337**(21): p. 1485-90.
47. Van Damme, L., et al., Preexposure prophylaxis for HIV infection among African women. *N Engl J Med*, 2012. **367**(5): p. 411-22.
48. Marrazzo, J.M., et al., Tenofovir-based preexposure prophylaxis for HIV infection among African women. *N Engl J Med*, 2015. **372**(6): p. 509-18.
49. Thigpen, M.C., et al., Antiretroviral preexposure prophylaxis for heterosexual HIV transmission in Botswana. *N Engl J Med*, 2012. **367**(5): p. 423-34.
50. Baeten, J.M., et al., Antiretroviral prophylaxis for HIV prevention in heterosexual men and women. *New England Journal of Medicine*, 2012. **367**(5): p. 399-410.
51. Grant, R.M., et al., Preexposure chemoprophylaxis for HIV prevention in men who have sex with men. *N Engl J Med*, 2010. **363**(27): p. 2587-99.
52. McCormack, S., et al., Pre-exposure prophylaxis to prevent the acquisition of HIV-1 infection (PROUD): effectiveness results from the pilot phase of a pragmatic open-label randomised trial. *Lancet*, 2016. **387**(10013): p. 53-60.
53. Choopanya, K., et al., Antiretroviral prophylaxis for HIV infection in injecting drug users in Bangkok, Thailand (the Bangkok Tenofovir Study): a randomised, double-blind, placebo-controlled phase 3 trial *The Lancet*, 2013. V 381, I 9883, P2083-2090

54. Lajoie, J., L. Mwangi, and K.R. Fowke, Preventing HIV infection without targeting the virus: how reducing HIV target cells at the genital tract is a new approach to HIV prevention. *AIDS Res Ther*, 2017. **14**(1): p. 46.
55. McLaren, P.J., et al., HIV-exposed seronegative commercial sex workers show a quiescent phenotype in the CD4+ T cell compartment and reduced expression of HIV-dependent host factors. *J Infect Dis*, 2010. **202 Suppl 3**: p. S339-44.
56. Chen, Y., et al., Implant delivering hydroxychloroquine attenuates vaginal T lymphocyte activation and inflammation. *J Control Release*, 2018. **277**: p. 102-113.
57. Morris, G.C., et al., MABGEL 1: first phase 1 trial of the anti-HIV-1 monoclonal antibodies 2F5, 4E10 and 2G12 as a vaginal microbicide. *PLoS One*, 2014. **9**(12): p. e116153.
58. Ledgerwood, J.E., et al., Safety, pharmacokinetics and neutralization of the broadly neutralizing HIV-1 human monoclonal antibody VRC01 in healthy adults. *Clin Exp Immunol*, 2015. **182**(3): p. 289-301.
59. Diseases, N.I.o.A.a.I., Evaluating the safety and efficacy of the VRC01 antibody in reducing acquisition of HIV-1 infection in women. Library of Medicine, Bethesda, MD, 2015.( <https://clinicaltrials.gov/ct2/show/NCT02568215>)
60. Choi, E.e.a., First Phase I human clinical trial of a killed whole-HIV-1 vaccine: demonstration of its safety and enhancement of anti-HIV antibody responses. *Retrovirology*, 2016. **13**(1):82
61. Pillay, V., et al., Dosage Forms for Microbicide Formulations: Advantages and Pitfalls. *Drug Delivery and Development of Anti-HIV Microbicides*, 2014: Pan Stanford Publishing; ISBN: 9789814463560 p. 193.

62. Traore, Y.L., Y. Chen, and E.A. Ho, Current State of Microbicide Development. *Clinical pharmacology and therapeutics*, 2018. 104(6):1074-1081
63. Rohan, L.C., Z. Vaginal microbicide films. *Drug Delivery and Development of Anti-HIV Microbicides*. CRC Press, Taylor & Francis Group 2014.
64. Bunge KE, Dezzutti CS, Rohan LC, Hendrix CW, Marzinke MA, Richardson-Harman N, Moncla BJ, Devlin B, Meyn LA, Spiegel HM, Hillier SL. A Phase 1 Trial to Assess the Safety, Acceptability, Pharmacokinetics, and Pharmacodynamics of a Novel Dapivirine Vaginal Film. *J Acquir Immune Defic Syndr*. 2016 Apr 15;71(5):498-505..
65. Robinson JA, Marzinke MA, Fuchs EJ, et al. Comparison of the Pharmacokinetics and Pharmacodynamics of Single-Dose Tenofovir Vaginal Film and Gel Formulation (FAME 05). *Journal of Acquired Immune Deficiency Syndromes (1999)*. 2018 Feb;77(2):175-182.
66. Kiser, P.F., T.J. Johnson, and J.T. Clark, State of the art in intravaginal ring technology for topical prophylaxis of HIV infection. *AIDS reviews*, 2012. **14**(1): p. 62-77.
67. Clark, M., et al., A hot-melt extruded intravaginal ring for the sustained delivery of the antiretroviral microbicide UC781. *Journal of pharmaceutical sciences*, 2012. **101**(2): p. 576-587.
68. Chen, Y., et al., Development of polyether urethane intravaginal rings for the sustained delivery of hydroxychloroquine. *Drug design, development and therapy*, 2014. **8**: p. 1801-1815.
69. Traore, Y.L., Y. Chen, and A.M. Bernier, Impact of Hydroxychloroquine-Loaded Polyurethane Intravaginal Rings on Lactobacilli. *Impact of Hydroxychloroquine-Loaded Polyurethane Intravaginal Rings on Lactobacilli*, 2015. 59(12):7680-6

70. Moss, J.A., et al., Pharmacokinetics of a multipurpose pod-intravaginal ring simultaneously delivering five drugs in an ovine model. *Antimicrob Agents Chemother*, 2013. **57**(8): p. 3994-7.
71. McKay, P., et al., Intravaginal immunization using a novel antigen delivery device elicits robust vaccine antigen-specific systemic and mucosal humoral immune responses. *Retrovirology*, 2012. **9**(Suppl 2): p. P192.
72. Kim, S., et al., Reversibly pH-responsive polyurethane membranes for on-demand intravaginal drug delivery. *Acta biomaterialia*, 2017. **47**: p. 100-112.
73. McGowan, The development of rectal microbicides for HIV prevention. *Expert opinion on drug delivery*, 2014. **1**(11) p 69-82
74. Anton, P.A., et al., First phase 1 double-blind, placebo-controlled, randomized rectal microbicide trial using UC781 gel with a novel index of ex vivo efficacy. *PLoS One*, 2011. **6**(9): e23243
75. Yang, H., uc781: Beta-cyclodextrin complexation and formulation as an anti-hiv microbicide. uc781: Beta-cyclodextrin complexation and formulation as an anti-hiv microbicide, 2008.
76. Carballo-Diéguez, A., et al., High levels of adherence to a rectal microbicide gel and to oral Pre-Exposure Prophylaxis (PrEP) achieved in MTN-017 among men who have sex with men (MSM) and transgender women. *PloS one*, 2017. **12**(7).
77. Cranston, R.D., J.R. Lama, and R.-B.A. , MTN-017: a rectal phase 2 extended safety and acceptability study of tenofovir reduced-glycerin 1% gel. *Clin Infect Dis*. 2017 Mar 1;64(5):614-620



78. Thomas, C.E., A. Ehrhardt, and M.A. Kay, Progress and problems with the use of viral vectors for gene therapy. *Nature Reviews Genetics*, 2003. **4**(5): p. 346.
79. das Neves J, Nunes R, Rodrigues F, Sarmiento B. Nanomedicine in the development of anti-HIV microbicides. *Adv Drug Deliv Rev*. 2016 Aug 1;103:57-75. doi: 10.1016/j.addr.2016.01.017.
80. Carballo-Diéguez, A., et al., “Tell Juliana”: Acceptability of the candidate microbicide VivaGel® and two placebo gels among ethnically diverse, sexually active young women participating in a .... *AIDS and Behavior*, 2012. **16**(7): 1761–1774.
81. Lakshmi, Y.S., et al., Triple combination MPT vaginal microbicide using curcumin and efavirenz loaded lactoferrin nanoparticles. *Scientific reports*, 2016. **6**:25479
82. Gu, J., S. Yang, and E.A. Ho, Biodegradable Film for the Targeted Delivery of siRNA-Loaded Nanoparticles to Vaginal Immune Cells. *Molecular pharmaceutics*, 2015. **12**(8): p. 2889-2903.
83. Maisel, K., et al., Nanoparticles coated with high molecular weight PEG penetrate mucus and provide uniform vaginal and colorectal distribution in vivo. *Nanomedicine (Lond)*. 2016 Jun;11(11):1337-43
84. Kish-Catalone T, Pal R, Parrish J, Rose N, Hocker L, Hudacik L, Reitz M, Gallo R, Devico A. Evaluation of -2 RANTES vaginal microbicide formulations in a nonhuman primate simian/human immunodeficiency virus (SHIV) challenge model. *AIDS Res Hum Retroviruses*. 2007 Jan;23(1):33-42..
85. Alukda D, Sturgis T, Youan BC. Formulation of tenofovir-loaded functionalized solid lipid nanoparticles intended for HIV prevention. *J Pharm Sci*. 2011 Aug;100(8):3345-3356.

86. Boyapalle, S., et al., A multiple siRNA-based anti-HIV/SHIV microbicide shows protection in both In Vitro and In Vivo models. *PloS one*, 2015. 10(9): e0135288
87. James, H.P., et al., Smart polymers for the controlled delivery of drugs—a concise overview. *Acta Pharmaceutica Sinica B*, 2014. 4(2):120–127
88. Nakano, F.Y., R.F. Leão, and S.C. Esteves, Insights into the role of cervical mucus and vaginal pH in unexplained infertility. *MedicalExpress*, 2015. 2(2).
89. Tevi-Bénissan C, Bélec L, Lévy M, Schneider-Fauveau V, Si Mohamed A, Hallouin MC, Matta M, Grésenguet G. In vivo semen-associated pH neutralization of cervicovaginal secretions. *Clin Diagn Lab Immunol*. 1997 May;4(3):367-74.
90. Mahalingam, A., et al., Inhibition of the transport of HIV in vitro using a pH-responsive synthetic mucin-like polymer system. *Biomaterials*, 2011. 32(33):8343-55
91. Clark, M.R., et al., Enzymatic triggered release of an HIV-1 entry inhibitor from prostate specific antigen degradable microparticles. *International Journal of Pharmaceutics* Volume 413, Issues 1–2, 15 July 2011, Pages 10-18
92. Coulibaly, F.S., M.J.M. Ezoulin, and P.-S.S. Molecular ..., Layer-by-Layer Engineered Microbicide Drug Delivery System Targeting HIV-1 gp120: Physicochemical and Biological Properties. *Mol Pharm*. 2017 Oct 2;14(10):3512-3527.
93. Ball, C. and W.-K.A. *Electrospun fibers for microbicide drug delivery. Drug Delivery and Development of Anti-HIV microbicides*; Jenny Stanford Publishing, 2014.
94. Huang, C., et al., Electrospun cellulose acetate phthalate fibers for semen induced anti-HIV vaginal drug delivery. *Biomaterials*, 2012. 33(3):962-9
95. Tyo, K.M., et al., pH-responsive delivery of Griffithsin from electrospun fibers. *European Journal of Pharmaceutics and biopharmaceutics*, 2018. 138:64-74

96. Palomino, Ñ., et al., Vaginal *Lactobacillus* inhibits HIV-1 replication in human tissues ex vivo. *Front Microbiol.* 2017 May 19;8:906.
97. Brichacek, B., et al., In vivo evaluation of safety and toxicity of a *Lactobacillus jensenii* producing modified cyanovirin-N in a rhesus macaque vaginal challenge model. *PloS one*, 2013. 8(11): e78817
98. Lagenaar, L.A., et al., Robust vaginal colonization of macaques with a novel vaginally disintegrating tablet containing a live biotherapeutic product to prevent HIV infection in .... *PloS one*, 2015. 10(4): e0122730
99. Liu, X., et al., Engineering of a human vaginal *Lactobacillus* strain for surface expression of two-domain CD4 molecules. *Applied and environmental ...*, 2008. 74(15):4626-35
100. Liu, J.J., et al., Activity of HIV entry and fusion inhibitors expressed by the human vaginal colonizing probiotic *Lactobacillus reuteri* RC-14. *Cell Microbiol.* 2007 Jan;9(1):120-30.
101. Vangelista, L., et al., Engineering of *Lactobacillus jensenii* to secrete RANTES and a CCR5 antagonist analogue as live HIV-1 blockers. *Antimicrob Agents Chemother.* 2010 Jul;54(7):2994-3001.
102. Damelin, L.H. and M.-D.-D. and ..., Plasmid Transduction Using Bacteriophage  $\Phi$ adh for Expression of CC Chemokines by *Lactobacillus gasseri* ADH. *Appl Environ Microbiol.* 2010;76(12):3878-3885.
103. Agashe, H., M. Hu, and L. Rohan, Formulation and delivery of microbicides. *Current HIV research*, 2012. **10**(1): p. 88-96.

104. Zhou, T., et al., Expression of transporters and metabolizing enzymes in the female lower genital tract: Implications for microbicide research. *AIDS Res Hum Retroviruses*. 2013 Nov;29(11):1496-503.
105. Klatt, N.R., et al., Vaginal bacteria modify HIV tenofovir microbicide efficacy in African women. *Science*. 2017 Jun 2;356(6341):938-945.
106. Gosmann, C., et al., Lactobacillus-deficient cervicovaginal bacterial communities are associated with increased HIV acquisition in young South African women. *Immunity*. 2017 Jan 17; 46(1): 29–37.
107. Molina, J.M., et al., On-demand preexposure prophylaxis in men at high risk for HIV-1 infection. *N Engl J Med* 2015; 373:2237-2246.
108. Keller, M.J., et al., A phase 1 randomized placebo-controlled safety and pharmacokinetic trial of a tenofovir disoproxil fumarate vaginal ring. *AIDS*, 2016. **30**(5): p. 743-51.
109. Baeten, J.M., T. Palanee-Phillips, Use of a vaginal ring containing dapivirine for HIV-1 prevention in women. *N. Engl J Med* 2016; 375:2121-2132
110. Morris, G.C., et al., MABGEL 1: first phase 1 trial of the anti-HIV-1 monoclonal antibodies 2F5, 4E10 and 2G12 as a vaginal microbicide. *PLoS One* 9(12): e116153.
111. Ledgerwood, J.E. and C.-E.E. ..., Safety, pharmacokinetics and neutralization of the broadly neutralizing HIV-1 human monoclonal antibody VRC01 in healthy adults. *Clin Exp Immunol*. 2015 Dec;182(3):289-301.
112. Friend, D.R., Intravaginal rings: controlled release systems for contraception and prevention of transmission of sexually transmitted infections. *Drug delivery and translational research*, 2011. **1**(3): p. 185-193.

113. Briselden, A.M. and S.L. Hillier, Evaluation of affirm VP Microbial Identification Test for *Gardnerella vaginalis* and *Trichomonas vaginalis*. Evaluation of affirm VP Microbial Identification Test for *Gardnerella vaginalis* and *Trichomonas vaginalis*., *J Clin Microbiol.* 1994 Jan;32(1):148-52..
114. Kiser, P.F., T.J. Johnson, and J.T. Clark, State of the art in intravaginal ring technology for topical prophylaxis of HIV infection. *AIDS reviews*, 2011. **14**(1): p. 62-77.
115. Koetsawang, S., et al., Microdose intravaginal levonorgestrel contraception: a multicentre clinical trial. II. Expulsions and removals. World Health Organization. Task Force on Long-Acting Systemic Agents for Fertility Regulation. *Contraception*, 1990. **41**(2): p. 125-141.
116. Malcolm, K.R., et al., Advances in microbicide vaginal rings. *Antiviral research*, 2010. **88 Suppl 1**: p. 9.
117. Thurman, A., et al., Intravaginal rings as delivery systems for microbicides and multipurpose prevention technologies. *International journal of women's health*, 2013. **5**: p. 695-708.
118. Novak, A., et al., The combined contraceptive vaginal ring, NuvaRing: an international study of user acceptability. *Contraception*, 2003. **67**(3): p. 187-94.
119. Peeters, M. and P. Piot, Adhesion of *Gardnerella vaginalis* to vaginal epithelial cells: variables affecting adhesion and inhibition by metronidazole. Adhesion of *Gardnerella vaginalis* to vaginal epithelial cells: variables affecting adhesion and inhibition by metronidazole., 1985. 61(6):391-5
120. Taylor, E., et al., *Gardnerella vaginalis*, anaerobes, and vaginal discharge. *Gardnerella vaginalis*, anaerobes, and vaginal discharge, 1982. 1(8286):1376-9

121. Kyongo, J.K., et al., A cross-sectional analysis of selected genital tract immunological markers and molecular vaginal microbiota in Sub-Saharan African women with relevance to HIV risk and prevention. *Clinical and Vaccine Immunology*, 2015. 22(5):526-38
122. Cole, A.M., et al., HIV-Enhancing Factors are Secreted by Reproductive Epithelia Upon Inoculation with Bacterial Vaginosis-Associated Bacteria. *Protein and peptide letters*, 2015. 22(8):672-80
123. Kenyon, C. and K. Osbak, Sexual networks, HIV, race and bacterial vaginosis. *AIDS* (London, England), 2015. 29(5): p. 641-642.
124. Gunawardana, M., et al., Microbial biofilms on the surface of intravaginal rings worn in non-human primates. *Journal of medical microbiology*, 2011. 60(Pt 6): p. 828-837.
125. Peer, D., Induction of therapeutic gene silencing in leukocyte-implicated diseases by targeted and stabilized nanoparticles: a mini-review. *Journal of controlled release : official journal of the Controlled Release Society*, 2010. 148(1): p. 63-68.
126. Ramalingam, D., et al., RNA aptamers directed to human immunodeficiency virus type 1 Gag polyprotein bind to the matrix and nucleocapsid domains and inhibit virus production. *J Virol*, 2011. 85(1): p. 305-14.
127. Duclair, S., et al., High-affinity RNA Aptamers Against the HIV-1 Protease Inhibit Both In Vitro Protease Activity and Late Events of Viral Replication. *Molecular Therapy - Nucleic Acids*, 2015. 4: p. e228.
128. Falkenhagen, A., et al., Control of HIV Infection In Vivo Using Gene Therapy with a Secreted Entry Inhibitor. *Molecular therapy. Nucleic acids*, 2017. 9: p. 132-144.
129. Mahmood ur, R., et al., RNA interference: the story of gene silencing in plants and humans. *Biotechnology advances*, 2007. 26(3): p. 202-209.

130. Elbashir, et al., Duplexes of 21-nucleotide RNAs mediate RNA interference in cultured mammalian cells. Duplexes of 21-nucleotide RNAs mediate RNA interference in cultured mammalian cells, *Nature*. 2001 May 24;411(6836):494-8.
131. Kurreck, J., RNA interference: from basic research to therapeutic applications. *Angewandte Chemie (International ed. in English)*, 2008. **48**(8): p. 1378-1398.
132. Novina, C.D., et al., siRNA-directed inhibition of HIV-1 infection. *Nature medicine*, 2002. **8**(7): p. 681-686.
133. Robbins, M., et al., Misinterpreting the therapeutic effects of small interfering RNA caused by immune stimulation. *Human gene therapy*, 2008. **19**(10): p. 991-999.
134. Yin, H., et al., Non-viral vectors for gene-based therapy. *Nature reviews. Genetics*, 2014. **15**(8): p. 541-555.
135. McCall, R.L. and R.W. Sirianni, PLGA nanoparticles formed by single- or double-emulsion with vitamin E-TPGS. *Journal of visualized experiments : JoVE*, 2012(82): p. 51015.
136. Uner, M. and G. Yener, Importance of solid lipid nanoparticles (SLN) in various administration routes and future perspectives. *International journal of nanomedicine*, 2007. **2**(3): p. 289-300.
137. Chu, L.Y., et al., Preparation of thermo-responsive core-shell microcapsules with a porous membrane and poly (N-isopropylacrylamide) gates. Preparation of thermo-responsive core-shell microcapsules with a porous membrane and poly (N-isopropylacrylamide) gates, *Journal of Membrane Science* 192 (2001) 27–39.
138. Camp, W., et al., Poly (acrylic acid) with disulfide bond for the elaboration of pH-responsive brush surfaces. *European Polymer Journal*, 2010. **46**(2): p. 195-201.

139. Zhou, H., et al., Preparation of Thermal and pH Dually Sensitive Polyurethane Membranes and Their Properties. *Journal of Macromolecular Science, Part B*, 2014. **53**(3): p. 398-411.
140. Huh, K., et al., pH-sensitive polymers for drug delivery. *Macromolecular Research*, 2012. **20**(3): p. 224-233.
141. Rastogi, R., et al., Osmotic pump tablets for delivery of antiretrovirals to the vaginal mucosa. *Antiviral Res*, 2013. **100**(1): p. 255-8.
142. Teller, R., R. Rastogi, and P. Kiser., A Simple Intravaginal Ring Pump for Sustained Vaginal Release of ARV Microparticles and Macromolecular Agents, *AIDS Research and Human Retroviruses* 2014 30:S1, A67-A68.
143. Frykberg, R.G. and J. Banks, Challenges in the treatment of chronic wounds. *Advances in wound care*, 2015. **4**(9): p. 560-582.
144. Kalra, S., et al., Understanding diabetes in patients with HIV/AIDS. *Diabetology & metabolic syndrome*, 2011. **3**(1): p. 2-2.
145. Gupta, A., G.K. Jain, and R. Raghbir, A time course study for the development of an immunocompromised wound model, using hydrocortisone. *Journal of Pharmacological and Toxicological Methods*, 1999. **41**(4): p. 183-187.
146. Burns, J. and B. Pieper, HIV/AIDS: impact on healing. *Ostomy Wound Manage*, 2000. **46**(3): p. 30-40, 42, 44 passim; quiz 48-9.
147. McMeeking, A., et al., Wounds in patients with HIV. *Adv Skin Wound Care*, 2014. **27**(9): p. 396-9.



148. Popovich, K.J., et al., Community-Associated Methicillin-Resistant *Staphylococcus aureus* Colonization Burden in HIV-Infected Patients. *Clinical Infectious Diseases*, 2013. **56**(8): p. 1067-1074.
149. Nunan, R., K.G. Harding, and P. Martin, Clinical challenges of chronic wounds: searching for an optimal animal model to recapitulate their complexity. *Dis Model Mech*. 2014 Nov;7(11):1205-13.
150. Reiber, G.E., B.A. Lipsky, and G.W. Gibbons, The burden of diabetic foot ulcers. *American journal of surgery*, 1998. **176**(2A Suppl).
151. Jeffcoate, W.J. and K.G. Harding, Diabetic foot ulcers. *Lancet (London, England)*, 2003. **361**(9368): p. 1545-1551.
152. Minniti, C.P., et al., Leg ulcers in sickle cell disease. *American journal of hematology*, 2010. **85**(10): p. 831-833.
153. Cristóbal, L., et al., Human skin model for mimic dermal studies in pathology with a clinical implication in pressure ulcers. *Histology and histopathology*, 2018: p. 11990.
154. Stojadinovic, A., et al., Topical advances in wound care. *Gynecol Oncol*. 2008 Nov;111(2 Suppl):S70-80..
155. Grice, E.A. and J.A. Segre, Interaction of the microbiome with the innate immune response in chronic wounds. *Current Topics in Innate Immunity II, Adv Exp Med Biol*. 2012;946:55-68.
156. Karin, M., T. Lawrence, and N.-V. Cell, Innate immunity gone awry: linking microbial infections to chronic inflammation and cancer. *Cell*, 2006. 124(4):823-35
157. Stojadinovic, A., et al., Topical advances in wound care. *Topical advances in wound care*, 2008. Nov;111(2 Suppl):S70-80

158. Salgado, R.M., et al., Maltodextrin/ascorbic acid stimulates wound closure by increasing collagen turnover and TGF- $\beta$ 1 expression in vitro and changing the stage of inflammation from chronic to acute in vivo. *Journal of tissue viability*, 2017. **26**(2): p. 131-137.
159. Nouvong, A., et al., Reactive oxygen species and bacterial biofilms in diabetic wound healing. *Physiological genomics*, 2016. **48**(12): p. 889-896.
160. Ennis, W.J., A. Sui, and B.-A. in wound care, Stem cells and healing: impact on inflammation. *Advances in wound care*, 2013. 2013;2(7):369-378
161. Stewart P, Mukherjee P, Ghannoum M. 2004. Biofilm Antimicrobial Resistance, p 250-268. In Ghannoum M, O'Toole G (ed), *Microbial Biofilms*. ASM Press, Washington, DC. doi: 10.1128/9781555817718.ch14.
162. Wolcott, R.D., K.P. Rumbaugh, and J.-G. of wound ..., Biofilm maturity studies indicate sharp debridement opens a time-dependent therapeutic window. *J Wound Care*. 2010 Aug;19(8):320-8..
163. James GA, Swogger E, Wolcott R, Pulcini Ed, Secor P, Sestrich J, Costerton JW, Stewart PS. Biofilms in chronic wounds. *Wound Repair Regen*. 2008 Jan-Feb;16(1):37-44.
164. Grice, E.A., et al., A diversity profile of the human skin microbiota. *Genome ...*, 2008. 18(7): 1043–1050.
165. Hooper, S.J., D.W. Thomas, and J.W. Costerton, A review of the scientific evidence for biofilms in wounds. *Wound repair and ...*, 2012. 20(5):647-57.
166. Zhao, G., et al., Biofilms and Inflammation in Chronic Wounds. *Advances in Wound Care*, 2013. **2**(7): p. 389-399.
167. Seth AK, Geringer MR, Gurjala AN, Abercrombie JA, Chen P, You T, Hong SJ, Galiano RD, Mustoe TA, Leung KP. Understanding the host inflammatory response to wound

- infection: an in vivo study of *Klebsiella pneumoniae* in a rabbit ear wound model. *Wound Repair Regen.* 2012 Mar-Apr;20(2):214-25.
168. Scherr TD, Hanke ML, Huang O, James DB, Horswill AR, Bayles KW, Fey PD, Torres VJ, Kielian T. *Staphylococcus aureus* Biofilms Induce Macrophage Dysfunction Through Leukocidin AB and Alpha-Toxin. *mBio.* 2015 Aug 25;6(4):e01021-15..
169. Secor, P.R., G.A. James, and F.-P. BMC ..., *Staphylococcus aureus* Biofilm and Planktonic cultures differentially impact gene expression, mapk phosphorylation, and cytokine production in human. *BMC Microbiol.* 2011; 11: 143..
170. Zhao, G., M.L. Usui, and U.-R.A. and ..., Time course study of delayed wound healing in a biofilm-challenged diabetic mouse model. *Wound Repair Regen.* 2012 May-Jun;20(3):342-52..
171. Wessels S, Ingmer H. Modes of action of three disinfectant active substances: a review. *Regul Toxicol Pharmacol.* 2013 Dec;67(3):456-67.
172. Sakarya, S.M. and N.M. Wounds, Hypochlorous acid: an ideal wound care agent with powerful microbicidal, antibiofilm, and wound healing potency. *Wounds*, 2014 26(12):342-50.
173. White, R. and C.-K. Wounds, Exploring the effects of silver in wound management-what is optimal? *Wounds*, 2006. 18(11):307-314
174. Cooper ML, Boyce ST, Hansbrough JF, Foreman TJ, Frank DH. Cytotoxicity to cultured human keratinocytes of topical antimicrobial agents. *J Surg Res.* 1990 Mar;48(3):190-5.
175. Akiyama H, Oono T, Saito M, Iwatsuki K. Assessment of cadexomer iodine against *Staphylococcus aureus* biofilm in vivo and in vitro using confocal laser scanning microscopy. *J Dermatol.* 2004 Jul;31(7):529-34..

176. Jan, S. and A. Seema, Polymers with Upper Critical Solution Temperature in Aqueous Solution. *Macromolecular Rapid Communications*, 2012. **33**(22): p. 1898-1920.
177. Vladimir, A., T. Heikki, and M.W. Françoise, *Advances in Polymer Science*. springer, 2011. **242**: p. 29-89.
178. Sahil Sandesh, G., Y. Huan, and K. Chanjoong, Thermoresponsive Gelatin Nanogels. *ACS Macro Letters*, 2014. **3**(11): p. 1210-1214.
179. Christine, J.-D., H. Dominique, and D. Madeleine, All Gelatin Networks: 1. Biodiversity and Physical Chemistry†. *Langmuir*, 2002. **18**(19): p. 7208-7217.
180. Farris, S., et al., Gelatin–pectin composite films from polyion-complex hydrogels. *Gelatin–pectin composite films from polyion-complex hydrogels*, 2011. *Food Hydrocolloids* 25 (2011) 61e7062
181. Byju, A.G. and A. Kulkarni, *Mechanics of Gelatin and Elastin based hydrogels as Tissue Engineered Constructs*. *Mechanics of Gelatin and Elastin based hydrogels as Tissue Engineered Constructs*, 2013.
182. Abdool Karim SS, Richardson BA, Ramjee G, Hoffman IF, Chirenje ZM, Taha T, Kapina M, Maslankowski L, Coletti A, Profy A, Moench TR, Piwowar-Manning E, Mâsse B, Hillier SL, Soto-Torres L; HIV Prevention Trials Network (HPTN) 035 Study Team. Safety and effectiveness of BufferGel and 0.5% PRO2000 gel for the prevention of HIV infection in women. *AIDS*. 2011 Apr 24;25(7):957-66..
183. Mulders TM, Dieben TO. Use of the novel combined contraceptive vaginal ring NuvaRing for ovulation inhibition. *Fertil Steril*. 2001 May;75(5):865-70.
184. Murray, S.M., C.M. Down, and D.R. Boulware, Reduction of immune activation with chloroquine therapy during chronic HIV infection. *J Virol*. 2010 Nov;84(22):12082-6.

185. Bothwell, B. and D.E. Furst, Hydroxychloroquine. Antirheumatic Therapy: Actions and Outcomes, 2005. pp 81-92
186. Sperber, K., et al., Hydroxychloroquine treatment of patients with human immunodeficiency virus type 1. Clinical therapeutics, 1995. **17**(4): p. 622-636.
187. Vatakis, D.N., C.C. Nixon, and J.A. Zack, Quiescent T cells and HIV: an unresolved relationship. Immunologic research, 2010. 48(1-3):110-21
188. Card, C.M., T.B. Ball, and K.R. Fowke, Immune Quiescence: a model of protection against HIV infection. Immune Quiescence: a model of protection against HIV infection, Retrovirology. 2013 Nov 20;10:141..
189. Savarino, A. and I.L. Shytaj, Chloroquine and beyond: exploring anti-rheumatic drugs to reduce immune hyperactivation in HIV/AIDS. Retrovirology, 2015. **12**: p. 51-51.
190. Chiang, G., et al., Inhibition of HIV-1 Replication by Hydroxychloroquine: Mechanism of Action and Comparison with Zidovudine. Clinical Therapeutics, 1996. **18**(6): p. 1080-1092.
191. Harraway, C., N.G. Berger, and N.H. Dubin, Semen pH in patients with normal versus abnormal sperm characteristics. American journal of obstetrics and gynecology, 2000. **182**(5): p. 1045-1047.
192. Sood, A., M.S. Granick, and N.L. Tomaselli, Wound Dressings and Comparative Effectiveness Data. Advances in wound care, 2014. **3**(8): p. 511-529.
193. Zarghami, N., et al., An Overview on Application of Natural Substances Incorporated with Electrospun Nanofibrous Scaffolds to Development of Innovative Wound Dressings. Mini reviews in medicinal chemistry, 2017. **17**.

194. Shurko, J.F., et al., Evaluation of LL-37 antimicrobial peptide derivatives alone and in combination with vancomycin against *S. aureus*. *The Journal of Antibiotics*, 2018. **71**(11): p. 971-974.
195. Zanetti, M., Cathelicidins, multifunctional peptides of the innate immunity. *J Leukoc Biol*, 2004. **75**(1): p. 39-48.
196. Sørensen, O.E., et al., Human cathelicidin, hCAP-18, is processed to the antimicrobial peptide LL-37 by extracellular cleavage with proteinase 3. *Blood*, 2001. **97**(12): p. 3951-9.
197. Steinstraesser, L., et al., Host Defense Peptides in Wound Healing. *Molecular Medicine*, 2008. **14**(7): p. 528-537.
198. Kang, J., M.J. Dietz, and B. Li, Antimicrobial peptide LL-37 is bactericidal against *Staphylococcus aureus* biofilms. *PloS one*, 2019. **14**(6): p. e0216676-e0216676.
199. Shahmiri, M., et al., Membrane Core-Specific Antimicrobial Action of Cathelicidin LL-37 Peptide Switches Between Pore and Nanofibre Formation. *Scientific Reports*, 2016. **6**(1): p. 38184.
200. Nagarajan, R., Antibacterial activities and modes of action of vancomycin and related glycopeptides. *Antimicrobial agents and chemotherapy*, 1991. **35**(4): p. 605-609.
201. Scheffers, D.J. and M.G. Pinho, Bacterial cell wall synthesis: new insights from localization studies. *Microbiol Mol Biol Rev*, 2005. **69**(4): p. 585-607.
202. Rohan, L.C. and A.B. Sassi, Vaginal drug delivery systems for HIV prevention. *AAPS J*, 2009. **11**(1): p. 78-87.

203. Ghosal, K., A. Ranjan, and B.B. Bhowmik, A novel vaginal drug delivery system: anti-HIV bioadhesive film containing abacavir. *J Mater Sci Mater Med*, 2014. **25**(7): p. 1679-89.
204. Garg, S., et al., Development and characterization of bioadhesive vaginal films of sodium polystyrene sulfonate (PSS), a novel contraceptive antimicrobial agent. *Pharm Res*, 2005. **22**(4): p. 584-95.
205. Gu, J., S. Yang, and E.A. Ho, Biodegradable Film for the Targeted Delivery of siRNA-Loaded Nanoparticles to Vaginal Immune Cells. *Mol Pharm*, 2015. **12**(8): p. 2889-903.
206. Garg, S., et al., Advances in development, scale-up and manufacturing of microbicide gels, films, and tablets. *Antiviral Res*, 2010. **88 Suppl 1**: p. S19-29.
207. Ndesendo, V.M., et al., A review of current intravaginal drug delivery approaches employed for the prophylaxis of HIV/AIDS and prevention of sexually transmitted infections. *AAPS PharmSciTech*, 2008. **9**(2): p. 505-20.
208. Machado, R.M., et al., Vaginal films for drug delivery. *J Pharm Sci*, 2013. **102**(7): p. 2069-81.
209. Park, J.S., J.W. Park, and E. Ruckenstein, A dynamic mechanical and thermal analysis of unplasticized and plasticized poly (vinyl alcohol)/methylcellulose blends. A dynamic mechanical and thermal analysis of unplasticized and plasticized poly (vinyl alcohol)/methylcellulose blends, *Journal of Applied Polymer Science*, Vol.80,1825–1834(2001).
210. Adel Ramezani Kakroodi, S.C., Mohini Sain, Abdullah Asiri, Mechanical, Thermal, and Morphological Properties of Nanocomposites Based on Polyvinyl Alcohol and Cellulose Nanofiber from Aloe vera Rind. *Journal of Nanomaterials*, 2014. **2014**: p. 7.

211. Sasa Mrkic, K.G., Marica Ivankovic, Effect of Temperature and Mechanical Stress on Barrier Properties of Polymeric Films Used for Food Packaging. *Journal of Plastic Film & Sheeting*, 2007. **23**(3): p. 239-256.
212. Ioannis Arvanitoyannis, E.P., Costas G. Biliaderis, Hiromasa Ogawa, Norioki Kawasaki, Atsuyoshi Nakayama, Biodegradable Films Made from Low Density Polyethylene (LDPE), Ethylene Acrylic Acid (EAA), PolyCaprolactone (PCL) and Wheat Starch for Food Packaging Applications: Part 3. *Starch*, 1997. **49**(7-8): p. 306-322.
213. E. Schaffer, S.H., R. Blossey, U. Steiner, Temperature-gradient-induced instability in polymer films. *Europhysics Letters*, 2002. **60**(2).
214. Bertoglio, P., S.E. Jacobo, and M.E. Daraio, Preparation and characterization of PVA films with magnetic nanoparticles: the effect of particle loading on drug release behavior. *Journal of applied polymer science*, 2010. **115**(3): p. 1859-1865.
215. Galya, T., et al., Antibacterial poly (vinyl alcohol) film containing silver nanoparticles: preparation and characterization. Antibacterial poly (vinyl alcohol) film containing silver nanoparticles: preparation and characterization, *Journal of Applied Polymer Science*, Vol. 110, 3178–3185 (2008).
216. Miral, F. and A.H. Emmanuel, Nanoparticles Encapsulated with LL37 and Serpin A1 Promotes Wound Healing and Synergistically Enhances Antibacterial Activity. *Molecular pharmaceutics*, 2016. **13**(7): p. 2318-2331.
217. Wu, S.Y., et al., Vaginal delivery of siRNA using a novel PEGylated lipoplex-entrapped alginate scaffold system. *Journal of controlled release*, 155(3):418-26.
218. Duncan, J., Principles and Applications of Mechanical Thermal Analysis 2008: Blackwell Publishing: Chap 4, P 119-163



219. Ehrenstein, G.W., Riedel, Gabriela, and Trawiel, Pia, Thermal Analysis of Plastics. Theory and Practice. 2004 Carl Hanser Verlag GmbH & Co. KG. 399
220. Ladipo, O.A., et al., A new vaginal antimicrobial contraceptive formulation: phase I clinical pilot studies. *Contraception*, 2000. **62**(2): p. 91-7.
221. Ding, C., M. Zhang, and G. Li, Preparation and characterization of collagen/hydroxypropyl methylcellulose (HPMC) blend film. *Carbohydr Polym*, 2015. **119**: p. 194-201.
222. Kaffashi, B., S. Davoodi, and E. Oliaei, Poly(epsilon-caprolactone)/triclosan loaded polylactic acid nanoparticles composite: A long-term antibacterial bionanocomposite with sustained release. *Int J Pharm*, 508 (2016) 10–21
223. Al-Kayiem, H.H. and M. Sidik, Study on the thermal accumulation and distribution inside a parked car cabin. Study on the thermal accumulation and distribution inside a parked car cabin, Volume 7 No. 6, 2010, 784-789
224. Lei, P., et al., Immobilization of TiO<sub>2</sub> nanoparticles in polymeric substrates by chemical bonding for multi-cycle photodegradation of organic pollutants. *J Hazard Mater*, 2012. **227-228**: p. 185-94.
225. Mauck, C.K., et al., A phase I comparative study of three contraceptive vaginal films containing nonoxynol-9. Postcoital testing and colposcopy. *Contraception*, 1997. **56**(2): p. 97-102.
226. Staab, R.J., Dissolvable device for contraception or delivery of medication. US Patent 5, 1995.
227. Sobel, J.D., Bacterial vaginosis, in *Annual Review of Medicine*. 2000. p. 349-356.

228. Ferris, D.G., et al., Treatment of bacterial vaginosis: A comparison of oral metronidazole, metronidazole vaginal gel, and clindamycin vaginal cream. *Journal of Family Practice*, 1995. **41**(5): p. 443-449.
229. Higgins, J.A., S. Hoffman, and S.L. Dworkin, Rethinking gender, heterosexual men, and women's vulnerability to HIV/AIDS. *American Journal of Public Health*, 2010. **100**(3): p. 435-445.
230. Ndesendo, V.M.K., et al., A review of current intravaginal drug delivery approaches employed for the prophylaxis of HIV/AIDS and prevention of sexually transmitted infections. *AAPS PharmSciTech*, 2008. **9**(2): p. 505-520.
231. Gu, J.H. and A. Emmanuel, Drug Delivery: Intravaginal, Advantages and Challenges. *Encyclopedia of Biomedical Polymers and Polymer Biomaterials*, 2015. **4**: p. 2712-2725.
232. Mahalingam, A., et al., Vaginal microbicide gel for delivery of IQP-0528, a pyrimidinedione analog with a dual mechanism of action against HIV-1. *Antimicrobial Agents and Chemotherapy*, 2011. **55**(4): p. 1650-1660.
233. Johal, H.S., et al., Advanced topical drug delivery system for the management of vaginal candidiasis. *Drug Delivery*, 2016. **23**(2): p. 550-563.
234. Thiery, M., et al., The medroxyprogesterone acetate intravaginal silastic ring as a contraceptive device. *Contraception*, 1976. **13**(5): p. 605-617.
235. Johnson, T.J., et al., A 90-day tenofovir reservoir intravaginal ring for mucosal HIV prophylaxis. *Antimicrobial Agents and Chemotherapy*, 2012. **56**(12): p. 6272-6283.
236. Ugaonkar, S.R., et al., An Intravaginal Ring for the Simultaneous Delivery of an HIV-1 Maturation Inhibitor and Reverse-Transcriptase Inhibitor for Prophylaxis of HIV Transmission. *Journal of Pharmaceutical Sciences*, 2015. **104**(10): p. 3426-3439.

237. Briselden, A.M. and S.L. Hillier, Evaluation of affirm VP microbial identification test for *Gardnerella vaginalis* and *Trichomonas vaginalis*. *Journal of Clinical Microbiology*, 1994. **32**(1): p. 148-152.
238. Boskey, E.R., et al., Acid production by vaginal flora in vitro is consistent with the rate and extent of vaginal acidification. *Infection and Immunity*, 1999. **67**(10): p. 5170-5175.
239. Klare, I., et al., Evaluation of new broth media for microdilution antibiotic susceptibility testing of lactobacilli, pediococci, lactococci, and bifidobacteria. *Applied and Environmental Microbiology*, 2005. **71**(12): p. 8982-8986.
240. Wagner, R.D., S.J. Johnson, and D.R. Tucker, Protection of vaginal epithelial cells with probiotic lactobacilli and the effect of estrogen against infection by *Candida albicans*. *Open J Med Microbiol*, 2012. **2**: p. 54-64.
241. Gali, Y., et al., Development of an in vitro dual-chamber model of the female genital tract as a screening tool for epithelial toxicity. *Journal of Virological Methods*, 2010. **165**(2): p. 186-197.
242. Gali, Y., et al., In vitro evaluation of viability, integrity, and inflammation in genital epithelia upon exposure to pharmaceutical excipients and candidate microbicides. *Antimicrobial Agents and Chemotherapy*, 2010. **54**(12): p. 5105-5114.
243. Van Damme, L., et al., Effectiveness of COL-1492, a nonoxynol-9 vaginal gel, on HIV-1 transmission in female sex workers: A randomised controlled trial. *Lancet*, 2002. **360**(9338): p. 971-977.
244. Mesquita, P.M.M., et al., Disruption of tight junctions by cellulose sulfate facilitates HIV infection: Model of microbicide safety. *Journal of Infectious Diseases*, 2009. **200**(4): p. 599-608.

245. Fernández-Romero, J.A., et al., Preclinical assessments of vaginal microbicide candidate safety and efficacy. *Advanced Drug Delivery Reviews*, 2015. **92**: p. 27-38.
246. Royce, R.A., et al., Bacterial vaginosis associated with HIV infection in pregnant women from North Carolina. *Journal of Acquired Immune Deficiency Syndromes and Human Retrovirology*, 1999. **20**(4): p. 382-386.
247. Sewankambo, N., et al., HIV-1 infection associated with abnormal vaginal flora morphology and bacterial vaginosis. *Lancet*, 1997. **350**(9077): p. 546-550.
248. Furst, D.E., Pharmacokinetics of hydroxychloroquine and chloroquine during treatment of rheumatic diseases. *Lupus*, 1996. **5**(SUPPL. 1): p. S11-S15.
249. Goldman, F.D., et al., Hydroxychloroquine inhibits calcium signals in T cells: A new mechanism to explain its immunomodulatory properties. *Blood*, 2000. **95**(11): p. 3460-3466.
250. Antonio, M.A.D., S.E. Hawes, and S.L. Hillier, The identification of vaginal *Lactobacillus* species and the demographic and microbiologic characteristics of women colonized by these species. *Journal of Infectious Diseases*, 1999. **180**(6): p. 1950-1956.
251. Rolain, J.M., P. Colson, and D. Raoult, Recycling of chloroquine and its hydroxyl analogue to face bacterial, fungal and viral infections in the 21st century. *International Journal of Antimicrobial Agents*, 2007. **30**(4): p. 297-308.
252. Owen, D.H. and D.F. Katz, A vaginal fluid simulant. *Contraception*, 1999. **59**(2): p. 91-95.
253. Ayehunie, S., et al., Development of an in vitro alternative assay method for vaginal irritation. *Toxicology*, 2011. **279**(1-3): p. 130-138.

254. Fowler, M.G., S.L. Melnick, and B.J. Mathieson, Women and HIV. *Epidemiology and global overview. Obstetrics and gynecology clinics of North America*, 1997. **24**(4): p. 705-729.
255. Ickovics, J.R. and J. Rodin, Women and AIDS in the United States: epidemiology, natural history, and mediating mechanisms. *Health psychology : official journal of the Division of Health Psychology, American Psychological Association*, 1992. **11**(1): p. 1-16.
256. García-Moreno, C., C. Zimmerman, and M.-G.-A. Lancet, Addressing violence against women: a call to action. *The Lancet*, 2015. 385(9978):1685-95.
257. Dimitrov, D.T., et al., How much do we know about drug resistance due to PrEP use? Analysis of experts' opinion and its influence on the projected public health impact. How much do we know about drug resistance due to PrEP use? Analysis of experts' opinion and its influence on the projected public health impact, 2016. 11(7): e0158620.
258. Grant, R.M., et al., Preexposure chemoprophylaxis for HIV prevention in men who have sex with men. *The New England journal of medicine*, 2010. **363**(27): p. 2587-2599.
259. Tuller, D., HIV Prevention Drug's Slow Uptake Undercuts Its Early Promise. *Health Affairs*, 2018. **37**(2): p. 178-180.
260. Knox, D.C., et al., Multidrug-Resistant HIV-1 Infection despite Preexposure Prophylaxis. *The New England Journal of Medicine*, 2017. **376**(5): p. 501-502.
261. Gengiah, T.N., et al., Adherence challenges with drugs for pre-exposure prophylaxis to prevent HIV infection. *International journal of clinical pharmacy*, 2014. **36**(1): p. 70-85.
262. Poynten, I.M., et al., The safety of candidate vaginal microbicides since nonoxynol-9: a systematic review of published studies. *AIDS*, 2009. **23**(10).

263. Van Damme, L., et al., Lack of effectiveness of cellulose sulfate gel for the prevention of vaginal HIV transmission. *N Engl J Med*, 2008. **359**(5): p. 463-72.
264. D'Cruz, O.J. and F.M. Uckun, Vaginal microbicides and their delivery platforms. *Expert Opin Drug Deliv*, 2014. **11**(5): p. 723-40.
265. Novák, A., et al., The combined contraceptive vaginal ring, NuvaRing: an international study of user acceptability. *Contraception*, 2003 **67**(3):187-94.
266. Baum, M.M., et al., An intravaginal ring for the simultaneous delivery of multiple drugs. *Journal of pharmaceutical sciences*, 2012. **101**(8): p. 2833-2843.
267. Keller, M.J., et al., Tenofovir disoproxil fumarate intravaginal ring for HIV pre-exposure prophylaxis in sexually active women: a phase 1, single-blind, randomised, controlled trial. *The lancet. HIV*, 2019. **6**(8): p. e498-e508.
268. Klatt, N.R., et al., Immune activation and HIV persistence: implications for curative approaches to HIV infection. *Immunological reviews*, 2013. **254**(1): p. 326-342.
269. McLaren, P.J., et al., HIV-exposed seronegative commercial sex workers show a quiescent phenotype in the CD4+ T cell compartment and reduced expression of HIV-dependent host factors. *The Journal of infectious diseases*, 2010. **202 Suppl 3**: p. 44.
270. Vatakis, D.N., C.C. Nixon, and J.A. Zack, Quiescent T cells and HIV: an unresolved relationship. *Immunologic research*, 2010. **48**(1-3): p. 110-121.
271. Lajoie, J., et al., Using safe, affordable and accessible non-steroidal anti-inflammatory drugs to reduce the number of HIV target cells in the blood and at the female genital tract. 2018. **21**(7):e25150
272. Lombard-Platlet, S., et al., Inhibition by chloroquine of the class II major histocompatibility complex-restricted presentation of endogenous antigens varies

- according to the cellular origin of the antigen-presenting cells, the nature of the T-cell epitope, and the responding T cell. *Immunology*, 1993. **80**(4): p. 566-573.
273. Schmidt, R.L.J., et al., Chloroquine inhibits human CD4+ T-cell activation by AP-1 signaling modulation. *Scientific reports*, 2017. 7:42191
274. Brown, T.R., Timothy Ray Brown's Continuing Activism Toward Curing HIV. *AIDS research and human retroviruses*, 2018. **34**(1): p. 9-11.
275. Gupta, R.K., et al., Evidence for HIV-1 cure after CCR5 $\Delta$ 32/ $\Delta$ 32 allogeneic haemopoietic stem-cell transplantation 30 months post analytical treatment interruption: a case report. *The lancet. HIV*, 2020. **7**(5).
276. Lopalco L. CCR5: From Natural Resistance to a New Anti-HIV Strategy. *Viruses*. 2010;2(2):574-600. doi:10.3390/v2020574.
277. Kim SS, Peer D, Kumar P, Subramanya S, Wu H, Asthana D, Habiro K, Yang YG, Manjunath N, Shimaoka M, Shankar P. RNAi-mediated CCR5 silencing by LFA-1-targeted nanoparticles prevents HIV infection in BLT mice. *Mol Ther*. 2010 Feb;18(2):370-6.
278. Kim, S., et al., Design and development of pH-responsive polyurethane membranes for intravaginal release of nanomedicines. *Acta Biomater*, 2018. **82**: p. 12-23.
279. Ghanbar, S., et al., A new strategy for battling bacterial resistance: Turning potent, non-selective and potentially non-resistance-inducing biocides into selective ones. *Nanomedicine: Nanotechnology, Biology and Medicine*, 2018. **14**(2): p. 471-481.
280. Rastogi R, Su J, Mahalingam A, Clark J, Sung S, Hope T, Kiser PF. Engineering and characterization of simplified vaginal and seminal fluid simulants. *Contraception*. 2016 Apr;93(4):337-346.

281. Rehan, N., A.J. Sobrero, and J.W. Fertig, The semen of fertile men: statistical analysis of 1300 men. *Fertil Steril*, 1975. **26**(6): p. 492-502.
282. Cooper, T.G., et al., World Health Organization reference values for human semen characteristics. *Hum Reprod Update*, 2010. **16**(3): p. 231-45.
283. Kiertiburanakul, S. and S.-S. research, Emerging of HIV drug resistance: epidemiology, diagnosis, treatment and prevention. *Current HIV research*, 2009, **7**(3):273-8.
284. Camara M, Dieye TN, Seydi M, Diallo AA, Fall M, Diaw PA, Sow PS, Mboup S, Kestens L, Jennes W. Low-level CD4+ T cell activation in HIV-exposed seronegative subjects: influence of gender and condom use. *J Infect Dis*. 2010 Mar 15;201(6):835-42.
285. Bégaud E, Chartier L, Marechal V, et al. Reduced CD4 T cell activation and in vitro susceptibility to HIV-1 infection in exposed uninfected Central Africans. *Retrovirology*. 2006;3:35.
286. Goldman FD, Gilman AL, Hollenback C, Kato RM, Premack BA, Rawlings DJ. Hydroxychloroquine inhibits calcium signals in T cells: a new mechanism to explain its immunomodulatory properties. *Blood*. 2000 Jun 1;95(11):3460-6.
287. Chen, Y., et al., Implant delivering hydroxychloroquine attenuates vaginal T lymphocyte activation and inflammation. *Journal of controlled release : official journal of the Controlled Release Society*, 2018. **277**: p. 102-113.
288. Wojnilowicz, M., et al., Super-resolution Imaging of Proton Sponge-Triggered Rupture of Endosomes and Cytosolic Release of Small Interfering RNA. *ACS Nano*, 2019. **13**(1): p. 187-202.
289. Kocak, G., C. Tuncer, and V. Bütün, pH-Responsive polymers. *Polymer Chemistry*, 2016. **8**(1): p. 144-176.



290. Thakral S, Thakral NK, Majumdar DK. Eudragit: a technology evaluation. *Expert Opin Drug Deliv.* 2013 Jan;10(1):131-49.
291. Miller, C.J., et al., Propagation and dissemination of infection after vaginal transmission of simian immunodeficiency virus. *Journal of virology*, 2005. **79**(14): p. 9217-9227.
292. Lai, S.K., Y.Y. Wang, and H.-J. drug delivery reviews, Mucus-penetrating nanoparticles for drug and gene delivery to mucosal tissues. *Advanced drug delivery reviews*, 2009, **61**(2):158-71.
293. Suk, J.S., et al., PEGylation as a strategy for improving nanoparticle-based drug and gene delivery. *Adv Drug Deliv Rev*, 2016. **99**(Pt A): p. 28-51.
294. Fox, C.A., S.J. Meldrum, and B.W. Watson, continuous measurement by radio-telemetry of vaginal pH during human coitus. *Reproduction*, 1973. **33**(1): p. 69-75.
295. Bouvet JP, Grésenguet G, Bélec L. Vaginal pH neutralization by semen as a cofactor of HIV transmission. *Clin Microbiol Infect.* 1997 Feb;3(1):19-23.
296. Wolters-Everhardt, E., et al., Buffering capacity of human semen. *Fertility and Sterility*, 1986. **46**(1): p. 114-119.
297. Järbrink, K., et al., The humanistic and economic burden of chronic wounds: a protocol for a systematic review. *Systematic reviews*, 2017. **6**(1): p. 15-15.
298. Dhivya, S., V.V. Padma, and E. Santhini, Wound dressings - a review. *BioMedicine*, 2015. **5**(4): p. 22-22.
299. Sorg, H., et al., Skin Wound Healing: An Update on the Current Knowledge and Concepts. *European Surgical Research*, 2017. **58**(1-2): p. 81-94.
300. Boer, M., et al., Structural and biophysical characteristics of human skin in maintaining proper epidermal barrier function. *Postepy dermatologii i alergologii*, 2016. **33**(1): p. 1-5.

301. Guo, S. and L.A. Dipietro, Factors affecting wound healing. *Journal of dental research*, 2010. **89**(3): p. 219-229.
302. Wallace, H.A., B.M. Basehore, and P.M. Zito, Wound Healing Phases, in *StatPearls*. 2020, StatPearls Publishing Copyright © 2020, StatPearls Publishing LLC.: Treasure Island (FL).
303. Attinger, C. and R. Wolcott, Clinically Addressing Biofilm in Chronic Wounds. *Advances in wound care*, 2012. **1**(3): p. 127-132.
304. Wu, Y.-K., N.-C. Cheng, and C.-M. Cheng, Biofilms in Chronic Wounds: Pathogenesis and Diagnosis. *Trends in Biotechnology*, 2019. **37**(5): p. 505-517.
305. Taylor, T.A. and C.G. Unakal, Staphylococcus Aureus, in *StatPearls*. 2020, StatPearls Publishing Copyright © 2020, StatPearls Publishing LLC.: Treasure Island (FL).
306. Li, J. and D.J. Mooney, Designing hydrogels for controlled drug delivery. *Nature reviews. Materials*, 2016. **1**(12): p. 16071.
307. Zheng, Y., et al., Gelatin-Based Hydrogels Blended with Gellan as an Injectable Wound Dressing. *ACS omega*, 2018. **3**(5): p. 4766-4775.
308. Han, G. and R. Ceilley, Chronic Wound Healing: A Review of Current Management and Treatments. *Advances in therapy*, 2017. **34**(3): p. 599-610.
309. Antonov, Y.A., et al., Effect of the Helix–Coil Transition in Bovine Skin Gelatin on Its Associative Phase Separation with Lysozyme. *Langmuir*, 2017. **33**(47): p. 13530-13542.
310. Bierman, W., The temperature of the skin surface. *Journal of the American Medical Association*, 1936. **106**(14): p. 1158-1162.
311. Dai, T., et al., Chitosan preparations for wounds and burns: antimicrobial and wound-healing effects. *Expert review of anti-infective therapy*, 2011. **9**(7): p. 857-879.

312. Ali Mirani, Z., et al., Ascorbic acid augments colony spreading by reducing biofilm formation of methicillin-resistant *Staphylococcus aureus*. *Iranian journal of basic medical sciences*, 2018. **21**(2): p. 175-180.
313. Mihai, M.M., et al., Nanomaterials for Wound Healing and Infection Control. *Materials* (Basel, Switzerland), 2019. **12**(13): p. 2176.
314. Byju, A.G. and A. Kulkarni, Mechanics of Gelatin and Elastin based hydrogels as Tissue Engineered Constructs. *ICF13*, 2013.
315. Rufián-Henares, J.A. and F.J. Morales, Microtiter plate-based assay for screening antimicrobial activity of melanoidins against *E. coli* and *S. aureus*. *Food chemistry*, 2008. **111**(4):1069-1074.
316. Müsken M, Di Fiore S, Römling U, Häussler S. A 96-well-plate-based optical method for the quantitative and qualitative evaluation of *Pseudomonas aeruginosa* biofilm formation and its application to susceptibility testing. *Nat Protoc*. 2010 Aug;**5**(8):1460-9..
317. Coenye, T. and H.J. Nelis, In vitro and in vivo model systems to study microbial biofilm formation. *Journal of Microbiological Methods*, 2010. **83**(2): p. 89-105.
318. Saghazadeh, S., et al., Drug delivery systems and materials for wound healing applications. *Advanced drug delivery reviews*, 2018. **127**: p. 138-166.
319. Zhao, G., et al., Delayed wound healing in diabetic (db/db) mice with *Pseudomonas aeruginosa* biofilm challenge: a model for the study of chronic wounds. *Wound Repair and Regeneration*, 2010. **18**(5): p. 467-477.
320. Joly-Duhamel, C., D. Hellio, and M. Djabourov, All Gelatin Networks: 1. Biodiversity and Physical Chemistry†. *Langmuir*, 2002. **18**(19): p. 7208-7217.

321. Tanaka, F. and Y. Tamura, Thermoreversible Gelation driven by Coil-to-Helix Transition of Polymers. AIP Conference Proceedings, 2004. **708**(1): p. 221-224.
322. Joly-Duhamel, C., et al., All Gelatin Networks: 2. The Master Curve for Elasticity†. Langmuir, 2002. **18**(19): p. 7158-7166.
323. Lee, D.H., et al., Mechanically Reinforced Gelatin Hydrogels by Introducing Slidable Supramolecular Cross-Linkers. Polymers, 2019. **11**(11): p. 1787.
324. Fumakia, M. and E.A. Ho, Nanoparticles Encapsulated with LL37 and Serpin A1 Promotes Wound Healing and Synergistically Enhances Antibacterial Activity. Molecular pharmaceutics, 2016. **13**(7): p. 2318-2331.
325. Dürr, U.H.N., U.S. Sudheendra, and A. Ramamoorthy, LL-37, the only human member of the cathelicidin family of antimicrobial peptides. Biochimica et biophysica acta, 2006. **1758**(9): p. 1408-1425.
326. Shurko, J.F., et al., Evaluation of LL-37 antimicrobial peptide derivatives alone and in combination with vancomycin against S. aureus. The Journal of antibiotics, 2018. 71, pages971–974
327. Kim, M.-H., Nanoparticle-Based Therapies for Wound Biofilm Infection: Opportunities and Challenges. IEEE transactions on nanobioscience, 2016. **15**(3): p. 294-304.
328. Simoni, R., et al., Effect of drying method on mechanical, thermal and water absorption properties of enzymatically crosslinked gelatin hydrogels. Anais da Academia Brasileira de Ciências, 2017. **89**.
329. Long, H., et al., Preparation and characteristics of gelatin sponges crosslinked by microbial transglutaminase. PeerJ, 2017. **5**: p. e3665-e3665.

330. Sieprawska-Lupa, M., et al., Degradation of human antimicrobial peptide LL-37 by *Staphylococcus aureus*-derived proteinases. *Antimicrob Agents Chemother*, 2004. **48**(12): p. 4673-9.
331. Coutinho, B. and R. Prasad, Emtricitabine/tenofovir (Truvada) for HIV prophylaxis. *Am Fam Physician*, 2013. **88**(8): p. 535-40.
332. Maenza, J. and C. Flexner, Combination antiretroviral therapy for HIV infection. *Am Fam Physician*, 1998. **57**(11): p. 2789-98.
333. Wolfarth, A.A., et al., A Human Microbiota-Associated Murine Model for Assessing the Impact of the Vaginal Microbiota on Pregnancy Outcomes. *Frontiers in Cellular and Infection Microbiology*, 2020. **10**(558).
334. Dinarvand, R. and A. D'Emanuele, The use of thermoresponsive hydrogels for on-off release of molecules. *Journal of Controlled Release*, 1995. **36**(3): p. 221-227.